

HELSINKI UNIVERSITY OF TECHNOLOGY  
Faculty of Information and Natural Sciences  
Degree Programme in Industrial Engineering and Management

Antti Eloranta

PRICING OF EXOTIC FOREIGN EXCHANGE RATE OPTIONS

Thesis submitted in partial fulfillment of the requirements for the degree of Master of  
Science (Technology)

Copenhagen, 24<sup>th</sup> January 2008

Supervisor: Professor Ahti Salo  
Instructor: M.Sc. Antti Parviainen

|                          |  |
|--------------------------|--|
| <b>Author:</b>           | Antti Eloranta   |
| <b>Department:</b>       | Industrial Engineering and Management  |
| <b>Major subject:</b>    | Strategy and International Business  |
| <b>Minor subject:</b>    | Systems and Operations Research  |
| <b>Title:</b>            | Pricing of Exotic Foreign Exchange Rate Options  |
| <b>Chair:</b>            | Mat-2 Applied Mathematics  |
| <b>Supervisor:</b>       | Professor Ahti Salo  |
| <b>Instructor:</b>       | M.Sc. Antti Parviainen   |
| <b>Abstract:</b>         | <p>The popularity of exotic foreign exchange rate options has grown rapidly during the past decade. High profit margins and rapid market growth have made the market particularly lucrative for the banks. On the other hand, the correct pricing of exotic options requires more sophisticated models than the traditional Black-Scholes. The objective of this thesis is to build, implement, and validate a pricing model for the exotic foreign exchange rate options.</p> <p>Based on previous research, this thesis models the stochastic behavior of the foreign exchange rates as a stochastic volatility – jump-diffusion process with piecewise constant model parameters. The process is defined in both continuous and discrete times. The continuous time process is used for pricing European options in a semi-closed form, which enables an efficient model calibration. The discrete time model is used for pricing exotic options with Monte Carlo. The model is calibrated using a method customized specifically for the purposes of this thesis.</p> <p>The model is validated by analyzing its performance with real market data from the beginning of July to the end of August 2007. The convergence of the closed-form and Monte Carlo solution option prices shows that the model is internally consistent. The comparison of the model implied and market implied option prices indicate that the model is market consistent. The analysis of the robustness suggests that the model and its calibration are mathematically meaningful.</p> |
| <b>Number of pages:</b>  | 110  |
| <b>Keywords:</b>         | Option pricing, exotic options, foreign exchange rates, stochastic volatility, jump-diffusion.   |
| <b>Department fills:</b> |  |
| <b>Approved:</b>         | <b>Library location:</b>   |

|                             |   |
|-----------------------------|---|
| <b>Tekijä:</b>              | Antti Eloranta  |
| <b>Osasto:</b>              | Tuotantotalouden osasto   |
| <b>Pääaine:</b>             | Yritysstrategia ja kansainvälinen liiketoiminta   |
| <b>Sivuaine:</b>            | Systeemi- ja operaatiotutkimus  |
| <b>Työn nimi:</b>           | Eksoottisten valuuttaoptioiden hinnoittelu  |
| <b>Professori:</b>          | Mat-2 Sovellettu matematiikka   |
| <b>Työn valvoja:</b>        | Professori Ahti Salo  |
| <b>Työn ohjaaja:</b>        | KTM Antti Parviainen  |
| <b>Tiivistelmä:</b>         | <p>Eksoottisten valuuttaoptioiden suosio on kasvanut voimakkaasti viimeisen vuosikymmenen aikana. Korkeiden tuottomarginaalien ja nopean kasvun vuoksi markkina on pankeille erittäin houkutteleva. Toisaalta eksoottisen optioiden oikea hinnoittelu vaatii perinteistä Black-Scholes mallia monimutkaisempien hinnoittelumallien käyttöä. Tämän työn tavoitteena on kehittää, implementoida ja validoida hinnoittelumalli eksoottisille valuuttaoptioille.</p> <p>Aiempiin tutkimustuloksiin nojaten, tämä tutkimus mallintaa valuuttakurssien käyttäytymistä stokastista volatiliteettia ja hyppydiffuusiota kuvaavalla yhdistelmämallilla, jonka parametrit ovat paloittain vakioita. Malli määritellään sekä jatkuvassa että diskreetissä ajassa. Jatkuvan ajan mallia käytetään eurooppalaisten optioiden hinnoitteluun puolisuuljetussa muodossa, jota tarvitaan mallin tehokasta kalibrointia varten. Diskreetin ajan mallia käytetään eksoottisten optioiden hinnoitteluun Monte Carlo simuloinnin avulla. Malli kalibroidaan tätä työtä varten räätälöidyllä menetelmällä.</p> <p>Mallin toiminta validoidaan testaamalla mallia todellisella markkinadatalla heinäkuun alusta elokuun loppuun 2007 ulottuvalla ajanjaksolla. Puolisuuljetun muodon ja Monte Carlo ratkaisujen optiohintojen yhtäpitävyys osoittaa mallin olevan sisäisesti konsistentti. Mallin tuottamien hintojen ja markkinahintojen yhtäpitävyys validoi mallin markkinakonsistenttiuden. Parametrien käyttäytyminen osoittaa, että malli ja sen kalibrointi ovat matemaattisesti mielekkäitä.</p> |
| <b>Sivumäärä:</b>           | 110   |
| <b>Avainsanat:</b>          | Optioiden hinnoittelu, eksoottiset optiot, valuuttaoptiot, stokastinen volatiliteetti, hyppydiffuusio.  |
| <b>Täytetään osastolla:</b> |   |
| <b>Hyväksytty:</b>          | <b>Kirjasto:</b>  |

---

# Acknowledgements

This thesis was conducted for Nordea Markets; a part of the Corporate and Institutional Banking division of Nordea Group. I would like to thank my colleagues at Markets for their comments and advices. In particular, I would like to thank M.Sc. Antti Parviainen for taking the time to instruct this thesis.

I would also like to express my gratitude to professor Ahti Salo for supervising this thesis.

Last but not least, I would like to thank Johanna, my family, and my friends for their support during my studies.

Copenhagen, 24<sup>th</sup> January 2008

Antti Eloranta

---

# Table of Contents

|        |  |    |
|--------|--|----|
| 1      | Introduction .....                           | 1  |
| 1.1    | Background .....                             | 1  |
| 1.2    | Research Problem.....                        | 1  |
| 1.3    | Research Objectives .....                    | 2  |
| 1.4    | Research Scope.....                          | 3  |
| 1.5    | Research Methods and Data Acquisition .....  | 3  |
| 1.6    | Structure of the Study.....                  | 4  |
| 2      | Foreign Exchange Rates.....                  | 5  |
| 2.1    | Interest Rate Parity .....                   | 6  |
| 2.1.1  | Covered Interest Rate Parity.....            | 6  |
| 2.1.2  | Uncovered Interest Rate Parity.....          | 6  |
| 2.1.3  | Empirical Relevance.....                     | 7  |
| 2.2    | Stochastic Modeling.....                     | 7  |
| 2.2.1  | Standard Brownian Motion .....               | 8  |
| 2.2.2  | Arithmetic Brownian Motion .....             | 9  |
| 2.2.3  | Geometric Brownian Motion.....               | 10 |
| 2.2.4  | Stable Distributions .....                   | 11 |
| 2.2.5  | ARCH and GARCH .....                         | 11 |
| 2.2.6  | Jump-Diffusion.....                          | 14 |
| 2.2.7  | Stochastic Volatility .....                  | 16 |
| 2.2.8  | Stochastic Volatility – Jump.....            | 19 |
| 2.2.9  | Two-Factor Stochastic Volatility – Jump..... | 21 |
| 2.2.10 | Stochastic Volatility – Double Jump.....     | 22 |
| 3      | Approaches to Option Pricing .....           | 25 |
| 3.1    | Black-Scholes Model .....                    | 26 |
| 3.2    | Analytical Models .....                      | 29 |

---

|       |   |    |
|-------|---|----|
| 3.2.1 | Biger-Hull.....   | 29 |
| 3.2.2 | Local Volatility Adjusted Biger-Hull.....                     | 31 |
| 3.2.3 | Merton Jump-Diffusion.....                                    | 32 |
| 3.2.4 | Hull-White Stochastic Volatility.....                         | 33 |
| 3.2.5 | Heston Stochastic Volatility.....                             | 34 |
| 3.2.6 | Heston-Nandi GARCH.....                                       | 37 |
| 3.2.7 | Bates Stochastic Volatility – Jump.....                       | 38 |
| 3.2.8 | Duffie-Pan-Singleton Stochastic Volatility – Double Jump..... | 40 |
| 3.3   | Monte Carlo Simulation.....                                   | 41 |
| 3.3.1 | Efficiency.....   | 41 |
| 3.3.2 | Sampling from the Data Generating Process.....                | 42 |
| 4     | Model Calibration.....  | 45 |
| 4.1   | Historical Returns Methods.....                               | 46 |
| 4.1.1 | Generalized Method of Moments.....                            | 46 |
| 4.1.2 | Quasi-Maximum Likelihood Methods.....                         | 46 |
| 4.1.3 | Approximated Maximum Likelihood Methods.....                  | 47 |
| 4.1.4 | Markov-Chain Monte Carlo Methods.....                         | 47 |
| 4.2   | Implied Option Price Methods.....                             | 48 |
| 4.2.1 | Option Price Time Series Methods.....                         | 49 |
| 4.2.2 | Implied Volatility Surface Methods.....                       | 49 |
| 5     | Option Pricing Model.....                                     | 50 |
| 5.1   | Data Generating Process.....                                  | 51 |
| 5.1.1 | Continuous Time Model.....                                    | 52 |
| 5.1.2 | Discrete Time Model.....                                      | 53 |
| 5.2   | Option Pricing.....   | 58 |
| 5.2.1 | Semi-Closed Form Solution for European Options.....           | 58 |
| 5.2.2 | Monte Carlo Solution for European Options.....                | 62 |
| 5.2.3 | Monte Carlo Solution for Exotic Options.....                  | 62 |
| 5.3   | Calibration.....  | 64 |
| 5.3.1 | Cost Function.....  | 65 |
| 5.3.2 | Additional Constraints.....                                   | 66 |

---

---

|       |                                 |    |
|-------|---------------------------------|----|
| 5.3.3 | Numerical Algorithm .....       | 67 |
| 5.4   | Implementation.....             | 70 |
| 5.4.1 | Numerical Integration.....      | 71 |
| 5.4.2 | Random Number Generation.....   | 73 |
| 6     | Numerical Tests.....            | 75 |
| 6.1   | Internal Consistency.....       | 76 |
| 6.2   | Market Consistency.....         | 77 |
| 6.3   | Robustness.....                 | 84 |
| 7     | Discussion and Conclusions..... | 91 |
| 7.1   | Summary .....                   | 91 |
| 7.2   | Concluding Remarks .....        | 93 |
|       | References .....                | 94 |

---

# List of Appendices

Appendix A: Abbreviations

Appendix B: Symbols

---

# List of Figures

|   |    |
|---|----|
| Figure 1: Mean absolute volatility difference and mean spread. ....                               | 79 |
| Figure 2: Maximum absolute volatility difference and mean and maximum spreads. ...                | 80 |
| Figure 3: Market and model implied volatilities for one month at-the-money tenor.....             | 81 |
| Figure 4: Market and model implied volatility surfaces on 11 <sup>th</sup> July 2007.....         | 81 |
| Figure 5: Market and model implied volatility surfaces on 16 <sup>th</sup> July 2007.....         | 82 |
| Figure 6: Market and model implied volatility surfaces on 28 <sup>th</sup> August 2007.....       | 83 |
| Figure 7: Time series of jump frequency ( $\lambda$ ). ....                                       | 85 |
| Figure 8: Time series of average jump size ( $\epsilon$ ). ....                                   | 85 |
| Figure 9: Time series of jump size standard deviation ( $\delta$ ). ....                          | 86 |
| Figure 10: Time series of volatility mean reversion rate ( $\kappa$ ). ....                       | 87 |
| Figure 11: Time series of volatility of volatility ( $\xi$ ). ....                                | 87 |
| Figure 12: Time series of spot-volatility correlation coefficient ( $\rho$ ). ....                | 88 |
| Figure 13: Time series of the average value of volatility mean reversion level ( $\theta$ ). .... | 89 |
| Figure 14: Time series of piecewise constant volatility mean reversion level ( $\theta$ ) .....   | 90 |

---

# List of Tables

|  |    |
|--|----|
| Table 1: The parameters of the option pricing model. ....                            | 53 |
| Table 2: Expiry tenor specific optimal cut-off points and abscissas.....             | 73 |
| Table 3: Comparison of semi-closed form and Monte Carlo solution option prices. .... | 77 |
| Table 4: Key statistics of the market consistency tests. ....                        | 83 |

# 1 Introduction

## 1.1 Background

Foreign exchange (FX) is one of the oldest asset classes traded in the financial market. There has been a need to exchange currencies as long as there has been trade between different countries with different currencies. In the past, FX trading was mostly a tool for international business, whereas in recent decades, investors have begun to use it for speculative purposes with an increasing pace.

Presently, there are hundreds of ways to speculate with the FX rates. The instruments vary from simple deposits to various exotic options. In simple products, the banks' profit margins are typically around a few basis points, whereas in exotic options, the margins vary from some tens of basis points to up to five percent. Combined with an annual market growth rate of 20% (Structured Products Association 2007), the market seems very lucrative for the banks.

One of the most important factors behind the popularity of the exotic options is the flexibility of exploiting different market views. Instead of only having a linear exposure on the FX spot rate, the investors can also have non-linear risk positions through exotic return profiles. From a mathematical perspective, the valuation of such instruments is highly sensitive to the higher moments of the FX returns, which in turn, are not captured by the traditional option pricing models. As a result, a successful exotic options business requires going beyond the traditional Black-Scholes framework.

## 1.2 Research Problem

The research problem of this thesis is to design a pricing model for exotic foreign exchange rate options, implement the model, create a calibration method for the model,

and validate the model in view of its performance requirements. The research problem can be further divided into four research questions:

- (1) How to model the stochastic behavior of the foreign exchange rates?
- (2) How to price exotic options on an underlying with the given stochastic behavior?
- (3) How to calibrate the model parameters?
- (4) How to evaluate the model:
  - (4.1) Is the model internally consistent?
  - (4.2) Is the model market consistent?
  - (4.3) Is the model mathematically meaningful?

### 1.3 Research Objectives

The first research objective is to assess the earlier approaches to FX rate modeling, option pricing, and model calibration. First, the capability of exchange rate models to explain the historical FX returns and the implied option prices should be assessed. Second, the suitability of option pricing models for exotic options should be analyzed. Third, the capability of calibration methods to align the models with the market implied option prices should be assessed.

The second objective is to develop an option pricing model, and the third to implement the model in practice. The first sub-objective of both is to create and implement a model for the stochastic behavior of the FX rates. The second is to create and implement a pricing model for the exotic FX options. The third is to create and implement a calibration method for the model parameters.

The fourth objective is to validate the model to meet its performance requirements. First, the internal consistency of the model should be validated in order to ensure that the implementation has been carried out correctly. Second, the market consistency should be validated in order to ensure that the model matches the market implied option prices. Third, the robustness of the model, or in other words, the stability of the calibrated

model parameters over time, should be validated in order to ensure that the model dynamics and the calibration are mathematically meaningful.

## 1.4 Research Scope

The scope of the theoretical part of the thesis can be further divided into three parts. First, the scope of the FX rate modeling is restricted to stochastic analysis, as the economic factors behind the stochastic behavior play no role in option pricing. Second, the scope of the option pricing is restricted to the most well-known models, as the number of models is far too large for making an extensive analysis of each. Third, the scope of the model calibration is restricted to methods applied to similar models by the previous studies, as the number of calibration methods is also exhaustive.

The scope of the empirical part is restricted to non-quanto, non-exercisable options on one underlying currency pair. Non-quanto refers to options where the underlying and the option itself are denominated in the same currency. Non-exercisable refers to options that are exercised automatically, instead of the option holder deciding whether or not, and when, to exercise the option. The pricing of quanto, exercisable, and basket options is left for the future research due to the limited time resources of this thesis.

## 1.5 Research Methods and Data Acquisition

The main research method in the theoretical part is literature review, whereas the research methods in the empirical part are threefold. First, the mathematical model is defined based on the conclusion from the theoretical part. Second, the model is implemented in Visual Basic programming language. Third, the model performance is validated using standard quantitative analysis techniques.

Data for the theoretical part is acquired from publicly available sources, academic journals being the most important source of data. In addition, some data is acquired from the online sources. All the market data for the empirical part is acquired from Bloomberg, which is one of the leading financial data providers in the world. In

addition, the source codes of some algebraic and numeric tools are acquired from online sources.

## 1.6 Structure of the Study

The *Introduction* Chapter is followed by the theoretical part of the thesis, consisting of *Foreign Exchange Rates*, *Approaches to Option Pricing*, and *Model Calibration* Chapters. *Foreign Exchange Rates* first describes the interest rate parity theory, which is essential for understanding the term structure of the FX rates. Subsequently, the Chapter discusses the stochastic modeling of the FX rates, which is needed for defining the data generating process of the option pricing model. *Approaches to Option Pricing* Chapter presents the most well-known analytical option pricing models and describes the use of Monte Carlo simulation in option pricing. *Model Calibration* Chapter concludes the theoretical part by reviewing different calibration methods for option pricing models.

The theoretical part is followed by the empirical part, consisting of *Option Pricing Model* and *Numerical Tests* Chapters. *Option Pricing Model* Chapter first defines the data generating process of the option pricing model in both continuous and discrete times. Subsequently, the Chapter builds a semi-closed for pricing model for European options in continuous time, which is needed for the efficient calibration of the model. Thereafter, it builds a Monte Carlo framework for pricing both European and exotic options in discrete time. *Numerical Tests* Chapter concludes the empirical part. It first assesses the internal consistency of the model, which ensures that the model is correctly implemented. Next, it verifies that the model is market consistent. Last, it ensures that the model parameters behave smoothly over time, which indicates that the model dynamics and the calibration are mathematically meaningful.

At the end, *Conclusions and Discussion* Chapter brings the thesis to a close. The Chapter first summarizes the research problem and concludes the most important findings. Subsequently, it analyzes the strengths and weaknesses of the thesis and presents suggestions for the future study.

## 2 Foreign Exchange Rates

Foreign exchange rates can be analyzed from different perspectives. On one hand, economic theorists strive to explain the behavior of foreign exchange rates as a part of the greater macroeconomic framework. On the other, industry practitioners seek for profitable ways to speculate with the FX rates, and to quantify and manage the associated risks.

From the economic theorist's perspective, the research regarding foreign exchange rates is focused on theories linking the behavior of FX rates to other economic and political phenomena. Particular areas of interest have been the efficiency of the foreign exchange market and the determination of the FX rates. Other frequently studied topics include the effectiveness of official intervention, foreign exchange rate behavior within target zones, and foreign exchange market microstructure. (Taylor 1995, pp. 13-47)

From the industry practitioner's perspective, the research regarding foreign exchange rates is focused on theories investigating the stochastic behavior of them. Particular areas of interest have been volatility modeling and derivatives pricing. Other frequently studied topics include the management of foreign exchange risk and the optimization of investment portfolios. (Poon & Granger 2003, pp. 478-539)

As defined in the research scope, this thesis approaches the FX rates from the industry practitioner's perspective. As a result, this Chapter begins with an introduction to the interest rate parity; one of the fundamental theories of FX rate behavior. Thereafter, this Chapter examines the most important stochastic models used for the FX rates.

## 2.1 Interest Rate Parity

According to the interest rate parity, the forward and future foreign exchange rates of a given currency pair are determined by the corresponding risk-free interest rates. Interest rate parity states that, under the assumption of risk neutral market participants and the absence of transaction costs, the forward and future foreign exchange rates must be determined by the cost-of-carry difference of the given currencies. The interest rate parity can be divided into covered interest rate parity (CIP) and uncovered interest rate parity (UIP) conditions. (Oldfield & Messina 1977, pp. 473-479)

### 2.1.1 Covered Interest Rate Parity

Covered interest rate parity condition states that it should be impossible to earn excess risk-free returns with the forward FX rates. The condition states that investment into domestic currency risk-free assets with a rate of ( $r_t$ ) for a period of ( $t$ ) must lead into the same result as buying the foreign currency at a spot rate ( $S_0$ ), investing the money into foreign currency risk-free assets with a rate of ( $r_t^*$ ) for a period of ( $t$ ), and selling a foreign currency forward ( $F_t$ ) for a delivery period of ( $t$ ),

$$(1 + r_t) - 1 = (1 + r_t^*) \cdot \frac{F_t}{S_0} - 1 \Leftrightarrow \frac{F_t}{S_0} = \frac{(1 + r_t)}{(1 + r_t^*)}. \quad (2.1)$$

### 2.1.2 Uncovered Interest Rate Parity

Uncovered interest rate parity condition states that it should be impossible, on average, to earn excess risk-free returns with unhedged FX positions. More precisely, buying foreign currency at a spot rate ( $S_0$ ), investing the money into foreign currency risk-free assets with a rate of ( $r_t^*$ ), and buying domestic currency after a period of ( $t$ ) at an estimated spot rate of ( $E(S_t)$ ), should lead into the same result as investing the money initially into domestic risk-free assets with a rate of ( $r_t$ ),

$$(1 + r_t^*) \cdot \frac{E(S_t)}{S_0} - 1 = (1 + r_t) - 1 \Leftrightarrow E(S_t) = \frac{S_0(1 + r_t)}{(1 + r_t^*)} = F_t. \quad (2.2)$$

### 2.1.3 Empirical Relevance

Since trading strategy (2.1) is risk-free, competitive markets always force CIP to hold so that arbitrage possibilities become extinct. Empirical research confirms CIP to hold well in developed markets, whereas in developing markets factors such as regulatory interference and the illiquidity of fixed income market may cause CIP not to hold (Chinn 2007, pp. 1-9). From the option pricing viewpoint, CIP can be utilized in the formulation of the option pricing problem, as discussed later in this thesis.

In contrast to CIP, trading strategy (2.2) is not risk-free, as  $(E(S_t))$  is only an estimate of the future FX spot rate. As a result, UIP does not necessarily hold even in competitive markets. In fact, numerous studies have tested UIP with a regression analysis and discovered that it systematically fails (Froot 1990, pp. 179-192). However, UIP does not have a similar relevance for option pricing purposes than CIP does, as UIP cannot be used as an arbitrage argument. As a result, this thesis does not analyze the “UIP anomaly” further, despite its importance for speculative purposes.

## 2.2 Stochastic Modeling

There are numerous stochastic models for describing the behavior of FX rates. Nevertheless, an exact formulation of the FX rate behavior still remains unsolved. Furthermore, none of the proposed models has proven universally superior to the others, but different models have proven optimal for different purposes.

The data generating process of the underlying FX rate has two important implications on option pricing. First, it affects the option price, as different processes model the uncertainty in different ways. Second, it affects the implementation of the option pricing model. If the data generating process has a known terminal probability distribution, one can price options in a closed form by utilizing the known properties of the terminal

probability distribution. Controversially, if the terminal probability distribution is unknown, more elaborate analytical or numerical methods are needed.

The rest of this Chapter reviews the most important stochastic models used for the FX rates. The review includes both models that have been used in the past, based on which the present models are build, and models that are used for practical applications at the time of writing this thesis. At the same time, the review includes models that focus on the terminal probability distribution and models that focus on the data generating process. The models are not mutually exclusive, but it is rather common to see a combination of several models used in practice. Furthermore, some models focus solely on volatility, and are not comprehensive for the option pricing purposes without a complementary spot process.

The models included are: standard Brownian motion, arithmetic Brownian motion, geometric Brownian motion, stable distributions, jump-diffusion (JD), autoregressive conditional heteroscedasticity (ARCH), generalized autoregressive conditional heteroscedasticity (GARCH), stochastic volatility (SV), stochastic volatility – jump (SVJ), two-factor stochastic volatility – jump (SVJ-2F), and stochastic volatility – double jump (SVDJ).

### 2.2.1 Standard Brownian Motion

Standard Brownian motion is also known as Wiener process. It was first discovered by botanist Robert Brown in 1827, as he was observing pollen particles movement in water. The first mathematical definition of the standard Brownian motion was presented by Thorvald Thiele in 1880. Thereafter, it has been one of the most widely used models for a random walk. (Nelson 1967, pp. 1-120)

One-dimensional standard Brownian motion is defined as the limiting ( $n \rightarrow \infty$ ) process, where a finite time interval  $[0, t]$  is divided into  $(n)$  subintervals, and the process state  $(S_t)$  increment for each subinterval is either  $(+\sqrt{t/n})$  or  $(-\sqrt{t/n})$  with equal

probabilities. The standard Brownian motion fulfils the Markov and martingale properties, meaning that the process is path independent and has no drift. The standard Brownian motion, in isolation, is an insufficient model for the FX rates. However, it is an essential building block in more complex models. (Hull 2005, pp. 263-280)

### 2.2.2 Arithmetic Brownian Motion

The stochastic analysis of financial assets started in 1900, when French doctoral student Louis Bachelier published his thesis *Théorie de la Spéculation* (Theory of Speculation). In his thesis, Bachelier propose that speculative market prices follow the arithmetic Brownian motion, generating normally distributed terminal probability distributions (Bachelier 1900, pp. 21-86. cited in Courtault et al. 2000, pp. 341-353). Compared to the standard Brownian motion, the arithmetic Brownian motion allows the process to have a continuous drift.

The arithmetic Brownian motion used by Bachelier is defined by stochastic differential equation (SDE)

$$dS_t = \mu dt + \sigma dW_t, \tag{2.3}$$

where the spot asset price ( $S_t$ ) depends on an instantaneous drift ( $\mu$ ), volatility ( $\sigma$ ), and a standard Wiener process ( $W_t$ ), ( $dt$ ) denoting a time differential. Using an arbitrary initial process state ( $S_0$ ), SDE (2.3) has an analytical solution

$$S_t = S_0 + \mu t + \sigma W_t. \tag{2.4}$$

Even though Bachelier's thesis was a trail-blazing piece of research, the arithmetic Brownian motion has proven inadequate for financial asset price modeling. This is also the case with the foreign exchange rates, as all the recent studies regarding their distributional properties have concluded the FX returns to be far too leptokurtic to satisfy normality (Tucker & Pond 1988, pp. 638-647).

### 2.2.3 Geometric Brownian Motion

Black and Scholes (1973, pp. 637-654) introduced their famous option pricing formula in 1973. Instead of using the arithmetic Brownian motion generating normally distributed returns, Black and Scholes assume the underlying spot price to follow the geometric Brownian motion generating log-normally distributed returns. Compared to the arithmetic Brownian motion, the geometric Brownian motion evolves in proportion to its current state, allowing the process to have only positive values.

The geometric Brownian motion used by Black and Scholes is defined by stochastic differential equation

$$dS_t = \mu S_t dt + \sigma S_t dW_t = S_t (\mu dt + \sigma dW_t), \quad (2.5)$$

where the spot price ( $S_t$ ) depends on itself, constant drift ( $\mu$ ), volatility ( $\sigma$ ), and a standard Wiener process ( $W_t$ ), ( $dt$ ) denoting a time differential. Using an arbitrary initial process state ( $S_0$ ), SDE (2.5) has an analytical solution

$$S_t = S_0 \exp\left(\sigma W_t - \frac{1}{2}\sigma^2 t + \mu t\right). \quad (2.6)$$

Even though superior to the arithmetic Brownian motion, the geometric Brownian motion does not capture the stochastic behavior of most financial assets satisfactorily either. From the time series perspective, several studies have noted that the historical returns of most financial assets, FX among them, are not log-normally distributed (Harrison 1998, pp. 55-79; Jorion 1988, pp. 427-445; Andersen et al. 2001, pp. 42-55). From the implied option price perspective, the option market would use the one and same implied volatility for all the options on one underlying, if the log-normality assumption was correct. However, it is commonly known that the implied volatilities of most financial assets vary depending on the option moneyness and the time to expiry. (Canina & Figlewski 1993, pp. 659-681)

#### 2.2.4 Stable Distributions

Since it was widely accepted that the FX returns do not satisfy log-normality, researchers needed to provide alternative explanations for them and the implied option prices. In the late 1970's and early 1980's, most foreign exchange rate studies focused on stable distributions. For example, Calderon-Rossell and Ben-Horim (1982, pp. 99-111) suggest to use Student's  $t$  distribution, whereas McFarland et al. (1982, pp. 693-715) suggest to use symmetric stable Paretian distributions with specific characteristic exponents.

Nevertheless, most studies pursuing to find stable distributions came to the conclusion that, if a stable distribution was used, its parameters could not be kept constant over time. As an example, McFarland et al. (1982, pp. 693-715) suggest to use different characteristics exponents for each weekday, because in their opinion, the nature of the US dollar FX market is different on each weekday. However, the lack of any remarkable research regarding the stable distributions since the 1980's indirectly indicates that they are not the optimal way to model the behavior of the FX rates.

#### 2.2.5 ARCH and GARCH

Until the early 1980s, financial asset returns were assumed to have constant volatilities. Autoregressive Conditional Heteroscedasticity (ARCH) model, introduced by Engle (1982, pp. 987-1008) in 1982, arose from an observation that the volatility changes from one period to another, and that the periods of higher or lower volatility have a tendency to cluster. As a result, Engle propose that the past random error terms can be utilized in forecasting the future volatility of the process.

The simplest ARCH family model is ARCH(p). The basic principle of ARCH(p) is to capture the random error term serial correlation of the asset price volatility. This is done by using AR(p) type of time series model, where (p) refers to the number of autoregressive lags. For example, let us assume that the asset price follows the

arithmetic random walk, where the present asset price ( $S_t$ ) equals the sum of the previous asset price ( $S_{t-1}$ ) and a random error term ( $\varepsilon_t$ ):

$$S_t = S_{t-1} + \varepsilon_t, \text{ where } \varepsilon \sim N(0, \sigma_t^2). \quad (2.7)$$

ARCH(p) assumes that the variance of the error term ( $\varepsilon_t$ ) is a linear combination of new volatility information ( $\omega$ ) and (p) previous error terms ( $\varepsilon_{t-1}, \varepsilon_{t-2}, \dots, \varepsilon_{t-p}$ ) with weights ( $\alpha_0, \alpha_1, \dots, \alpha_p$ ):

$$\sigma_t^2 = \omega + \alpha_0 \varepsilon_t^2 + \alpha_1 \varepsilon_{t-1}^2 + \dots + \alpha_p \varepsilon_{t-p}^2, \text{ where } \omega, \alpha_0, \alpha_1, \dots, \alpha_p \geq 0. \quad (2.8)$$

In the Engle's initial proposition, the weights are estimated using the least squares method.

Only four years after the introduction of ARCH, Bollerslev (1986, pp. 307-327) presented the Generalized Autoregressive Conditional Heteroscedasticity (GARCH) model in 1986. The basic principle of GARCH(p,q) is to capture the volatility random error term serial correlation and the volatility moving average properties. This is done by using ARMA(p,q) type of time series model, where (p) refers to the number of autoregressive lags and (q) to the number of moving average lags.

For example, let us assume that the asset price follows the arithmetic random walk, where the present asset price ( $S_t$ ) equals the sum of the previous asset price ( $S_{t-1}$ ) and a random error term ( $\varepsilon_t$ ):

$$S_t = S_{t-1} + \varepsilon_t, \text{ where } \varepsilon \sim N(0, \sigma_t^2). \quad (2.9)$$

GARCH(p,q) assumes that the volatility of the price process ( $\sigma_t^2$ ) is a linear combination of new volatility information ( $\omega$ ), (p) previous error terms ( $\varepsilon_{t-1}, \varepsilon_{t-2}, \dots, \varepsilon_{t-p}$ ) with weights

$(\alpha_0, \alpha_1, \dots, \alpha_p)$ , and  $(q)$  previous volatility terms  $(\sigma^2_{t-1}, \sigma^2_{t-2}, \dots, \sigma^2_{t-q})$  with weights  $(\beta_1, \beta_2, \dots, \beta_q)$ :

$$\sigma_t^2 = \omega + \alpha_0 \varepsilon_t^2 + \alpha_1 \varepsilon_{t-1}^2 + \dots + \alpha_p \varepsilon_{t-p}^2 + \beta_1 \sigma_{t-1}^2 + \beta_2 \sigma_{t-2}^2 + \dots + \beta_q \sigma_{t-q}^2. \quad (2.10)$$

In Bollerslev's initial proposition, the weights of historical data decline exponentially without ever going to zero.

Since the Bollerslev's initial proposition, numerous GARCH models have been introduced. As an example, the asymmetric GARCH assumes market decreases to have a greater impact on the volatility than same size market increases. Multivariate models in turn, use also exogenous variables, such as the volatilities of other financial assets, to forecast the volatility of a certain asset. (Engle 2001, pp. 157-168)

The prediction power of ARCH and GARCH has been subject to several studies, but the results are not unanimous. For example, Jorion (1995, pp. 507-528) conclude that the GARCH volatility estimates for several major trading currencies are outperformed by the Black-Scholes implied volatilities. On the other hand, Bali (2000, pp. 191-215) conclude that the GARCH models in general, and nonlinear GARCH models in particular, predict the one-week volatility of U.S. government bonds well. Andersen and Bollerslev (1998, pp. 885-905) in turn, add that the explanatory power of the GARCH models can be significantly improved by the use of high-frequency intraday data. All in all, most studies finding GARCH useful addressed asymmetric, multivariate, or high-frequency models, whereas the predicting power of simpler models was only considered superior to naive time series methods. (Poon & Granger 2003, pp. 478-539).

To be precise, ARCH and GARCH do not characterize the whole asset price process, but merely predict the future volatility of it. As a consequence, several studies (Poon & Granger 2003, pp. 478-539; Nelson 1992, pp. 61-90) emphasize that it makes little sense to use ARCH and GARCH as the data generating process of an option pricing model,

because they are designed for producing variance estimates based on the historical data. Furthermore, ARCH and GARCH can only be calibrated against the historical returns, making them less attractive from the industry practitioner's perspective.

### 2.2.6 Jump-Diffusion

Whereas the most late 1970's and early 1980's FX rate studies focused on stable distributions, some pioneering equity studies focused on the data generating process instead. Among the early pioneers, Merton (1976, pp. 125-144) suggested that the total fluctuation of a stock price could be divided into normal and abnormal components, where the normal component represents stock price's continuous daily fluctuation and the abnormal component unexpected shocks that sometimes occur in the market.

The JD process of Merton is defined by stochastic differential equation

$$dS_t = S_t [(\mu - \lambda \varepsilon)dt + \sigma dW_t + J_t N_t], \text{ where} \quad (2.11)$$

$$N_t \sim \text{Poisson}(\lambda t),$$

$$J_t = 1, \text{ if } N_t = 0,$$

$$J_t = \prod_{j=1}^{N_t} J_j, \text{ if } N_t \geq 1.$$

The diffusion component is modeled as a geometric Brownian motion, similarly to SDE (2.5). The jump component is modeled as a Poisson process ( $N_t$ ), where the jumps arrive with an intensity of ( $\lambda$ ), random variable ( $J_j$ ) determining the size of an individual jump and ( $\varepsilon$ ) the average jump size. Successive drawings  $\{J_j\}$  are assumed to be non-negative and i.i.d. Non-zero jump intensity ( $\lambda$ ) causes the jump component to be "activated" and a non-zero average jump size ( $\varepsilon$ ) requires a martingale compensation term ( $\lambda \varepsilon$ ) to be added into the spot process. Using an arbitrary initial process state ( $S_0$ ), SDE (2.11) has an analytical solution

$$S_t = S_0 \exp\left(\sigma W_t + \left(\mu - \frac{1}{2}\sigma^2 - \lambda\varepsilon\right)t\right) J_t. \quad (2.12)$$

The usefulness of the jump process has been subject to several studies. On equity side, Ball and Torous (1983, pp. 53-65) analyzed 47 New York Stock Exchange listed stocks, and conclude that most of them had discontinuous price shocks unexplainable by the diffusion process. On FX side, Akgiray and Booth (1988, pp.631-637) report that the US dollar had discontinuous shocks against the West German mark, the British pound, and the French franc. Furthermore, Jorion (1988, pp. 427-445) conclude that the historical returns from both FX and equity markets contain systematic discontinuities.

In 1988, Tucker and Pond (1988, pp. 638-647) compared four candidate processes for explaining the historical returns of the US dollar against six major trading currencies. The tested processes were scaled- $t$  distribution, general stable distribution, compound normal distributions, and jump-diffusion. After a series of statistical analysis and pair wise comparisons, Tucker and Pond conclude that JD had the best explanatory power for all the currencies studied.

In 1999, Das and Sundaram (1999, pp. 211-239) analyzed the capability of JD model to match both the historical returns and the implied option prices of S&P500 equity index. In terms of historical returns, Das and Sundaram observed JD to produce reasonable skewness and kurtosis for the short expiries, but the effect to vanish too rapidly as a function of time. The results were similar with implied volatility as well, as JD was discovered to match the short expiries well, but the implied volatility smile to flatten too rapidly as a function of the time to expiry. Furthermore, Das and Sundaram report JD to be only able to create monotonously increasing volatility term structures, which is not in line with the observed market behavior.

In 2003, Bollen and Rasiel (2003, pp. 33-64) tested the capability of the Black-Scholes, regime-switching, GARCH, and jump-diffusion models to fit the implied US dollar –

British pound and US dollar - Japanese yen option prices. They conclude that JD had the tightest fit, both in-sample and out-of-sample. They also conclude that JD provides the least profit and loss volatility when using the model for hedging purposes.

Even though some studies indicate jump-diffusion not to explain the historical returns and the implied option prices to a sufficient degree, all the studies reviewed for this thesis conclude FX rates to jump. On the other hand, several pieces of literature (Bates 1996, pp. 69-107; Honoré 1998, pp. 1-36) report it to be difficult to distinguish jumps from the historical time series, as jump intensities tend to be low. It is also hard to distinguish the value of jump fears from the implied option prices, as the jump-risk premium is unobservable (Bates 1996, pp. 69-107). Lately though, there have been some attempts to distinguish the jumps more efficiently from both the historical time series (Aït-Sahalia 2004, pp. 487-528) and the implied option prices (Pan 2002, pp. 3-50).

### 2.2.7 Stochastic Volatility

Similarly to ARCH, the stochastic volatility (SV) model does not assume constant volatility. However, whereas ARCH and GARCH predict the future volatility based on past information, SV seeks to model the dynamics of the volatility process. The first SV model was introduced by Hull and White (1987, pp. 281-300) in 1987, and the topic has been frequently studied ever since.

The SV process of Hull and White is defined by stochastic differential equations

$$dS_t = \mu(S_t, \sigma, t)dt + \sigma S_t W_{S_t}, \quad (2.13)$$

$$dV_t = \phi(\sigma, t)V_t dt + \xi(\sigma, t)dW_{V_t}, \quad (2.14)$$

where (2.13) defines the spot process and (2.14) the volatility process. As illustrated in them, the spot price ( $S_t$ ) depends on an instantaneous drift ( $\mu$ ), volatility ( $\sigma$ ), and the spot price itself. The instantaneous drift ( $\mu$ ) is further allowed to depend on time ( $t$ ), spot price ( $S_t$ ), and volatility ( $\sigma$ ). Volatility ( $\sigma$ ) in turn, evolves as the square root of the state

process ( $V_t$ ), the behavior of which is determined by the drift ( $\phi$ ) and volatility ( $\xi$ ) components, which are both allowed to depend on volatility ( $\sigma$ ) and time ( $t$ ). In addition, the SDEs of Hull-White SV process contain a time differential ( $dt$ ) and two Wiener processes ( $W_{St}$ ) and ( $W_{Vt}$ ), which Hull and White assume to be uncorrelated for the model purposes, still recognizing the possibility of them being correlated in reality.

By modeling the volatility as a stochastic variable, Hull-White SV process is able to generate excess kurtosis, observed in the returns of most financial assets. However, due to the assumption of Wiener processes ( $W_{St}$ ) and ( $W_{Vt}$ ) being uncorrelated, the process is not able to generate excess skewness, which is also observed in the market. As a solution, Heston (1993, pp. 327-343) presented an alternative SV process in 1993, which allows a non-zero correlation between the spot price and the volatility processes.

The SV process of Heston is defined by stochastic differential equations

$$dS_t = \mu S_t dt + \sqrt{V_t} S_t W_{St}, \quad (2.15)$$

$$dV_t = \kappa(\theta - V_t)dt + \xi \sqrt{V_t} W_{Vt}, \quad (2.16)$$

where (2.15) defines the spot process and (2.16) the volatility process. As illustrated in them, the spot price ( $S_t$ ) depends on an instantaneous drift ( $\mu$ ), volatility ( $V_t$ ), and the spot price itself. Volatility in turn, evolves as a mean reverting Ornstein-Uhlenbeck process, as proposed by Stein and Stein (1991, pp. 727-752). The behavior of the volatility depends on mean a reversion rate ( $\kappa$ ), mean reversion level ( $\theta$ ), volatility itself ( $V_t$ ), and the volatility of volatility ( $\xi$ ). In addition, the SDEs of the Heston SV process contain a time differential ( $dt$ ), and two standard Wiener processes ( $W_{Vt}$ ) and ( $W_{St}$ ), allowed to have an arbitrary correlation ( $\rho$ ).

If the assumptions of Hull, White, and Heston are relaxed, a generic SV process can be defined as by Alizadeh et al. (2002, pp. 1047-1091). The generic SV process is defined by stochastic differential equations

$$dS_t = \mu(S_t, V_t)dt + \sigma(S_t, V_t)dW_{S_t}, \quad (2.17)$$

$$dV_t = \varphi(S_t, V_t)dt + \xi(S_t, V_t)dW_{V_t}, \quad (2.18)$$

where (2.17) defines the spot process and (2.18) the volatility process. As illustrated in them, the spot price ( $S_t$ ) depends on an instantaneous drift ( $\mu$ ) and the volatility of the spot process ( $\sigma$ ), which are both allowed to depend on the spot price ( $S_t$ ) and the volatility ( $V_t$ ). Volatility in turn, depends on the drift ( $\varphi$ ) and the volatility ( $\xi$ ) of the volatility process, which in turn, are both allowed to depend on the spot price ( $S_t$ ) and the volatility ( $V_t$ ). In addition, the SDEs of the generic SV process contain time a differential ( $dt$ ), and two standard Wiener processes ( $W_{S_t}$ ) and ( $W_{V_t}$ ), allowed to have a state-dependent arbitrary correlation  $dW_{S_t}dW_{V_t} = \theta(S_t, V_t)dt$ .

In fact, all the stochastic volatility processes can be derived from the generic SV process by selecting functional forms for  $\mu(S_t, V_t)$ ,  $\sigma(S_t, V_t)$ ,  $\varphi(S_t, V_t)$ , and  $\xi(S_t, V_t)$ . As a result, there exists no single SV process, but rather a family of processes having the in common feature of modeling the volatility as a stochastic process.

The performance testing of SV models has proven challenging due to several reasons. First, the SV models are not homogenous, so most findings only apply for certain types of SV models. Second, an unsuccessful model calibration might cause a model to perform badly in tests, even if its dynamics were correct. Nevertheless, there still exists a wide range of literature analyzing the performance of the SV models, but partly due to the challenges above, ending up to various conclusions.

Among the first papers, Heynen and Kat (1994, pp. 50-65) compare SV and GARCH volatility estimates for seven equity indices and five FX rates in 1994. They conclude SV to provide better forecasts, but on the other hand, also ten times larger forecast errors. Hol and Koopman (2000, pp. 1-27) in turn, compare SV equity index volatility forecasts to the implied volatility, and discover the implied volatility to perform better. Poon and Granger (2003, pp. 478-539) in turn, compare different models pair wise by

reviewing the result of 66 earlier studies. They discover three studies concluding SV superior to simple time series methods and three concluding SV superior to GARCH. On the other hand, one paper concluded GARCH and one paper implied volatility superior to SV.

Das and Sundaram (1999, pp. 211-239) conducted a more thorough analysis of the general properties of the SV model, not only the volatility prediction power, in 1999. From the historical returns perspective, Das and Sundaram conclude SV to generate sufficient levels of short term skewness and kurtosis, but the skewness and kurtosis to dissipate too slowly as a function of time. From an implied option price perspective, they discover SV to be in line with the observed term structure of at-the-money volatilities, but on the other hand, not to generate a deep enough short term volatility smile. Furthermore, the flattening of the smile as function of time to expiry was discovered to be too slow. Nevertheless, Das and Sundaram still conclude SV to provide a high degree of flexibility in explaining the observed market behavior, even though not being able to capture the behavior to a full degree.

The benefits of SV model are obvious, even though some studies conclude the volatility prediction power of SV inferior to the implied volatility and GARCH, and some studies SV to be incapable of fully fitting the implied option prices. However, the literature still undisputedly verifies the volatility to be time-dependent, and SV to explain several phenomena observed in the market. Furthermore, the large number of published studies and the extensive use of SV models among the industry practitioners strongly favor its usefulness.

### 2.2.8 Stochastic Volatility – Jump

Numerous studies indicate that both the jump-diffusion and the stochastic volatility processes outperform the geometric Brownian motion in explaining both the historical returns and the implied option prices. However, the literature also conclude JD to provide a good short expiry fit, while having problems in the longer expiries, whereas

SV has just the opposite problem. As a solution, Bates (1996, pp. 69-107) introduced the nested stochastic volatility – jump (SVJ) process in 1996.

The SVJ process of Bates is defined by stochastic differential equations

$$dS_t = S_t \left[ (\mu - \lambda \varepsilon) dt + \sqrt{V_t} W_{S_t} + J_t dN_t \right], \quad (2.19)$$

$$dV_t = (\theta - \kappa V_t) dt + \xi \sqrt{V_t} W_{V_t}, \quad (2.20)$$

$$dN_t \sim \text{Poisson}(\lambda t), \text{ where} \quad (2.21)$$

$$\ln(1 + J_t) \sim N \left( \ln(1 + \varepsilon) - \frac{1}{2} \delta^2, \delta^2 \right),$$

where (2.19) defines the spot process, (2.20) the volatility process, and (2.21) the jump process. As illustrated in them, the spot price ( $S_t$ ) depends on itself, instantaneous drift ( $\mu$ ), martingale compensation term ( $\lambda \varepsilon$ ), volatility ( $V_t$ ), Poisson distributed jump intensity ( $\lambda$ ), and log-normal distributed jump size ( $J_t$ ). The jump size further depends on the average jump size ( $\varepsilon$ ) and jump size standard deviation ( $\delta$ ). Volatility ( $V_t$ ) in turn, evolves as a mean reverting Ornstein-Uhlenbeck process, which depends on a mean reversion level ( $\theta$ ), mean reversion rate ( $\kappa$ ), volatility itself ( $V_t$ ), and the volatility of volatility ( $\xi$ ). In addition, the SDEs of the Bates SVJ process contain a time differential ( $dt$ ) and two standard Wiener processes ( $W_{V_t}$ ) and ( $W_{S_t}$ ) with an arbitrary correlation ( $\rho$ ).

In 1997, Bakshi et al. (1997, pp. 2003-2049) extended the Bates SVJ process by allowing the interest rate to be stochastic (SVJ-SI). However, they conclude the stochastic interest rate to have only a small impact on the long expiry option prices and practically no impact on the short expiry option prices. As a result, this thesis considers SVJ-SI as a special case of SVJ, instead of treating it as a separate process.

In terms of the model performance, both Bates and Bakshi et al. conclude SVJ to clearly outperform JD and SV in explaining both the historical returns and the implied option prices, but on the other hand, the parameter estimates based on the historical returns and

the implied option prices not to be in line. Calibrating the model parameters against the historical returns, Bates discovers his model to produce lower option prices than the ones traded in the market. Calibrating the model parameters against the implied option prices instead, Bakshi et al. obtain parameter values implausible from the historical returns perspective.

To reduce the mismatch, Pan (2002, pp. 3-50.) introduces a risk premium for the volatility and jump risks. He concludes it to diminish the mismatch, but the model to be still unable to explain the whole implied volatility surface with constant parameters. As a further extension, Galluccio and Le Cam (2005, pp. 1-40) conclude SVJ to match the whole implied volatility surface, if piecewise constant model parameters are used.

As a result, SVJ is a potential data generating process for an exotic option pricing model, as it can match the whole implied volatility surface, provided that piecewise constant model parameters are used. Furthermore, the extensive use of SVJ among the industry practitioners strongly favors its usefulness.

### 2.2.9 Two-Factor Stochastic Volatility – Jump

To address the parameter instability problem of SVJ in another way, Bates (2000, pp. 69-107) introduced a two-factor SVJ (SVJ-2F) process in 2000.

The SVJ-2F process of Bates is defined by stochastic differential equations

$$dS_t = S_t \left[ (\mu - \lambda \varepsilon) dt + \sqrt{V_{1t}} W_{S1t} + \sqrt{V_{2t}} W_{S2t} + J_t dN_t \right], \quad (2.22)$$

$$dV_{it} = (\theta_i - \kappa_i V_{it}) dt + \xi_i \sqrt{V_{it}} W_{Vit}, \quad (i = 1, 2), \quad (2.23)$$

$$dN_t \sim \text{Poisson}(\lambda t), \text{ where} \quad (2.24)$$

$$\ln(1 + J_t) \sim N \left( \ln(1 + \varepsilon) - \frac{1}{2} \delta^2, \delta^2 \right),$$

where (2.22) defines the spot process, (2.23) the two identical volatility processes, and (2.24) the jump process. As illustrated in the SDEs, the spot price ( $S_t$ ) follows a similar process than in one-factor SVJ, except that it depends on two identical mean reverting volatility processes instead of one. The volatility processes as such, are identical to the one of one-factor SVJ. All the variables are also denoted similarly to the one-factor SVJ.

Bates tested the capability of the SVJ-2F to fit the implied option prices of S&P500 equity index options. He concludes SVJ-2F to outperform SVJ, but on the other hand, SVJ-2F to still have a pricing error larger than the market bid-offer spread. In addition, Bates tests the consistency of the market implied parameters against the ones estimated from the historical returns, and discovers them not to be in line.

Unfortunately, no other studies testing the SVJ-2F model could be found for this thesis. As a result, the added value of the second SV factor is questionable. On one hand, Bates himself reports the SVJ-2F to outperform the SVJ, but on the other, more degrees of freedom naturally improve the fit, without guaranteeing the process to be more correct per se. Furthermore, one can consider the lack of further research to be an indirect piece of evidence against the usefulness of the SVJ-2F. As a result, the SVJ-2F is not considered to be a potential data generating process for the option pricing model of this thesis.

#### 2.2.10 Stochastic Volatility – Double Jump

Also motivated by the problems of the one-factor SVJ, Duffie et al. (2000, pp. 1343-1376) introduced the stochastic volatility – double jump (SVDJ) process in 2000. In SVDJ, both the spot price and the volatility processes incorporate discontinuous jumps. As another extension to the Bates SVJ, the process uses the logarithm of spot price ( $X_t$ ) instead of the spot price ( $S_t$ ) itself, enabling the process to be defined as a two-dimensional affine state-space model.

The SVDJ model of Duffie et al. is defined by stochastic differential equation

$$d \begin{pmatrix} X_t \\ V_t \end{pmatrix} = \begin{pmatrix} \mu - \lambda\varepsilon - \frac{1}{2}V_t \\ \kappa(\theta - V_t) \end{pmatrix} dt + \sqrt{V_t} \begin{pmatrix} 1 & 0 \\ \rho\xi & \sqrt{1-\rho^2}\xi \end{pmatrix} dW_t + dZ_t, \quad (2.25)$$

where the logarithm of the spot price ( $X_t$ ) depends on an instantaneous drift ( $\mu$ ), martingale compensation term ( $\lambda\varepsilon$ ), volatility ( $V_t$ ), and the first dimension of a two-dimensional jump process ( $Z_t$ ). Volatility ( $V_t$ ) in turn, depends on a mean reversion rate ( $\kappa$ ), mean reversion level ( $\theta$ ), volatility itself ( $V_t$ ), the volatility of volatility ( $\xi$ ), and the second dimension of the two-dimensional jump process ( $Z_t$ ). In addition, the SDE contains a time differential ( $dt$ ) and a two-dimensional standard Wiener process ( $W_t$ ) with an arbitrary correlation ( $\rho$ ) between its dimensions.

SVDJ has drawn a lot of attention since its introduction. In 2003, Eraker et al. (2003, pp. 1269-1300) extended the work of Duffie et al. by comparing two special cases of SVDJ: one where jump arrivals in the spot price and volatility processes are independent (SVIDJ) and another where the arrivals are correlated (SVCDJ). In 2004, Eraker (2004, pp. 1367-1404) extended the process further by allowing the volatility mean reversion rate ( $\kappa$ ) to depend on the volatility ( $V_t$ ), the process being referred as the stochastic volatility – state-dependent correlated double jump (SVSCDJ).

In terms of model performance, Duffie et al. (2000, pp. 1343-1376), Eraker et al. (2003, pp. 1269-1300), and Eraker (2004, pp. 1367-1404) all conclude the different SVDJ variants to outperform the SVJ in fitting both the historical returns and the implied option prices. Nevertheless, Eraker (2004, pp. 1367-1404) still concludes the process parameters to be unstable over time, and the pricing error to be larger than the market bid-offer spread. As a result, similarly to SVJ, also SVDJ requires a non-zero volatility and jump risk premiums to align the historical returns and the implied option prices, and non-constant model parameters to fit all the implied option prices simultaneously.

As a result, the SVDJ is a potential data generating process for an exotic option pricing model, provided that piecewise constant model parameters are used. However, the parameter instability problem requires the model to be recalibrated whenever the market implied option prices move. As a result, one is faced with a trade-off between the increased market fit and the increased difficulty of implementation and calibration, when choosing between the SVJ and SVDJ.

### 3 Approaches to Option Pricing

Options have been used for hundreds, perhaps even for thousands of years. As an example, the “tulipmania” swept across Holland in the 17<sup>th</sup> century causing tulip producers, brokers, and retailers to make future and option type of agreements with each others (Garber 1989, pp. 535-560). Some pieces of literature even suggest that option type of agreements were used already in the Ancient Greece circa 600 years before the Common Era (Malkiel & Quandt 1969, p. 8). Exchange-based option trading dates back to 1973, when Chicago Board Options Exchange launched the trading of listed options. Thereafter, the number of exchanges, underlying, and option styles has increased tremendously. Nowadays, a huge number of both vanilla and exotic options are traded both in the exchanges and in the over-the-counter (OTC) market. (Cox & Rubinstein 1985, pp. vii-ix; Bank for International Settlements 2007, pp. 1-26)

The foundation of modern option pricing was also laid in 1973, when Black and Scholes (1973, pp. 637-654) introduced their famous option pricing model. In those days, the limited computing capacity compelled the researchers to focus on analytical models, as the practical applications of the non-analytical ones were few. In the recent decades instead, the exploded computing capacity has brought more interest to alternative methods, such as Monte Carlo (MC) simulation. Compared to the analytical methods, they allow more exotic payout structures and more complex underlying dynamics to be modeled, enabling the efficient pricing of exotic options. (Hull 2005, pp. 181-550; Scholes 1998, pp. 350-370)

This Chapter begins with the derivation of the Black-Scholes model. It is commonly considered as the fundamental theory of modern option pricing, even if Samuelson (1965, pp. 13-31), Merton (Samuelson & Merton 1969, pp. 17-46), and Chen (1970, pp. 1041-1059), among many others, had already studied the theory of option and warrant

pricing before the introduction of the Black-Scholes. After the Black-Scholes, this Chapter reviews the most well-known analytical option pricing models. At the end, this Chapter describes the Monte Carlo approach to option pricing.

### 3.1 Black-Scholes Model

Black and Scholes (1973, pp. 637-654) created the basis for modern option pricing by publishing *The Pricing of Options and Corporate Liabilities* in 1973. Based on the standard arbitrage arguments, Black and Scholes assume that a risk-free portfolio consisting of long and short option and stock positions should have a yield equal to the risk-free interest rate. As a result, Black and Scholes deduct that if it is possible to hedge an option position by dynamically rebalancing a stock position, the price of a European call option ( $C$ ) should only depend on the underlying spot price ( $S$ ) and the time to option expiry ( $T$ ). In order to be able to form such a hedge position, Black and Scholes assume the so called ideal market conditions, listed below, to hold:

- Short-term risk-free interest rate ( $r$ ) is known and constant.
- Stock price ( $S_t$ ) follows the geometric Brownian motion with known and constant drift ( $\mu$ ) and volatility ( $\sigma$ ).
- Stock pays no dividends.
- Option can be exercised only at the final valuation time.
- No transaction costs exist.
- Trading takes place continuously in time.
- Money can be borrowed and lent at the same risk-free interest rate.
- Short selling is allowed.

If the ideal market conditions hold, an option position can be perfectly hedged using the so called delta-hedging. The delta-hedging is based on a principle that the option delta ( $C_1(S,t)$ ), the first partial derivative of option price with respect to the underlying price, determines how many shares of stock offset the change in the option value, when the underlying price is subject to an incremental change ( $\Delta S$ ). As a result, a long stock position is hedged by the number of sold call options equal to the inverse of delta:

$$S - \frac{C}{C_1(S, t)}. \quad (3.1)$$

The change in the value of such position in a short time interval ( $\Delta t$ ) can be written

$$\Delta S - \frac{\Delta C}{C_1(S, t)}. \quad (3.2)$$

On the other hand, the value of the option is assumed to only depend on the underlying spot price ( $S$ ) and the time to option expiry ( $T$ ). As a result, the change in the option value ( $\Delta C$ ) can be written

$$\Delta C = C(S + \Delta S, t + \Delta t) - C(S, t). \quad (3.3)$$

By using stochastic calculus and by denoting the volatility of the underlying stock with ( $\sigma$ ), (3.3) can be expanded into form

$$\Delta C = C_1 \Delta S + \frac{1}{2} C_{11} \sigma^2 S \Delta t + C_2 \Delta t. \quad (3.4)$$

Furthermore, substituting ( $\Delta C$ ) in (3.2) with (3.4), gives

$$\frac{-\left(\frac{1}{2} C_{11} \sigma^2 S^2 + C_2\right) \Delta t}{C_1}. \quad (3.5)$$

Because it was assumed to be impossible to gain excess risk-free returns, the perfectly hedged position (3.1) should provide the same yield as the risk-free interest rate ( $r$ ). Thus, (3.5) should be equal to the yield of risk-free interest rate ( $r\Delta t$ ). That in turn, requires the option price to satisfy partial differential equation

$$C_2 = rC - rSC_1 - \frac{1}{2}\sigma^2 S^2 C_{11}. \quad (3.6)$$

By denoting the option exercise price with (K), (3.6) must satisfy boundary conditions

$$\begin{aligned} C(S, t^*) &= S - K & , S \geq K, \\ C(S, t^*) &= 0 & , S < K, \end{aligned} \quad (3.7)$$

at the time of the option expiry ( $t^*$ ).

By making an appropriate substitution to (3.6), one observes it to be equal to a heat-transfer equation in physics, the solution of which is presented in the mathematical literature (Churchill 1963, p. 155). As a result, Black and Scholes succeeded in defining a closed form solution for the price of a European call option, subject to the ideal market conditions. By denoting the cumulative normal density function with ( $N(\cdot)$ ), Black-Scholes equation can be written in the familiar form:

$$C(S, t) = SN(d_1) - Ke^{-rt} N(d_2), \text{ where} \quad (3.8)$$

$$d_1 = \frac{\ln(S/K) + \left(r + \frac{1}{2}\sigma^2\right)T}{\sigma\sqrt{T}},$$

$$d_2 = d_1 - \sigma\sqrt{T}.$$

Even though the Black-Scholes model revolutionized the theory of option pricing, it was soon discovered to have several shortcomings. Among the first critics, Merton (1973, pp. 141-183) reassessed the ideal market conditions assumed by the model. Merton concludes that the model could be easily adjusted for non-constant interest rate, dividend paying stocks, and early exercisable options. On the other hand, Merton concludes that the assumptions of log-normally distributed returns and continuous trading are critical for the model. Without them, the delta-hedging would not give a perfect hedge, making

the arbitrage argument invalid. As known from the previous Chapter, the returns of most financial assets do not unfortunately satisfy log-normality.

## 3.2 Analytical Models

Black-Scholes too is an analytical model. However, as this thesis considers it as the starting point for the study, this part of the Chapter reviews the most important closed form and semi-closed form models introduced after the Black-Scholes. The models included are Biger-Hull, local volatility adjusted Biger-Hull, Merton jump-diffusion, Hull-White stochastic volatility, Heston stochastic volatility, Heston-Nandi GARCH, Bates stochastic volatility – jump, and Duffie-Pan-Singleton stochastic volatility – double jump.

### 3.2.1 Biger-Hull

Even though Black and Scholes published their model already in 1973, it took ten more years before the first FX option pricing models were introduced. The late arrival of the FX models is largely explained by the fact that FX options were not traded in any exchange until 1982, when Philadelphia Stock Exchange took them into its lists (Philadelphia Stock Exchange 2004, pp. 1-26). Once the silent period ended, there were three independent FX option pricing papers published nearly simultaneously in 1983.

The first of three papers was published by Biger and Hull (1983, pp. 24-28) in spring 1983. It considers the problem of pricing an option on FX analogous to the one of pricing an option on a stock paying continuous dividend; a problem to which Merton (1973, pp. 141-183) proposed a solution in 1973. In Merton's solution, the price of a European call option is defined similarly to BS, except that the drift of underlying is adjusted with a continuous dividend yield ( $q_c$ ):

$$C(S, t) = e^{-q_c T} SN(d_1) - e^{-rT} KN(d_2), \text{ where} \quad (3.9)$$

$$d_1 = \frac{\ln(S/K) + \left(r + q_c + \frac{1}{2}\sigma^2\right)T}{\sigma\sqrt{T}},$$

$$d_2 = d_1 - \sigma\sqrt{T}.$$

In Biger and Hull's approach, the risk-free interest rate of foreign currency ( $r^*$ ) has the same impact on the FX option price as the continuous dividend yield ( $q_c$ ) on the stock option price. More precisely, by assuming the CIP to hold and the underlying FX rate to follow the geometric Brownian motion, the logarithmic difference between the forward (F) and spot (S) FX rates can be explained by the spread between the domestic ( $r$ ) and foreign ( $r^*$ ) risk-free interest rates:

$$\ln(F/S) = (r - r^*)T. \quad (3.10)$$

By replacing the continuous dividend yield ( $q_c$ ) in (3.9) with the foreign interest rate ( $r^*$ ), and by using (3.10), Biger and Hull write the price of the European FX call option (C) in the form

$$C(S, t) = e^{-rT} FN(d_1) - e^{-r^*T} KN(d_2), \text{ where} \quad (3.11)$$

$$d_1 = \frac{\ln(F/K) + \frac{1}{2}\sigma^2T}{\sigma\sqrt{T}},$$

$$d_2 = d_1 - \sigma\sqrt{T},$$

where ( $r$ ) denotes the domestic risk-free interest rate, (T) time to option expiry, (F) forward FX rate, (K) option exercise price, and ( $\sigma$ ) the volatility of the underlying FX rate.

Shortly after the introduction of the Biger-Hull, two other FX option pricing models were introduced on December 1983. Similarly to the Biger-Hull, also the models by

Garman and Kohlhagen (1983, pp. 231-237) and Grabbe (1983, pp. 239-254) are based on the idea of combining the Black-Scholes and the CIP. As a result, both end up to the same pricing formula than Biger and Hull.

The main contribution of the Biger-Hull, Garman-Kohlhagen, and Grabbe models is to combine the Black-Scholes model with the interest rate parity theory. However, the models do not fulfill the objectives of this thesis, as they assume the FX spot rate to follow the geometric Brownian motion, and thus ignore the higher moments of the FX return distributions.

### 3.2.2 Local Volatility Adjusted Biger-Hull

As discussed in the previous Chapter, the market implied option prices reject the log-normality assumption of FX returns. This is proved by the fact that the market implied Black-Scholes volatilities calculated from the traded option prices typically give different implied volatilities for different moneyness and time to expiry tenors. As a result, pricing FX options with the constant volatility Biger-Hull model, would lead a market maker to open arbitrage possibilities for the other market participants.

A naive solution to the problem above is to use the Biger-Hull model, but to use different volatilities for different moneyness and expiry tenors. This approach, referred as the local volatility concept, was officially introduced by Derman and Kani (1994, pp. 1-20) as a part of their implied volatility tree model in 1994. In practice though, the method has been used since the introduction of the Black-Scholes model.

As long as one only considers vanilla options, the local volatility concept offers a non-elegant but yet working solution for dealing with the non-constant implied volatility. In the case of exotic options instead, the problem becomes that the local volatility adjusted Biger-Hull still fails to capture the higher moments of the FX return distributions. As a result, one would need separate local volatility surfaces for each exotic option style, as the implied volatilities calculated from the vanilla option prices do not necessarily give the correct exotic option prices. However, the fact that exotic options are only traded

over-the-counter, means that there are no public price records available. That in turn, makes the local volatility concept useless in practical exotic option pricing applications.

### 3.2.3 Merton Jump-Diffusion

The first remarkable extension to the Black-Scholes was proposed by Merton (1976, pp. 125-144) in 1976, as he introduced the jump-diffusion model (Merton JD). The model rises from an observation that the historical returns of most stocks contain far too many outliers to satisfy log-normality. As a result, Merton suggests modeling the underlying price as a nested jump-diffusion process, defined by SDE (2.11).

However, the existence of jumps invalidates the “local Markov property”, which allows the spot price to have only small changes in a short time interval. As a consequence, the BS model’s basic principle of perfectly hedging a long stock position by a short option position becomes invalid, as the discrete shocks in the underlying price make an efficient delta-hedging impossible at the time of a shock.

As a result, Merton does not find a way to price European options in a closed form. However, by assuming the jumps to only represent non-systematic market risk, Merton proves that the price of a European call option must satisfy

$$C(S, t) = \sum_{n=0}^{\infty} \frac{e^{-\lambda T} (\lambda T)^n}{n!} \{E_n [C_{BS}(S J_n e^{-\lambda \epsilon T}, T, K, \sigma^2, r)]\}, \quad (3.12)$$

the solution of which can be approximated with a reasonable computational effort if the density function of the jump size  $\{J_n\}$  is not too complex. In the equation,  $(\lambda)$  denotes Poisson jump intensity,  $(n)$  the number of jumps,  $(E_n[\cdot])$  expectation operator over  $\{J_n\}$ ,  $(\epsilon)$  the average jump size, and  $C_{BS}(S, T, K, \sigma^2, r)$  the Black-Scholes formula, defined in (3.8).

Even though the Merton JD model was a major extension to the Black-Scholes, it still lacks many features that an exotic FX option pricing model should have. Most severely, Merton JD does not take the stochastic nature of the volatility into account, as the jumps are produced by a Poisson process having no memory. As a result, the model fails to produce enough kurtosis for long expiries, as discussed in the previous Chapter. That in turn, makes it impossible to calibrate the model against the long expiry implied option prices, meaning that the model does not fulfill the objectives of this thesis.

### 3.2.4 Hull-White Stochastic Volatility

Similarly to Merton, also Hull and White (1987, pp. 281-300) considers the geometric Brownian motion to be a too simplified data generating process for the most option underlying. However, whereas Merton keeps the underlying volatility constant and adds jumps to the spot price process, Hull and White allows the volatility to be stochastic, as defined in SDEs (2.13) and (2.14).

Despite the attractiveness of the data generating process, Hull and White's approach turns out to be challenging from the option pricing perspective. In order to use the standard arbitrage arguments, one should have a perfect hedge for the option. That is not a problem under the ideal market conditions, as an option then incorporates only delta risk, which can be hedged by buying or selling the underlying. However, an option on asset with a stochastic volatility also incorporates vega risk, defined as the option's price sensitivity to the volatility of underlying. As a result, creating a perfect hedge would require the volatility to be either a traded asset, or perfectly correlated with some other traded asset. As that is rarely the case in reality, Hull and White are not able to find a closed form solution for the price of a European call option.

However, by assuming the spot price and volatility to be uncorrelated, the volatility process to have no drift ( $\varphi = 0$ ), and the volatility of volatility ( $\xi$ ) to be constant, Hull and White define the price of a European call option in a Taylor series form:

$$\begin{aligned}
 C(S, t, \sigma) = & C_{BS}(S, t) + \frac{1}{2} \frac{\sqrt{T} N'(d_1)(d_1 d_2 - 1)}{4\sigma^3} \cdot \left[ \frac{2\sigma^4 (e^k - k - 1)}{k^2} - \sigma^4 \right] + \\
 & + \frac{1}{6} \frac{S \sqrt{T} N'(d_1) [(d_1 d_2 - 3)(d_1 d_2 - 1) - (d_1^2 d_2^2)]}{8\sigma^5} \\
 & \cdot \sigma^6 \left[ \frac{e^{3k} - (9 + 18k)e^k + (8 + 24k + 18k^2 + 6k^3)}{3k^3} \right] + \dots,
 \end{aligned} \tag{3.13}$$

where  $C_{BS}(S, t)$ ,  $(d_1)$ , and  $(d_2)$  refer to the Black-Scholes formula (3.8). Further on,  $(T)$  denotes the time to option expiry,  $(N(\cdot))$  cumulative normal density function,  $(\sigma)$  the volatility of underlying, and  $(k)$  a short hand notation for  $(\xi^2 T)$ . With a reasonably short time to expiry  $(T)$  and low volatility of volatility  $(\xi)$ , Hull and White conclude the series to convergence rapidly.

Nevertheless, the assumptions required for the series form solution are remarkably strong, as Hull and White point out themselves as well. Most critically, the assumption of zero correlation between the spot price and volatility allows the model to generate only symmetric volatility smiles, which is clearly against the observed market behavior. As a result, the model does not fulfill the objectives of this thesis.

### 3.2.5 Heston Stochastic Volatility

Similarly to the Hull-White model, Heston SV model from 1993 (Heston 1993, pp. 327-343) assumes the volatility to be stochastic. However, whereas Hull-White SV assumes the spot price and volatility to be uncorrelated, Heston SV allows an arbitrary correlation between them, enabling the process to generate both excess kurtosis and skewness. Even more importantly, Heston introduces a method for pricing European options in a semi-closed form by utilizing the characteristic functions of the data generating process.

More precisely, by assuming the underlying spot price and volatility to follow processes defined in SDEs (2.15) and (2.16), Heston uses Ito's lemma and standard arbitrage arguments to obtain Garman's partial differential equation

$$\begin{aligned} & \frac{1}{2}VS^2 \frac{\partial^2 C}{\partial S^2} + \rho\xi VS \frac{\partial^2 C}{\partial S \partial V} + \frac{1}{2}\xi^2 V \frac{\partial^2 C}{\partial V^2} + \mu S \frac{\partial C}{\partial S} \\ & + [\kappa(\theta - V) - \Gamma_V] \frac{\partial C}{\partial V} - \mu C + \frac{\partial C}{\partial t} = 0, \end{aligned} \quad (3.14)$$

which the solution of the call option price (C) is required to fulfill. The variables of (3.14) are denoted similarly to SDEs (2.15) and (2.16), in addition to which ( $\Gamma_V$ ) denotes the market price of the volatility risk.

In the spirit of the Black-Scholes, Heston assumes the solution to have a form

$$C(S, v, t) = S_t P_1 - e^{-rT} K P_2, \quad (3.15)$$

where ( $S_t$ ) denotes the spot asset price, ( $K$ ) option exercise price, ( $r$ ) risk-free interest rate, ( $T$ ) time to option expiry, ( $P_1$ ) option delta, and ( $P_2$ ) the conditional probability for the option to expire in-the-money.

Substituting (C) in (3.14) with (3.15) then gives

$$\begin{aligned} & \frac{1}{2}V \frac{\partial^2 P_j}{\partial X^2} + \rho\xi V \frac{\partial^2 P_j}{\partial X \partial V} + \frac{1}{2}\xi^2 V \frac{\partial^2 P_j}{\partial V^2} + (\mu + u_j \xi) \frac{\partial P_j}{\partial X} \\ & + (a - b_j \xi) \frac{\partial P_j}{\partial V} + \frac{\partial P_j}{\partial t} = 0, \text{ where for } j = 1, 2 \end{aligned} \quad (3.16)$$

$$X = \ln(S), \quad u_1 = \frac{1}{2}, \quad u_2 = -\frac{1}{2}, \quad a = \kappa\theta, \quad b_1 = \kappa + \Gamma_V - \rho\xi, \quad b_2 = \kappa + \Gamma_V,$$

which both ( $P_1$ ) and ( $P_2$ ) must satisfy.

(P<sub>1</sub>) and (P<sub>2</sub>) in turn, can be obtained by inverting the corresponding characteristic functions (Ψ<sub>1</sub>) and (Ψ<sub>2</sub>) via Fourier transformation

$$P_j(X, V, T; \ln(K)) = \frac{1}{2} + \frac{1}{\pi} \int_0^{\infty} \operatorname{Re} \left[ \frac{e^{-i\Phi \ln(K)} \Psi_j(X, V, T; \Phi)}{i\Phi} \right] d\Phi, \quad (3.17)$$

where (X) denotes the natural logarithm of the spot asset price, (V) the state of the volatility process, (T) time to option expiry, (K) option exercise price, (i) imaginary unit, and (Φ) integration variable.

Furthermore, by assuming the characteristic functions (Ψ<sub>1</sub>) and (Ψ<sub>2</sub>) to have a form

$$\Psi_j(X, V, T; \Phi) = \exp(C(T; \Phi) + D(T; \Phi)V + i\Phi X), \quad (3.18)$$

Heston concludes that (Ψ<sub>1</sub>) and (Ψ<sub>2</sub>) can be obtained by solving Riccati equations

$$C(T; \Phi) = r\Phi T + \frac{\kappa\theta}{\xi^2} \left[ (b_j - \rho\xi\Phi i + d)T - 2 \ln \left( \frac{1 - ge^{dT}}{1 - g} \right) \right], \quad (3.19)$$

$$D(T; \Phi) = \frac{b_j - \rho\xi\Phi i + d}{\xi^2} \left( \frac{1 - e^{dT}}{1 - ge^{dT}} \right), \text{ where for } j = 1, 2 \quad (3.20)$$

$$g = \frac{b_j - \rho\xi\Phi i + d}{b_j - \rho\xi\Phi i - d},$$

$$d = \sqrt{(\rho\xi\Phi i - b_j)^2 - \xi^2(2u_j\Phi i - \Phi^2)},$$

$$b_1 = \kappa + \Gamma_V - \rho\xi,$$

$$b_2 = \kappa + \Gamma_V.$$

The value of the European call option is then obtained by replacing (Ψ<sub>1</sub>) and (Ψ<sub>2</sub>) in (3.17) with (3.18), and (P<sub>1</sub>) and (P<sub>2</sub>) in (3.15) with (3.17).

Despite its elegance, the Heston's formulation of the characteristic functions turned out to be problematic. The problem arises from the fact that the complex valued integral in (3.17) is non-singular, due to the complex logarithm in (3.18) having a branch cut along the negative real axis. The problem has been documented by several studies (Kahl & Jäckel 2005, pp. 94-103; Albrecher et al. 2007, pp. 83-92), and it can be overcome by either using the so called rotation count algorithm (Lord & Kahl, 2006, pp. 1-31), or writing the characteristic functions in another way, described for example by Lipton (2002, pp. 61-65).

Despite the problematic numerical implementation, multiple studies (Das & Sundaram 1999, pp. 211-239; Mikhailov & Nögel 2003, pp. 74-79) conclude that Heston SV provides a good fit against the implied option prices. Nevertheless, the model is still reported not to generate steep enough volatility smiles for short expiries, without setting the model parameters to implausible levels. Furthermore, the whole implied volatility surface cannot be typically fit with constant model parameters, but an acceptable fit requires the model parameters to be piecewise constant, as proposed by Schlögl and Schlögl (2000, pp. 183-209). Even then, the model is often not able to generate steep enough volatility smiles for short expiries (Mikhailov & Nögel 2003, pp. 74-79), causing it not to fulfill the objectives of this thesis.

### 3.2.6 Heston-Nandi GARCH

Heston and Nandi (2000, pp. 585-625) presented an alternative semi-closed form option pricing model (Heston-Nandi GARCH) in 2000. The model assumes the volatility of the underlying to follow a discrete-time GARCH(p,q) process. Similarly to Heston SV, Heston-Nandi GARCH takes the stochastic nature of the volatility and the correlation between the spot asset price and the volatility into account. In contrast to Heston SV instead, the model can only be calibrated against the historical asset returns, but not against the implied option prices. As a result, the model does not fulfill the objectives of this thesis, and further analysis is therefore omitted.

### 3.2.7 Bates Stochastic Volatility – Jump

Bates (1996, pp. 69-107) combined the jump and the stochastic volatility elements in 1996, and introduced the first stochastic volatility -jump model (Bates SVJ). It enables the excess kurtosis and skewness to arise either due to stochastic volatility, jumps, or a combination of both, allowing richer model dynamics than JD or SV as independent models. The dynamics of the spot asset price and the volatility processes of the Bates SVJ are defined by SDEs (2.19), (2.20), and (2.21).

In order to price European call options in a semi-closed form, Bates adopts the Heston's characteristic functions technique. As a consequence, the Bates SVJ price of a European call option is also given by (3.15), where  $(P_1)$  and  $(P_2)$  are likewise obtained similarly to Heston SV, by inverting the characteristic functions  $(\Psi_1)$  and  $(\Psi_2)$  via Fourier transformation

$$\begin{aligned}
 P_j(\Phi | S_0, T) &= \text{prob}(S_T > K | \Psi_j) & (3.21) \\
 &= \frac{1}{2} + \frac{1}{2\pi} \int_{-\infty}^{\infty} \frac{\Psi_j(i\Phi) e^{-i\Phi X}}{i\Phi} d\Phi \\
 &= \frac{1}{2} + \frac{1}{\pi} \int_0^{\infty} \frac{\text{Im}[\Psi_j(i\Phi) e^{-i\Phi X}]}{\Phi} d\Phi, \text{ where for } j = 1, 2
 \end{aligned}$$

$$X \equiv \ln(K / S_0),$$

where  $(S_t)$  denotes the spot asset price,  $(T)$  time to option expiry,  $(K)$  option strike,  $(i)$  imaginary unit, and  $(\Phi)$  integration variable.

Different from the Heston SV instead, the more complex data generating process causes the characteristic functions of Bates SVJ,

$$\Psi_j(\Phi | V_t, T) = \exp\{ C_j(T; \Phi) + D_j(T; \Phi)V_t + \lambda T(1 + \varepsilon)^{\mu_j + 1/2} \cdot [(1 + \varepsilon)^\Phi \exp(\delta^2(\mu_j \Phi + \Phi^2 / 2)) - 1] \}, \quad (3.22)$$

to take a more complex form than the ones of Heston SV. The same applies for the Riccati equations

$$C_j(T, \Phi) = (b - \lambda \varepsilon)\Phi T - \frac{\theta T}{\xi^2} (\rho \xi \Phi - \beta_j - \gamma_j) - \frac{2\theta}{\xi^2} \ln \left( 1 + \frac{1}{2} (\rho \xi \Phi - \beta_j - \gamma_j) \frac{1 - e^{\gamma_j T}}{\gamma_j} \right), \quad (3.23)$$

$$D_j(T; \Phi) = -2 \frac{\mu_j \Phi + \frac{1}{2} \Phi^2}{\rho \xi \Phi - \beta_j + \gamma_j \frac{1 + e^{\gamma_j T}}{1 - e^{\gamma_j T}}}, \text{ where for } j = 1, 2 \quad (3.24)$$

$$\gamma_j = \sqrt{(\rho \xi \Phi - \beta_j)^2 - 2\xi^2 \left( \mu_j \Phi + \frac{1}{2} \Phi^2 \right)},$$

$$\mu_1 = +\frac{1}{2}, \quad \mu_2 = -\frac{1}{2}, \quad \beta_1 = \kappa - \rho \xi, \quad \text{and} \quad \beta_2 = \kappa.$$

Not surprisingly, the Bates SVJ provides a better fit against the implied option prices than the Heston SV. In particular, the incorporation of jumps improves the short expiry fit. In addition, the long expiry fit is also improved, as the calibration of the SV parameters is no longer “contaminated” by the short expiry kurtosis. It is also worth pointing out that the form of the characteristic functions used by Bates has the same non-singularity problem as the Heston SV does. Fortunately, the problem can also be solved similarly, by either writing the characteristic functions in a different form, or using the rotation count algorithm.

Despite the improved fit compared to the Merton JD and Heston SV, multiple studies still report Bates SVJ not to fit the whole implied volatility surface simultaneously,

without allowing the model parameters to be piecewise constant (Galluccio & Le Cam 2005, pp. 1-40). As a result, the Bates SVJ can potentially fulfill the objectives of this thesis, provided that piecewise constant model parameters are used.

### 3.2.8 Duffie-Pan-Singleton Stochastic Volatility – Double Jump

Duffie, Pan, and Singleton (2000, pp. 1343-1376) extended the approach of Heston and Bates even further in 2000, by introducing the stochastic volatility – double jump model (DPS SVDJ). The model can be extended from the Bates SVJ by allowing also the volatility process to incorporate discrete jumps, as illustrated in SDE (2.25), defining the state transform dynamics of the DPS SVDJ model.

The pricing of European options in the DPS SVDJ is conducted similarly to Heston SV and Bates SVJ, by inverting the characteristic functions of the data generating process via Fourier transformation. Due to length and complexity, the characteristic functions and their Fourier transformations are not presented in this thesis, but the full derivation can be found in the original source.

Compared to the Bates SVJ, the DPS SVDJ provides a better fit to both the historical returns and the implied option prices due to the increased degrees of freedom. The improved fit is documented for example, by Eraker et al. (2003, pp. 1269-1300), who tests the fit of the different versions of SV, SVJ, and SVDJ models against the historical returns and the implied option prices.

On the other hand, Galluccio and Le Cam (2005, pp. 1-40), conclude that the complexity of the DPS SVDJ model's data generating process makes the efficient calibration of the model against the implied option prices extremely difficult, if not impossible. Unfortunately, no piece of research presents a robust calibration method for the DPS SVDJ model by the time of writing this thesis. As a result, the suitability of the DPS SVDJ for the purposes of this thesis is twofold. On one hand, the theoretical performance of the model is superior to the others' reviewed in this Chapter, but on the other, the suitability of the model for practical applications has not been validated.

### 3.3 Monte Carlo Simulation

The credit for inventing the Monte Carlo method (MC) is often given to Metropolis and Ulam (1949, pp. 335-341), who published *The Monte Carlo method* in 1949, even though W. S. Gossett, using a well-known pen name “Student” (1908a, pp. 1-25.; 1908b, pp. 302-310), studied a similar method already 40 years earlier. Whatever the truth, the method has been used for various statistical and probability modeling problems since the 1950s, and for option pricing purposes since 1977, when Boyle (1977, pp. 323-338) introduced the first Monte Carlo option pricing model.

The largest advantage of the Monte Carlo is its flexibility, as it makes the modeling of the data generating process and the pricing of options technically independent, whereas in the analytical methods they are strictly dependent on each others. As a result, the Monte Carlo enables the pricing of exotic options without analytical solutions, even if the data generating process was complex. On the other hand, the largest disadvantage of the Monte Carlo is its extensive computational burden, which is caused by the slow convergence rate, necessitating a large number of simulation replications to obtain an accurate output. (Boyle et al. 1997, pp. 1267-1321; Haug 1998, pp. 139-142)

This part of the Chapter first reviews the definitions and interdependencies of computing time, variance, and bias; commonly considered as the determinants of an efficient Monte Carlo model. Subsequently, this part of the Chapter discusses the sampling from the data generating process, which is an essential part of Monte Carlo option pricing model, especially if the data generating process is complex.

#### 3.3.1 Efficiency

Literature (Glasserman 2003, pp. 1-38) determines three requirements for an efficient Monte Carlo model. The model should have a short computing time, low variance, and low bias. The computing time refers to the calculation time of simulation, variance to the variation of simulation outputs, and bias to a possible difference between the real value of studied random event, and the value to which the Monte Carlo simulation converges.

Computing time and variance are related to each others through convergence rate, and are generally negatively dependent. As a result, variance can be reduced by increasing the computing time, and vice versa. In addition, variance can be reduced by variance reduction techniques, which are commonly based on either adjusting the simulation outputs by utilizing the tractable features of the model, or reducing the variance of the simulation inputs. The most well-known variance reduction techniques are antithetic variates, control variates, moment matching methods, stratified sampling, hypercube sampling, and importance sampling. (Glasserman 2003, pp. 185-276; Boyle et al. 1997, pp. 1267-1321)

Unlike variance, bias cannot necessarily be eliminated at the cost of the computing time. In option pricing applications, bias can typically arise from three sources. First, a model discretization error may occur when continuous time dynamics are modeled in a discrete time. Second, a payoff discretization error may occur when the option payout depends on an infinite set of underlying fixing values, whereas MC can only handle a finite number of them. Third, the non-linear functions of mean may exist in conjunction with conditional probabilities, which in practice is related to exercisable options, such as American and Bermudan ones. Bias caused by the model discretization or payoff discretization errors can be usually eliminated by increasing the number of simulation time steps, whereas a bias caused by the non-linear functions of mean cannot. However, as the exercisable options are not a part of the research scope, this thesis omits further analysis regarding the problem.

### 3.3.2 Sampling from the Data Generating Process

In order to price options with Monte Carlo, one needs to generate random trajectories from the data generating process. In an ideal situation, one has an explicit sampling scheme, meaning that one is able to draw non-biased trajectories from the data generating process with an arbitrary time step length. Of the processes reviewed for this thesis, standard Brownian motion, arithmetic Brownian motion, geometric Brownian motion, and jump-diffusion have explicit sampling schemes. As an example, the explicit sampling scheme of the geometric Brownian motion is given by (2.6).

Unfortunately, there are no explicit sampling schemes for the SV, SVJ, and SVDJ processes, as their terminal probability distributions are unknown. Nevertheless, one is still able to sample from them, by using approximated sampling schemes. Unfortunately, the approximated schemes often cause discretization bias, necessitating a short time step length to keep the discretization bias in an acceptable level. On the other hand, the time step length cannot be reduced infinitely, as the computational burden would at some point make the scheme useless for practical applications. As a result, an efficient sampling scheme is vital for the Heston SV, Bates SVJ, and DPS SVDJ model MC applications.

In fact, the Heston SV, Bates SVJ, and DPS SVDJ models are close to each others in terms of the data generating process sampling, as they only differ by the number of Poisson jump processes without a memory. As a result, both the Bates SVJ and DPS SVDJ schemes can be easily derived from the Heston SV ones. Thus, this Chapter only discusses the simulation of the Heston SV process, reminding the reader to keep in mind that the results are valid for the Bates SVJ and DPS SVDJ processes as well.

Given the popularity of the Heston SV, there are surprisingly few studies regarding its sampling. In fact, the first bias-free sampling scheme for the Heston SV process was not proposed until 2003, when Broadie and Kaya (2006, pp. 217-231) published the first draft of their exact simulation scheme. Even though the scheme provides a bias-free simulation method, its computational inefficiency restricts it from being used in the practical applications. Instead, the scheme has merely been used as a benchmark for others, computationally more efficient schemes.

Some studies, such as the one by Eraker et al. (2003, pp. 1269-1300), suggest that a simple Euler discretization scheme would provide a sufficient accuracy for the Heston SV. However, the obvious problem with the Euler discretization is that, while the continuous time mean reverting square root volatility process is guaranteed to be non-negative, its Euler discretization is not. As a result, one needs to equip the scheme with a fix for the negative volatility problem.

To find an optimal fix, Lord et al. (2006, pp. 1-32) compared five simple fixes in 2006. The ones included were absorption, reflection (Berkaoui et al. 2006, pp. 1-18), Higham and Mao (Higham & Mao 2005, pp. 35-62), partial truncation (Deelstra & Delbaen 1998, pp. 77-84), and full truncation. Lord et al. conclude their full truncation scheme to be the best out of five, in addition to which, they also conclude it to outperform the more complex IJK-IMM scheme by Kahl and Jäckel (2006, pp. 513-536).

However, a recent study by Andersen (2007, pp. 1-38) claims that the majority of the earlier studies have used “too easy” model parameter values in their tests. More precisely, Andersen states that most studies have used too high mean reversion level ( $\theta$ ), too high mean reversion rate ( $\kappa$ ), too low volatility of volatility ( $\xi$ ), and too low correlation ( $\rho$ ) values compared to the ones typically obtained if calibrating the model against the implied option prices. As a result, Andersen concludes the simple Euler discretization not to provide a satisfactory accuracy, despite whatever “quick fix” for the negative volatility problem is used. Andersen also concludes the IJK-IMM not to provide a satisfactory accuracy either. Instead, Andersen states that one must use a more sophisticated sampling scheme, such as the Quadratic Exponential (QE) scheme proposed in his paper. As a result, the literature fails to give a unanimous answer to the question of how to sample the SV, SVJ and SVDJ processes in an optimal manner.

## 4 Model Calibration

Even the finest option pricing model has no practical applications, unless it can be calibrated against the market. As a result, literature provides a vast array of calibration methods, which can be roughly divided into two schools of thought. The first takes a time series approach, pursuing to make the model output consistent with the historical returns. The second takes an implied option price approach, pursuing to make the model output consistent with the implied option prices. It has been acknowledged since the introduction of the Black-Scholes that the historical returns and the implied option price based model parameter estimates differ from each others, but the issue has drawn surprisingly little attention until the recent years.

Traditionally, the academics have mostly focused on the historical returns, perhaps due to the more robust theoretical framework. The industry practitioners instead, have mostly focused on the implied volatility, due to the necessity of matching the market implied option prices in order to close arbitrage. In recent years though, several studies have tried to fill in the gap by, for example, introducing the volatility and jump risk premiums. (Pan 2002, pp. 3-50; Eraker 2004, pp. 1367-1404)

In this thesis, both the traditional historical returns methods and the recent methods trying to fill in the gap between the two schools of thought are described under the historical returns methods. Implied option price methods in turn, only cover the methods focusing purely on the implied option prices. This Chapter first discusses the historical returns methods and then the implied option price methods.

## 4.1 Historical Returns Methods

The basic idea of the historical returns methods is to optimize the model parameters to explain the historical asset returns. The historical returns methods can be further divided into four categories, namely: generalized method of moments (GMM), quasi-maximum likelihood (QML) methods, approximated maximum likelihood (AML) methods, and Markov-chain Monte Carlo (MCMC) methods. Of these, GMM is merely a stand-alone technique, whereas all the other three are maximum likelihood techniques.

### 4.1.1 Generalized Method of Moments

Generalized method of moments (GMM) was derived from the method of moments (MM) by Hansen (1982, pp. 1029-1054). The basic principle of the GMM is to define a set of moment conditions, which the sampled model posterior distribution is calibrated to match. The conditions are not actually required to be moments at all, but a rich selection of conditions can be used. In fact, the optimal moment conditions depend on the problem itself, so the selection of right moment conditions is highly essential in GMM.

The largest advantage of GMM is its suitability for a wide range of calibration problems, as the moments of an unknown distribution are typically easier to generate than the whole likelihood function. On the other hand, the selection of wrong moment conditions may ignore some essential information, causing GMM to produce highly biased estimates. In reference literature, GMM is used for the SV (Melino & Turnbull 1990, pp. 239-265) and SVJ-SI (Pan 2002, pp. 3-50) models.

### 4.1.2 Quasi-Maximum Likelihood Methods

The basic principle of the quasi-maximum likelihood (QML) methods is to treat non-Gaussian asset returns as if they were Gaussian. By doing so and by accepting the presence of an estimation error, standard Gaussian maximum likelihood techniques can be applied with an unknown accuracy. In practice though, the requirement of nearly

Gaussian returns would require the distribution of returns to be characterizable by only two moments, which is not the case with the most practical problems.

The largest advantage of QML is the ease of computation and implementation. On the other hand, the accuracy of the method may severely suffer, if the returns are non-Gaussian, which is often the case with complex models. In addition, the estimation of the model error is typically difficult, or impossible. In fact, the QML was more frequently used in the past decades, when it was applied for both JD (Ball & Torous 1983, pp. 53-65) and SV (Harvey et al. 1994, pp. 247-264) models. However, also some recent studies use the QML for the SV (Alizadeh et al. 2002, pp. 1047-1091) and JD (Aït-Sahalia 2004, pp. 487-528) models.

#### 4.1.3 Approximated Maximum Likelihood Methods

Unlike the QML, the approximated maximum likelihood (AML) methods do not assume the returns to be Gaussian. Instead, the AML approximates the unknown likelihood function in order to apply a modified likelihood measure to non-Gaussian time series. Typically used approximation techniques include numerical integration, Monte Carlo integration, and various sampling techniques.

The largest advantage of the AML is its flexibility, but on the other hand, the estimation of the method error is difficult. Furthermore, the AML methods are designed for specific purposes, so their convertibility for other types of calibration problems is generally poor. In reference literature, the AML is used for the SV (Fridman & Harris 1998, pp. 284-291; Aït-Sahalia & Kimmel 2007, pp. 413-452), JD (Honoré 1998, pp. 1-36), two-factor SV (Durham 2006, pp. 273-305), and SVDJ (Johannes et al. pp. 1-52) models.

#### 4.1.4 Markov-Chain Monte Carlo Methods

Similarly to the AML, the Markov-chain Monte Carlo (MCMC) methods do not try to solve the exact maximum likelihood function. Instead, the MCMC estimates the model parameters ( $\Theta$ ) and the state variables ( $X$ ) conditional on the observed prices ( $C$ ) by

generating draws from a recursively estimated a priori distribution  $p(\Theta, X|C)$ . The recursive estimation of  $p(\Theta, X|C)$  is conducted by utilizing the modular structure of the underlying data generating process, Clifford-Hammersley theorem stating that  $p(X|\Theta, C)$  and  $p(\Theta|X, C)$  completely characterize their joint distribution  $p(\Theta, X|C)$ , and the fact that it is typically easier to draw samples from  $p(X|\Theta, C)$  and  $p(\Theta|X, C)$  than directly from  $p(\Theta, X|C)$ . As the number of simulation runs increases, the draws from the a priori distribution form a Markov-chain converging to the target distribution, while simultaneously giving the optimal calibration. (Eraker 2001, pp. 177-191)

The largest advantage of the MCMC is its flexibility and computational efficiency. On the other hand, the accuracy of MCMC is difficult to measure. Despite that, the MCMC has become one of the dominating historical returns calibration methods, especially among the models having complex data generating processes. In reference literature, the MCMC is used for the SV (Jacquier et al. 1994, pp. 371-389; Shephard & Pitt 1997, pp. 653-667; Eraker 2001, pp. 177-191), JD (Johannes & Polson 2006, pp. 1-95), SVJ (Johannes & Polson 2006, pp. 1-95), and SVDJ (Eraker et al. 2003, pp. 1269-1300; Eraker 2004, pp. 1367-1404) models.

## 4.2 Implied Option Price Methods

The basic idea of the implied option price methods is to optimize model parameters to explain the implied option prices. The implied option price methods can be further divided into two categories. The first uses the historical time series of option prices and calibrates the model parameters by minimizing the sum of pricing errors over time. The second calibrates the model parameters by matching the model implied volatility surface to the market implied one at a given point in time. This part of the Chapter first describes the option price time series methods and then the implied volatility surface methods.

#### 4.2.1 Option Price Time Series Methods

The basic principle of the option price time series methods is to minimize the cumulative pricing error over time, which is usually done by minimizing either the absolute or the relative sum of the squared errors (SSE). As a result, the method is only suitable for stationary models, in which the parameters are constant over time. That in turn, prevents a misspecified model from fitting all the option prices simultaneously, explaining the limited interest of the industry practitioners.

The largest advantage of the method is its simplicity and robustness. However, the method suffers severely from the curse of dimensionality, as minimizing the SSE over a large range of historical data requires an extensive amount of computational capacity, especially if the number of free parameters is large. In reference literature, Bollen and Rasiel (2003, pp. 33-64) use the method for the JD model, Bates (1996, pp. 69-107) for the SVJ model, and Bakshi et al. (1997, pp. 2003-2049) for the SVJ-SI model.

#### 4.2.2 Implied Volatility Surface Methods

In contrast to the option price time series methods, the implied volatility surface methods focus on fitting all the implied option prices simultaneously at one point in time. That is typically done by minimizing either the absolute or the squared sum of pricing errors across the whole implied volatility surface, using either equal or unequal weights for the different moneyness and expiry tenors.

The largest advantage of the method is its market consistency, which explains its popularity among the industry practitioners. On the other hand, the method is challenging to apply for models with complex data generating processes, as the calibration of them is often an ill-posed non-linear optimization problem, which requires elaborate numerical techniques to be used. In reference literature, Cont and Tankov (2004, pp. 1-43) use the method for the JD model, Galluccio and Le Cam (2005, pp. 1-40) for the SVJ model, and Duffie et al. (2000, pp. 1343-1376) for the SVDJ model.

## 5 Option Pricing Model

As the theoretical part of the thesis illustrated, literature provides numerous alternatives for the stochastic modeling of FX rates. The potential data generating processes vary from very simple ones, such as the geometric Brownian motion, to very complex ones, such as the stochastic volatility – double jump. Nevertheless, none of the processes was concluded to perfectly explain the observed FX rate behavior, even though a positive correlation between the process complexity and the market fit seemed to exist. This leaves us with the problem mentioned earlier – finding an optimal trade-off between the model fit and the ease of implementation and calibration.

As this thesis seeks to fulfill the industry practitioners business needs, the model must both match the market implied option prices and be possible to implement in practice, as stated in the research objectives. As the theoretical part of the thesis concluded, all the geometric Brownian motion based models, JD model, and SV model do not fulfill the first requirement, as they fail to capture the higher moments of the FX return distributions. The SVDJ family models instead, provide a sound theoretical framework for the FX rate modeling, but the difficulty of calibration makes them impossible to implement in practice, given the resource constraints of this thesis.

As a result, this thesis models the behavior of the FX rates as an extended stochastic volatility – jump process, where the model parameters are allowed to be piecewise constant along the lines of Schlögl and Schlögl (2000, pp. 183-209). According to Galluccio and Le Cam (2005, pp. 1-40), the given data generating process provides the richest possible model dynamics, while still keeping the model efficient to calibrate.

Related to the efficiency of calibration, this thesis provides both semi-closed form and Monte Carlo solutions for the price of a European call option. Even though developing

the semi-closed form solution for the European options was not a direct objective of the thesis, the large number of model parameters requires it to be developed, in order to efficiently calibrate the model against the implied option prices, as concluded by the previous studies (Bakshi et al. 1997, pp. 2003-2049; Galluccio & Le Cam 2005, pp. 1-40).

The efficient calibration in turn, creates the basis for pricing exotic options with Monte Carlo simulation. However, the efficient calibration does not yet guarantee the Monte Carlo model to work adequately, but a successful implementation also requires a sampling scheme of good quality, and a thorough numerical implementation, as concluded by the previous studies (Broadie & Kaya 2006, pp. 217-231; Andersen 2007, pp.1-38).

This Chapter begins with the mathematical definition of the data generating process of the model, both in continuous and discrete times. Subsequently, it describes how the model is used for option pricing, by giving exact semi-closed form and Monte Carlo solutions for European options, and by describing how to extend the Monte Carlo solution for exotic options. At the end, the Chapter presents a calibration method for the model, and describes the details of the model implementation.

### 5.1 Data Generating Process

As already stated, the option pricing model of this thesis uses the stochastic volatility – jump (SVJ) data generating process with piecewise constant model parameters. The given process nests Bates SVJ, Heston SV, Merton JD, and Biger-Hull models as special cases, which means that the model can be collapsed to any of these by an appropriate selection of model parameter values. This part of the Chapter first defines the data generating process in the continuous time and then in the discrete time.

### 5.1.1 Continuous Time Model

The continuous time model is defined by three stochastic differential equations: one for spot price process ( $S_t$ ), one for stochastic volatility process ( $V_t$ ), and one for jump process ( $N_t$ ):

$$dS_t = S_t \left( (b_t - \lambda_t \varepsilon_t) dt + \sqrt{V_t} W_{S_t} + (J_t - 1) dN_t \right), \quad (5.1)$$

$$dV_t = \kappa_t (\theta_t - V_t) dt + \xi_t \sqrt{V_t} \left( \rho_t W_{S_t} + \sqrt{1 - \rho_t^2} W_{V_t} \right), \quad (5.2)$$

$$dN_t \sim \text{Poisson}(\lambda_t t), \text{ where} \quad (5.3)$$

$$J_t \sim \exp \left( \gamma_t - \frac{1}{2} \delta_t^2 + \delta_t N(\cdot) \right),$$

$$E[\ln(J_t)] = \gamma_t - \frac{1}{2} \delta_t^2,$$

$$\text{var}[\ln(J_t)] = \delta_t^2,$$

$$\gamma_t = \ln(\varepsilon_t + 1).$$

The state equations are dependent on nine model parameters, namely: risk-free domestic interest rate ( $r_t$ ), risk-free foreign interest rate ( $r_t^*$ ), the annual frequency of jumps ( $\lambda_t$ ), average jump size ( $\varepsilon_t$ ), jump size standard deviation ( $\delta_t$ ), volatility mean reversion level ( $\theta_t$ ), volatility mean reversion rate ( $\kappa_t$ ), the volatility of volatility ( $\xi_t$ ), and the correlation ( $\rho_t$ ) between the spot and volatility standard Wiener processes ( $W_{S_t}$ ) and ( $W_{V_t}$ ). In addition,  $N(\cdot)$  denotes a standard normal distributed random number and ( $b_t$ ) the spread between the domestic and foreign interest rates.

Even though the structure of the model allows all the parameters to be piecewise constant, not all of them are required to be piecewise constant in order to match the market implied option prices, as discussed later in this Chapter. Furthermore, this thesis assumes CIP to hold, meaning that the drift of the spot process is derived from the interest rate spread between the foreign and domestic currencies. However, if using the model for minor currencies, for which the CIP does not hold, the forward FX rate should

be explicitly defined instead of deriving it from the CIP. All the model parameters and their definitions are listed in Table 1.

**Table 1: The parameters of the option pricing model.**

| Parameter       | Definition   |
|-----------------|--|
| $S_t$           | FX spot rate   |
| $V_t$           | Stochastic volatility  |
| $J_t$           | Random percentage jump conditional on a jump occurring                           |
| $N_t$           | Time-inhomogeneous Poisson process with a frequency of $\lambda_t$               |
| $r_t$           | Risk-free domestic interest rate   |
| $r_t^*$         | Risk-free foreign interest rate  |
| $b_t$           | Interest rate spread between the foreign and domestic interest rates             |
| $\lambda_t$     | Annual frequency of jumps  |
| $\varepsilon_t$ | Average jump size  |
| $\delta_t$      | Jump size standard deviation   |
| $\theta_t$      | Volatility mean reversion level  |
| $\kappa_t$      | Volatility mean reversion rate   |
| $\xi_t$         | Volatility of volatility   |
| $\rho_t$        | Correlation between spot and volatility Wiener processes $W_{S_t}$ and $W_{V_t}$ |
| $W_{S_t}$       | Standard Wiener process in the spot process                                      |
| $W_{V_t}$       | Standard Wiener process in the stochastic volatility process                     |

### 5.1.2 Discrete Time Model

Whereas the continuous time model defines stochastic differential equations for the process state transitions, the discrete-time model defines a sampling scheme for generating new process states from the previous ones. Unfortunately, the SVJ process has no explicit sampling scheme, as discussed earlier in this thesis. As a result, the discrete time model must be implemented using an approximated scheme.

Due to conflicting conclusions in the reference literature, it was decided to begin with a simple Euler discretization, and fix the negative volatility problem with the full truncation scheme, as recommended by Lord et al. (2006, pp. 1-32) However, the resulting scheme turned out to be highly biased, when the market implied model parameters and any practical number of time steps were used. As a result, it was decided to implement the scheme of this thesis based on Andersen's (2007, pp. 1-38) Quadratic Exponential (QE) scheme. More precisely, the spot and volatility processes are sampled using the approximated schemes proposed by Andersen, whereas the jump process is sampled using an explicit scheme. This part of the Chapter first defines the scheme for the volatility process, and then the ones for the jump and spot processes.

The volatility process sampling scheme is implemented in five steps.

The first calculates the first ( $m$ ) and the second ( $s^2$ ) moments of the volatility process:

$$m = \theta_t + \left( \hat{V}_t - \theta_t \right) e^{-\kappa_t \Delta}, \quad (5.4)$$

$$s^2 = \frac{\hat{V}_t \xi_t^2 e^{-\kappa_t \Delta}}{\kappa_t} \left( 1 - e^{-\kappa_t \Delta} \right) + \frac{\theta_t \xi_t^2}{2\kappa_t} \left( 1 - e^{-\kappa_t \Delta} \right)^2. \quad (5.5)$$

The second calculates the ratio of the squared moments ( $\psi$ ):

$$\psi = \frac{s^2}{m^2}. \quad (5.6)$$

The third generates a uniform random number ( $U_V$ ). All the variables in the above equations are denoted as in Table 1, in addition to which, the time discretization step length is denoted with ( $\Delta$ ) and the discretized equivalents of the process state variables with ( $\hat{\cdot}$ ).

The fourth and fifth steps apply the switching logic between the so called quadratic and exponential schemes. More precisely, if the calculated ratio of the squared moments ( $\psi$ ) is equal to, or less than, a predetermined critical value ( $\psi_c$ ), the quadratic sampling scheme is used. If the reverse is true, the exponential sampling scheme is used.

The logic behind the switching rule is that the ratio of the moments tells how “far” the process is from zero in the given probability space. If one is far from zero, the exponential scheme provides a sufficient accuracy. If one is close to zero, the exponential scheme would decay far too fast. As a result, one then uses the quadratic scheme constructed using the Dirac’s delta function. As the quadratic scheme can only be moment-matched for  $(\psi) \leq 2$  and the exponential scheme for  $(\psi) \geq 1$ , the critical value ( $\psi_c$ ) must be set into interval  $[1, 2]$ . Andersen concludes the exact value to have only little significance and sets it to 1.5, so this thesis does the same.

Once the critical value ( $\psi_c$ ) has been assigned, one performs the final step of the volatility process sampling scheme.

If  $(\psi) \leq (\psi_c)$ , one first computes

$$b^2 = 2\psi^{-1} - 1 + \sqrt{2\psi^{-1} - 1} \sqrt{2\psi^{-1} - 1}, \quad (5.7)$$

$$a = \frac{m}{1 + b^2}. \quad (5.8)$$

Next, one generates an inverse-normal random number

$$Z_v = \Phi_N^{-1}(U_v), \quad (5.9)$$

after which the new volatility process state is given by

$$\hat{V}_{t+\Delta} = a(b + Z_v)^2. \quad (5.10)$$

If  $(\psi) > (\psi_c)$  instead, one first computes

$$p = \frac{\psi - 1}{\psi + 1}, \quad (5.11)$$

$$\beta = \frac{1 - p}{m}, \quad (5.12)$$

after which the new volatility process state is given by

$$\hat{V}_{t+\Delta} = \Psi^{-1}(U_v; p, \beta) = \begin{cases} 0 & , 0 \leq U_v \leq p \\ \beta^{-1} \ln\left(\frac{1-p}{1-U_v}\right) & , p < U_v \leq 1. \end{cases} \quad (5.13)$$

The jump process has an explicit sampling scheme, which is used in this thesis as well. More precisely, the random number of jumps ( $N_t$ ) is sampled from a Poisson distribution

$$\hat{N}_{t+\Delta} = RNG_{Poisson}(\lambda_t \Delta). \quad (5.14)$$

The corresponding number of the random jump sizes ( $\{J_t^n\}$ ) is sampled from a log-normal distribution

$$\hat{J}_{t+\Delta}^n = RNG_{LN}(\varepsilon_t + 1, \delta_t), \text{ for } n = 1 \text{ to } \hat{N}_{t+\Delta}. \quad (5.15)$$

The variables are denoted similarly to Table 1, in addition to which,  $(RNG_X(\cdot))$  denotes the random number generator of a distribution (X) with parameters ( $\cdot$ ).

The sampling scheme for the full SVJ model is then completed by a sampling scheme for the spot process. Similarly to the volatility process, the spot process is also sampled

along the lines of Andersen. However, as Andersen only considers the Heston SV model, this thesis extends the Andersen's original scheme with the jump process above. As a result, the spot process sampling scheme is given by

$$\hat{S}_{t+\Delta} = \hat{S}_t \cdot \exp\left(K_0 + K_1 \hat{V}_t + K_2 \hat{V}_{t+\Delta} + \sqrt{K_3 \hat{V}_t + K_4 \hat{V}_{t+\Delta}} \cdot Z_S\right) \cdot \prod_{n=0}^{\hat{N}_{t+\Delta}} \hat{J}_{t+\Delta}^n, \text{ where} \quad (5.16)$$

$$K_0 = -\frac{\rho_t \kappa_t \theta_t}{\xi_t} \Delta,$$

$$K_1 = \gamma_1 \Delta \left( \frac{\kappa_t \rho_t}{\xi_t} - \frac{1}{2} \right) - \frac{\rho_t}{\xi_t},$$

$$K_2 = \gamma_2 \Delta \left( \frac{\kappa_t \rho_t}{\xi_t} - \frac{1}{2} \right) + \frac{\rho_t}{\xi_t},$$

$$K_3 = \gamma_1 \Delta (1 - \rho_t^2),$$

$$K_4 = \gamma_2 \Delta (1 - \rho_t^2),$$

where the variables are denoted similarly to the previous equations and Table 1. In addition,  $(Z_S)$  denotes a standard normal distributed random number, and  $(\gamma_1)$  and  $(\gamma_2)$  the weighting factors of a simple time integral. Both  $(\gamma_1)$  and  $(\gamma_2)$  are set to 0.5 along the lines of Andersen.

All in all, the discrete time model is defined jointly by the volatility, spot, and jump process sampling schemes. When using the discrete time model, one first generates one time step from the jump process scheme using (5.14) and (5.15), then one time step from the volatility process scheme using (5.4) – (5.13), and finally one time step from the spot process scheme using (5.16).

## 5.2 Option Pricing

As pointed out by several studies (Bakshi et al. 1997, pp. 2003-2049; Galluccio & Le Cam 2005, pp. 1-40), an efficient calibration of the SVJ model against the implied option prices is practically impossible, due to the extensive computational burden, without an analytical solution for the price of a European call option. As a result, this part of the Chapter first defines the analogous semi-closed form and Monte Carlo solutions for the price of a European call option, and then describes how the Monte Carlo solution can be extended to various exotic option styles.

### 5.2.1 Semi-Closed Form Solution for European Options

The semi-closed form solution for European options follows the basic idea of Heston (1993, pp. 327-343) and Bates (1996, pp. 69-107), whereas the practical implementation is to a large extent conducted along the lines of Lipton (2002, pp. 61-65) and Sepp (2007, pp. 1-148). More precisely, the general solution of the European call option price and the implementation of the characteristic functions are done as proposed by Lipton, in order to avoid the non-singularity problem with the complex logarithms. The general solution of the Riccati equations in turn, is done along the lines of Sepp, in order to allow piecewise constant model parameters.

The basic idea of the Lipton's revised solution for the European call option price is to abandon the initial Black-Scholes originated form, in which the option price is defined with the help of delta ( $P_1$ ) and the conditional probability for the option to expire in-the-money ( $P_2$ ). Instead, the price of a European call option ( $C$ ) is defined directly through a Fourier integral

$$C(S, t) = e^{-rT} F(T) - \frac{e^{-rT} K}{2\pi} \int_{-\infty}^{\infty} \frac{e^{(-i\Phi+1/2)\ln(F(T)/K)} + \Psi(T, \Phi)}{\Phi^2 + 1/4} d\Phi, \quad (5.17)$$

where ( $r$ ) denotes the risk-free interest rate, ( $T$ ) time to option expiry, ( $F(T)$ ) the forward price of the underlying at the time of option expiry, ( $K$ ) option strike, ( $i$ ) imaginary unit,

and  $(\Psi(T, \Phi))$  the characteristic function of the data generating process. For the sake of easier numerical integration, the equation is convenient to write in an alternative form

$$C(S, t) = e^{-rT} F(T) - \frac{e^{-rT} K}{\pi} \int_0^{\infty} \text{Re} \left[ \frac{e^{(-i\Phi+1/2)\ln(F(T)/K)} + \Psi(T, \Phi)}{\Phi^2 + 1/4} \right] d\Phi, \quad (5.18)$$

where  $\text{Re}[\cdot]$  denotes the real part of a complex number.

Applying Ito's lemma and standard arbitrage arguments for the data generating process defined in SDEs (5.1), (5.2), and (5.3) gives Garman's PDE

$$\begin{aligned} \frac{\partial C}{\partial t} + \frac{1}{2} V S^2 \frac{\partial^2 C}{\partial S^2} + \frac{1}{2} \xi^2 V \frac{\partial^2 C}{\partial V^2} + \rho \xi V S \frac{\partial^2 C}{\partial S \partial V} + (b - \lambda \varepsilon) S \frac{\partial C}{\partial S} + \\ \kappa(\theta - V) \frac{\partial C}{\partial V} - (b - \lambda \varepsilon) C + \lambda \int_{-\infty}^{\infty} C(JS) J dJ = 0, \end{aligned} \quad (5.19)$$

which the price of the European call option is required to satisfy. Due to length and complexity, the full derivation of the Garman's PDE is not presented in this thesis. The thorough derivation is presented for example by Sepp (2007, pp. 1-148) or Bakshi et al. (1997, pp. 2003-2049).

In order to use the revised call option price (5.18) in the Garman's PDE, one must assign a functional form for the characteristic function  $(\Psi(T, \Phi))$ . Following the example of Lipton (2002, pp. 61-65) and Sepp (2007, pp. 1-148),  $(\Psi(T, \Phi))$  is defined in an exponential affine form

$$\Psi(T, \Phi) = \exp\left(\alpha^{(SV)}(T, \Phi) + \beta^{(SV)}(T, \Phi) + \alpha^{(JD)}(T, \Phi)\right), \quad (5.20)$$

where  $(\alpha^{(SV)}(T, \Phi))$  and  $(\beta^{(SV)}(T, \Phi))$  jointly define the stochastic volatility part, and  $(\alpha^{(JD)}(T, \Phi))$  the jump part of the characteristic function.

The pricing problem is then completed by solving  $(\alpha^{(SV)}(T, \Phi))$ ,  $(\beta^{(SV)}(T, \Phi))$ , and  $(\alpha^{(JD)}(T, \Phi))$  from the ordinary differential equation system

$$\begin{cases} \dot{\alpha}^{(SV)} + \kappa\theta = 0 & , \alpha^{(SV)}(T, T) = 0 \\ \dot{\beta}^{(SV)} + \frac{1}{2}\xi^2\beta^{(SV)2} - \kappa - \rho\xi\Phi + \frac{1}{2}\Phi^2 + \frac{1}{2}\Phi = 0 & , \beta^{(SV)}(T, T) = -\beta^{(SV)} , \\ \dot{\alpha}^{(JD)} + \int_{-\infty}^{\infty} \lambda \left( e^{-\gamma\left(i\Phi - \frac{1}{2}\right) - \frac{\delta^2}{2}\left(\Phi^2 + \frac{1}{4}\right)} - 1 + \varepsilon\left(i\Phi - \frac{1}{2}\right) \right) dt = 0 & , \alpha^{(SV)}(T, T) = 0 \end{cases} \quad (5.21)$$

consisting of three Riccati equations. As concluded by Sepp (2007, pp. 44-68), the solution is well-defined and given by

$$\alpha^{(SV)}(\tau, \Phi) = -\frac{\kappa\theta}{\xi^2} \left[ \psi_+ \tau + 2 \ln(\hat{C} + C_-) \right], \quad (5.22)$$

$$\beta^{(SV)}(\tau, \Phi) = -\frac{-\psi_- \hat{C} + \psi_+ C_-}{\xi^2 (\hat{C} + C_-)}, \quad (5.23)$$

$$\alpha^{(JD)}(T, \Phi) = \lambda T \left[ e^{-\gamma\left(i\Phi - \frac{1}{2}\right) - \frac{\delta^2}{2}\left(\Phi^2 + \frac{1}{4}\right)} - 1 + \varepsilon\left(i\Phi - \frac{1}{2}\right) \right], \text{ where} \quad (5.24)$$

$$\hat{C} = C_+ e^{-\zeta\tau},$$

$$C_{\pm} = \frac{1}{2\zeta} (\psi_{\pm} \mp \xi^2 \beta^{(SV)}),$$

$$\psi_{\pm} = \zeta \mp (i\Phi \rho \xi + \hat{\kappa}),$$

$$\zeta = \sqrt{\Phi^2 \xi^2 (1 - \rho^2) + 2i\Phi \xi \rho \hat{\kappa} + \hat{\kappa}^2 + \xi^2 / 4},$$

$$\hat{\kappa} = \kappa - \rho \xi / 2,$$

$$\tau = T - t,$$

where the time dependency of the parameters is omitted in order to lighten the notation.

In the case of constant model parameters, the solution of the Riccati equations is obtained by setting the initial value of  $(\beta^{(SV)})$  to zero, and thereafter computing  $(\alpha^{(SV)}(T, \Phi))$ ,  $(\beta^{(SV)}(T, \Phi))$ , and  $(\alpha^{(JD)}(T, \Phi))$  from (5.22), (5.23), and (5.24). In the case of piecewise constant model parameters, one needs to calculate  $(\alpha^{(SV)}(T, \Phi))$  and  $(\beta^{(SV)}(T, \Phi))$  recursively as presented by Mikhailov and Nögel (2003, pp. 74-79), whereas  $(\alpha^{(JD)}(T, \Phi))$  can be integrated straight forwardly over time.

More precisely, let time to option expiry ( $T$ ) be divided into  $n$  sub-intervals such that the model parameters are constant at each sub-interval, and allowed to have discontinuity points at the sub-interval interceptions. In the first sub-interval from the expiry  $[T, \tau_1]$ , one can apply the special solution of Riccati equations used for the constant model parameter case to obtain  $\alpha^{(SV)}(\tau_1, \Phi)$ ,  $\beta^{(SV)}(\tau_1, \Phi)$ , and  $\alpha^{(JD)}(\tau_1, \Phi)$ . In the next subinterval from the expiry  $[\tau_1, \tau_2]$ ,  $\beta^{(SV)}(\tau_2, \Phi)$  is computed using  $\beta^{(SV)}(\tau_1, \Phi)$  as the initial condition, whereas  $\alpha^{(SV)}(\tau_2, \Phi)$  is computed as the sum of  $\alpha^{(SV)}$  terms from the subintervals  $[T, \tau_1]$  and  $[\tau_1, \tau_2]$ . Similarly to  $\alpha^{(SV)}$ ,  $\alpha^{(JD)}(\tau_2, \Phi)$  is computed as the sum of  $\alpha^{(JD)}$  terms from the subintervals  $[T, \tau_1]$  and  $[\tau_1, \tau_2]$ . However, whereas  $\alpha^{(JD)}$  is a pure time integral,  $\alpha^{(SV)}$  depends on both time and  $\beta^{(SV)}$ . As a result,  $\alpha^{(JD)}$  can be computed independently on the SV part, whereas  $\alpha^{(SV)}$  and  $\beta^{(SV)}$  must be calculated recursively, in conjunction with each others.

All in all, the process of pricing European call options with the piecewise constant model parameters in a semi-closed form consists of three phases. First, one runs the recursion algorithm over all ( $n$ ) sub-intervals to obtain  $(\alpha^{(SV)}(0, \Phi))$ ,  $(\beta^{(SV)}(0, \Phi))$ , and  $(\alpha^{(JD)}(0, \Phi))$ . Second, one defines the characteristic function (5.20) using  $(\alpha^{(SV)}(0, \Phi))$ ,  $(\beta^{(SV)}(0, \Phi))$ , and  $(\alpha^{(JD)}(0, \Phi))$ . Third, one uses the characteristic function to calculate the option price, as defined in (5.18). The procedure is the same for constant model parameters, except that  $(\alpha^{(SV)}(0, \Phi))$ ,  $(\beta^{(SV)}(0, \Phi))$ , and  $(\alpha^{(JD)}(0, \Phi))$  can be computed at one step without the recursion algorithm. A method for the numerical integration needed for (5.18) is presented later in this Chapter.

### 5.2.2 Monte Carlo Solution for European Options

Monte Carlo solution for the European options is trivial to implement once a proper sampling scheme for the data generating process has been defined. More precisely, the Monte Carlo solution then only consists of generating a sufficient number of random trajectories and computing the option price as the discounted arithmetic mean of the trajectory terminal values:

$$C(S_0, t) = e^{-rT} \cdot \frac{1}{N} \cdot \sum_{n=1}^N S_T^n, \quad (5.25)$$

where  $(S_0)$  denotes the underlying spot price at time zero,  $(r)$  domestic risk-free interest rate,  $(T)$  time to option expiry,  $(N)$  the chosen number of simulation replications, and  $(S_T^n)$  the simulated terminal value of random trajectory  $(n)$ .

As a result, the simulation only requires the discretization time step length  $(\Delta)$  and the number of simulation replications  $(N)$  to be determined, in addition to the model parameter values. Furthermore, it should be acknowledged that if any model parameters are constant, the speed of the algorithm can be enhanced by calculating the feasible parts of (5.4), (5.5), and (5.16) outside the simulation replications.

### 5.2.3 Monte Carlo Solution for Exotic Options

Extending the Monte Carlo solution further to exotic options is also straightforward, the exact implementation naturally being dependent on the characteristics of the specific exotic option style in question. Nevertheless, what is in common for all the exotic option styles is that the option value is defined as the discounted value of the expected payout at expiry, whereas the expected payout at expiry is defined by the underlying spot value(s) at certain point(s) in time.

As a result, the problem of pricing an exotic option becomes a three-step process. First, one needs to apply the given sampling scheme to produce trajectory values at the

predefined fixing points. Second, one needs to compute the trajectory specific payouts at the expiry from the simulated underlying values using the option payout formula. Third, one needs to compute the option value as the discounted arithmetic mean of option payouts at the expiry for each trajectory, similarly to what is done for the European options.

To give a practical example,

$$C(S, T) = \max\left(\frac{1}{J} \cdot \sum_{j=1}^J S_j - K, 0\right) \quad (5.26)$$

illustrates the payout formula of a discrete Asian option, where the option payout at the expiry is defined as the average underlying spot price ( $S_j$ ) across ( $J$ ) fixing points minus the option strike ( $K$ ).

As another example,

$$C(S, T) = \begin{cases} 0\%, & S_T < 0.85 \\ 10\%, & 0.85 \leq S_T < 0.92 \\ 20\%, & 0.92 \leq S_T < 1.03 \\ 30\%, & 1.03 \leq S_T. \end{cases} \quad (5.27)$$

illustrates the payout formula of a specific “wedding cake” option, where the option payout at the expiry is either 0%, 10%, 20%, or 30%, depending on the underlying spot value at the time of the option expiry ( $S_T$ ).

In both cases, the option value can be determined using Monte Carlo, by generating a sufficient number of underlying trajectories ( $N$ ), and calculating the discounted value of the expected payout at the option expiry. What should be acknowledged in the practical implementation is that the optimal time discretization step length ( $\Delta$ ) and the number of

simulation replications ( $N$ ) vary according to the option style. As an example, path-dependent options, such as the discrete Asian option used as an example, generally require a shorter time step length. Options with digital payout structures in turn, such as the wedding cake option used as an example, generally require a larger number of simulation replications. However, the only reliable way to optimize ( $\Delta$ ) and ( $N$ ) is to conduct a separate variance and bias analysis for each option style.

### 5.3 Calibration

The calibrated model should at the same time be market consistent with the whole range of implied option prices, and give a robust and meaningful calibration. In other words, the model output option prices should be within the market bid-offer spread, the fluctuation of the model parameter values should be explainable by the fluctuation of the market implied option prices, while the model parameter values should be plausible compared to the historical asset returns.

The requirement of market consistency excludes the use of historical returns calibration methods, as they do not force the calibration to match the market implied option prices. That is also the case with the implied option price time series methods, as neither Bates (1996, pp. 69-107) nor Bakshi et al. (1997, pp. 2003-2049) was able to fit the whole implied volatility surface simultaneously. As a result, only the implied volatility surface methods can fulfill the requirement of market consistency. However, the use of them may, on the other hand, also endanger the robustness of calibration.

More precisely, the fundamental challenge of applying the implied volatility surface method for the SVJ model is that the problem of optimizing the model parameters against a given implied volatility surface is generally ill-posed. What is meant here by an ill-posed problem, is that the relationship between the model parameter values and the resulting implied volatility surface is not a bijection, but several different model parameter sets can give the same implied volatility surface. As a result, the inverse

problem of finding an optimal parameter set for a given implied volatility surface is generally ill-defined.

In this thesis, the problem of defining an implied calibration method for an SVJ model is structured to consist of three interrelated phases. First, one needs to define a cost function to be optimized. Second, one needs to define a set of additional optimization constraints to force the ill-posed problem to give meaningful solutions. Third, one needs to implement a numerical algorithm for solving the optimization problem in as robust and computationally efficient manner as possible. The rest of this part of the Chapter addresses these problems in the order above.

### 5.3.1 Cost Function

This thesis defines the optimization cost function as the average quadratic distance between the model implied and the market implied Black-Scholes volatilities, using equal weights for all the expiry tenors and strike levels:

$$\Theta^* = \arg \min_{\Theta} \frac{1}{N_s N_e} \cdot \sum_{s=1}^{N_s} \sum_{e=1}^{N_e} [\sigma^{SVJ}(K_s, T_e, \Theta) - \sigma^M(K_s, T_e)]^2. \quad (5.28)$$

In the equation,  $(\Theta^*)$  denotes the optimal set of the SVJ model parameters,  $(N_s)$  the number of strike levels in the implied volatility surface,  $(N_e)$  the number of expiry tenors in the implied volatility surface,  $(K_s)$  option strike related to strike level  $(s)$ ,  $(T_e)$  option time to expiry related to expiry tenor  $(e)$ ,  $\sigma^{SVJ}(K_s, T_e, \Theta)$  the SVJ model implied volatility for a given triplet  $(K_s, T_e, \Theta)$ , and  $\sigma^M(K_s, T_e)$  the market implied volatility for a given pair  $(K_s, T_e)$

The main reason for choosing the implied Black-Scholes volatility instead of the option price is the ease of weighting between the different expiry tenors and strike levels. If the pure option price was used, one would encounter a situation where the values of the long expiry in-the-money options would be hundreds of times higher than the ones of short

expiry out-of-the-money options. That in turn, would mean that the expensive long expiry in-the-money options would be highly over-weighted in the optimization, if no additional weighting logic was used. The problem is also to some extent present with the implied Black-Scholes volatility, but as the minimum and maximum implied volatilities across the whole surface typically only differ by a factor of 1.5 - 4, it is considered reasonable to use equal weights across the whole volatility surface. The same is also done by Galluccio and Le Cam (2005, pp. 1-40) and Duffie et al. (2000, pp. 1343-1376).

The main reason for choosing the quadratic distance is twofold. First, the quadratic distance includes a natural “absolute value adjustment”, meaning that only the absolute deviation from the market mid volatility matters, not the direction of the deviation. Second, choosing the quadratic distance instead of the pure absolute value distance enables the use of certain efficient non-linear optimization methods, such as the Levenberg-Marquardt.

### 5.3.2 Additional Constraints

As the non-constrained optimization problem is generally ill-posed, one needs to force the optimization algorithm to stay in the plausible parameter value space. There are generally two alternative ways of doing that. First, one can use a hard constraint optimization by giving each model parameter ranges within which the solution is required to stay. Second, one can use a soft constraint optimization by defining an a priori model parameter set and complementing the optimization cost function with a convex penalty term, which prevents the calibrated solution from drifting too far from the a priori one. The first approach is used for example by Cont and Tankov (2004, pp. 1-43) and the latter for example by Galluccio and Le Cam (2005, pp. 1-40).

The largest advantage of the hard constraint approach is that it does not change the original cost function, which gives a better accuracy, provided that the hard constraint barriers are well-set. On the other hand, poorly selected hard constraints will cause the algorithm to get stuck into a local minimum. The largest advantage the soft constraint approach in turn, is that it does not restrict the solution into any sub-space. Furthermore,

the penalty term increases the convexity of the initial problem, making it numerically more stable. On the other hand, the additional penalty term also changes the cost function, which makes the optimal solution dependent on both the a priori parameter set, and the form and the parameterization of the penalty function. That in turn, introduces a bias into the initial problem, which means that a badly chosen a priori may cause the calibration to fail severely.

Given the pros and cons of each alternative, this thesis decided to use the hard constraint approach. The decision was made based on two arguments. First, the hard constraint approach is non-biased, as the cost function maintains its original form. That is particularly important, as the literature does not provide any reliable way to define a good a priori model parameter set, which means that the use of the soft constraint approach would introduce a significant risk of compromising the model's market fit due to a badly chosen a priori parameter set.

Second, any potential problems with the hard constraint approach should be clearly revealed by the numerical tests conducted later in this thesis, which reduces the risk of introducing a faulty calibration method. More precisely, any robustness problems caused by the non-convex optimization problem should be detected as a model parameter fluctuation that cannot be explained by the implied option price fluctuation. Problems with the hard constraint barrier values instead, should be detected as model parameters constantly hitting their constraint barriers.

### 5.3.3 Numerical Algorithm

As Galluccio and Le Cam (2005, pp. 1-40) provide a comprehensive implied calibration method for the SVJ model with piecewise constant model parameters, this thesis first tried to implement that in its original form. However, the method was discovered to have some severe drawbacks, most likely because of Galluccio and Le Cam optimizing their method for equities, whereas this thesis focuses on FX. Even if the same SVJ process applies to both equities and FX, there still exist some essential differences in their typical shapes of implied volatility surfaces.

The first drawback of the Galluccio and Le Cam method was that it assumes the jumps to only occur at short expiries, referred as the Gamma region, and the jumps to “die out” according to a certain functional form. This holds well for equities, the implied volatility surfaces of which are typically characterized by high, fast decaying short expiry volatilities. Unfortunately the same characteristics do not apply for FX, but one seldom sees steep implied volatility increases in the short expiries. As a result, the Galluccio and Le Cam method was discovered to either give too high short expiry implied volatilities, or alternatively a bad fit at the interception of the Gamma and Vega regimes.

The second drawback of the Galluccio and Le Cam method was that it assumes all the SV parameters, except  $(\kappa)$ , to be piecewise constant. Using the same assumption for the model of this thesis, the piecewise constant parameter values of  $(\theta)$ ,  $(\xi)$ , and  $(\rho)$  were discovered to fluctuate heavily over expiry tenors, which indicates the optimization problem to be over-fitted, or the numerical implementation to be inaccurate.

To overcome the problems above, this thesis implemented two structural changes to the calibration method of Galluccio and Le Cam. First, the jumps are not assumed to die out in the Vega regime, but  $(\lambda)$ ,  $(\varepsilon)$ , and  $(\delta)$  are assumed to be constant across all the expiries. Second, only the volatility mean reversion level  $(\theta)$  is set piecewise constant, while the rest SV parameters;  $(\kappa)$ ,  $(\xi)$ , and  $(\rho)$ ; are assumed to be constant.

The reason behind the first change is that the FX volatility surfaces are typically not characterized by high, fast decaying short expiry volatilities, which eliminates the need for a separate Gamma regime. The reason behind the second change is twofold. First,  $(\theta)$  must be piecewise constant, as otherwise the model could only generate monotonously increasing or decreasing volatility term structures, which would clearly be against the observed market behavior. Second, setting  $(\kappa)$ ,  $(\xi)$ , and  $(\rho)$  piecewise constant was not discovered to significantly improve the market fit, but merely to cause the parameter values to oscillate across expiry tenors, and to make the whole calibration method computationally less efficient.

In terms of the optimization algorithm implementation, this thesis follows Galluccio and Le Cam, and breaks the calibration into smaller optimization problems, instead of trying to globally calibrate all the model parameters simultaneously. More precisely, this thesis uses a recursive calibration method, where each recursion round consist of four distinctive optimization problems. Within each recursion, no user intervention is needed, but the calibration algorithm solves the four optimization problems automatically. After each recursion round, the user must define whether the next recursion round is needed, or whether a sufficient calibration has breached. To give some intuition, already one recursion round was often discovered to give an accurate calibration, if the market had not moved much. On the other hand, up to ten recursion rounds were needed, if the market had been highly turbulent.

The first of the four distinctive optimization problems within each recursion round optimizes the piecewise constant volatility mean reversion level ( $\theta_t$ ). That is done tenor by tenor, starting from the shortest expiry. The second problem optimizes the jump frequency ( $\lambda$ ), the third the average jump size ( $\varepsilon$ ) and jump size standard deviation ( $\delta$ ), and the fourth the volatility mean reversion rate ( $\kappa$ ), the volatility of volatility ( $\xi$ ), and the correlation between the spot and volatility processes ( $\rho$ ).

Each of the four optimization problems is solved using a customized Levenberg-Marquardt algorithm, which is a widely used pseudo-second order method for solving non-linear quadratic optimization problems (Roweis 2007, pp. 1-5). The basic idea of the Levenberg-Marquardt is to interpolate between the traditional Gauss-Newton and gradient descent algorithms, using the second order information obtained by approximating the Hessian matrix using the sum of the outer products of the gradients.

More precisely, the standard Levenberg-Marquardt iterates recursively according to

$$\Theta_{i+1} = \Theta_i - (H + w \cdot \text{diag}[H])^{-1} J, \quad (5.29)$$

where  $(\Theta_i)$  denotes the parameter vector subject to optimization at iteration step (i), (H) the approximated Hessian matrix, (J) the approximated Jacobian matrix,  $(\text{diag}[\cdot])$  diagonal of matrix ( $\cdot$ ), and (w) a dumping factor that determines the blending between the Gauss-Newton and the gradient descent methods

Different from the standard Levenberg-Marquardt, the customized algorithm of this thesis uses a plain identity matrix (I) instead of the Hessian diagonal ( $\text{diag}[H]$ ) one. On one hand, that means moving from the Levenberg-Marquardt algorithm back to the simple Levenberg algorithm. On the other, it was discovered efficient to use the combination of identity matrix (I) and a three-scenario update scheme for the dumping factor (w), rather than using the Hessian diagonal ( $\text{diag}[H]$ ) and a simple increase-decrease update method for (w), as done in the standard Levenberg-Marquardt.

More precisely, the customized algorithm of this thesis iterates recursively according to

$$\Theta_{i+1} = \Theta_i - (H + w \cdot I)^{-1} J, \quad (5.30)$$

where  $(\Theta_i)$  denotes the optimization parameter set at iteration step (i), (H) the approximated Hessian matrix, (J) the approximated Jacobian matrix, (I) an identity matrix, and (w) the dumping factor determining the blending between the Gauss-Newton and gradient descent methods. The dumping factor ( $w_{i+1}$ ) in turn, is the one from the triplet  $\{0.1 \cdot w_i; 1 \cdot w_i; 10 \cdot w_i\}$ , giving the smallest cost function value at step (i+1), the cost function values being computed according to (5.28).

## 5.4 Implementation

The model was implemented in Visual Basic programming language, which provides a very limited number of ready-made algebraic and numerical tools. As a result, many tools had to be implemented specifically for this thesis. This part of the Chapter briefly describes the implementation of the numerical integration algorithm and the random

number generators. The first plays an important role in the semi-closed form solution for the European options, whereas the latter is essential for the Monte Carlo simulation.

#### 5.4.1 Numerical Integration

The numerical integration of the Fourier transformation is conducted using a customized Gaussian quadrature algorithm. The basic principle of the Gaussian quadrature is to truncate a finite integration domain  $[a, b]$  into  $[-1, 1]$  domain, and estimate the integral of a given function  $(f)$  as the weighted sum of the function values at (i) predefined abscissas  $(\{t_i\})$ , using predefined weights  $(\{w_i\})$ . The abscissas are derived from the roots of the associated Legendre polynomials, and can be found from the literature dealing with the numerical integration (Kythe & Schaferkötter 2005, pp. 108-186). The method is illustrated in (5.31), (5.32), and (5.33), where

$$I = \int_a^b f(x)dx \tag{5.31}$$

presents the integral problem to be estimated,

$$I = \int_{-1}^{+1} f(c + mt)dt, \text{ where} \tag{5.32}$$

$$c = \frac{1}{2}(b + a),$$

$$m = \frac{1}{2}(b - a).$$

the truncated form of the integral, and

$$GI = m \sum_{i=1}^n w_i f(c + mt_i) \tag{5.33}$$

the Gaussian quadrature estimate of the integral value.

Unfortunately for the purposes of this thesis, the Gaussian quadrature only accepts finite integration domains, whereas the option pricing problem (5.18) has a semi-infinite integration domain. Fortunately though, the integrand of (5.18) converges rapidly to zero, which enables one to cut-off the right-hand side tail without a loss of information.

In fact, the determination of the optimal cut-off point is highly essential for the numerical accuracy and the efficiency of the model. One on hand, if one cuts off “too early”, the model will give incorrect option prices, as a part of the probability mass would be ignored. On the other, if one cuts off “too late”, more Gaussian quadrature abscissas are needed for the desired accuracy, as some abscissas would fall into the “empty tail”, which contains no information about the integrand behavior. As the characteristic function needs to be solved as many times as there are abscissas, a too large number of abscissas increase the computing time unnecessarily.

To give some indication of a suitable cut-off point, a previous study by S nderby (2003, pp. 43-48) states 300 to be a safe cut-off point for the Bates SVJ model. Nevertheless, this thesis decided to conduct a simple estimate for the optimal cut-off point and the optimal number of the Gaussian quadrature abscissas. Motivated by the fact that the time to expiry has the most effect on the speed of the integrand convergence, it was decided to analyze the optimal cut-off point and the number of abscissas separately for each expiry tenor.

In the beginning, the initial cut-off point was conservatively set to 500, and the number of Gaussian quadrature abscissas to 512, in order to guarantee an excellent numerical accuracy at the initial point. Thereafter, the cut-off point was gradually moved closer to zero, separately for each expiry tenor, to find the expiry tenor specific critical cut-off points for the different model parameter sets. The critical point was defined to be the closest point to zero, where no implied volatility in tenors ( $T$ ) and below moved by more than 0.0009% in terms of an absolute value, compared to the initial cut-off point. The test was then repeated with different model parameter sets. At the end, the expiry tenor

specific optimal cut-off points were defined to be the furthest critical points from zero, across all the tested model parameter sets.

Once the optimal cut-off points were assigned, the optimal expiry tenor specific numbers of abscissas were determined in a similar manner. The initial number of abscissas was again set to 512, and the cut-off points to their previously assigned expiry tenor specific optimal levels. Thereafter, the number of abscissas was gradually decreased, separately for each expiry tenor, to find the expiry tenor-specific critical numbers of abscissas for the different model parameter sets. The critical number of abscissas was defined to be the smallest number of abscissas leading into an absolute value implied volatility change of less than 0.0009%, compared to the initial number of abscissas. The test was then repeated with different model parameter sets. At the end, the expiry tenor specific optimal numbers of abscissas were defined to be the largest critical numbers of abscissas across the tested model parameter sets. The obtained expiry tenor specific optimal cut-off points and the number of abscissas are presented in Table 2.

**Table 2: Expiry tenor specific optimal cut-off points and abscissas.**

| <b>Tenor</b>  | <b>1m</b> | <b>3m</b> | <b>6m</b> | <b>1y</b> | <b>2y</b> | <b>3y</b> | <b>5y</b> |
|---------------|-----------|-----------|-----------|-----------|-----------|-----------|-----------|
| Cut-off point | 270       | 220       | 140       | 80        | 70        | 60        | 40        |
| Abscissas     | 128       | 128       | 128       | 128       | 64        | 64        | 64        |

Given the optimal cut-off points and the number of abscissas, the Fourier integral in (5.18) can be solved numerically by using (5.33) and the corresponding cut-off points and the number of abscissas presented in Table 2.

#### 5.4.2 Random Number Generation

The model of this thesis requires random number generators for normal, log-normal, Poisson, and inverse-normal distributions. The normal distributed random numbers are generated with the polar-form of the Box-Muller transformation (Box & Muller 1958, pp. 610-611), the log-normal distributed random numbers with an algorithm presented by Kalvelagen (2005, pp. 8-10), the Poisson distributed random numbers with an

algorithm presented by Knuth (1997, pp. 1-193), and the inverse-normal distributed random numbers with an algorithm presented by Acklam (2004). This thesis does not discuss the logic and the implementation of each algorithm further, as it uses the standard forms of each. Instead, the details of each algorithm can be found in the original references.

## 6 Numerical Tests

In order to ensure that the option pricing model meets the research objectives, a series of numerical tests were performed. The tests were performed with EUR/USD FX rate on a two-month period ranging from the beginning of July to the end of August 2007. Fortunately from this thesis's point-of-view, this particular period turned out to be an excellent test environment for an option pricing model, as the period started with a one-and-half month stable period, after which the "subprime" crisis caused the credit and equity markets to crash on mid-August, causing the implied volatilities of all the asset classes to peak sharply.

As the exotic options are traded only over-the-counter, there are no public price records available. This makes it impossible to test the model with exotic options per se, without actively trading at the market and seeing at which prices the trades are executed. As a result, the initial testing of any exotic option pricing model is typically conducted using indirect methods, after which the model is taken into production step by step, by gradually increasing the risk positions and extending the model to new option styles. As the timeframe of this thesis was limited, it only reports the results of the indirect tests, as the model is not taken into production before the thesis has already been cased in.

On each business day in the test period, the required market data was downloaded from Bloomberg and the model calibrated against the downloaded market data. The data was always downloaded between 14.00 and 15.00 CET, as EUR/USD foreign exchange, EUR fixed income, and USD fixed income markets are all liquid at that time of the day, reducing the risk of non-synchronized market data.

The rest of this Chapter reports the key results of the indirect tests performed for the model. First, the internal consistency of the model is tested in order to ensure the model

implementation to have been carried out correctly. Second, the market consistency of the model is tested in order to ensure the model output vanilla option prices to be in line with the market. Third, the robustness of the model is tested in order to ensure the model dynamics to be mathematically meaningful, and the calibration method to give plausible parameter values.

## 6.1 Internal Consistency

In this thesis, an option pricing model is defined internally consistent, if the observed output of the model matches the expected one. In other words, the internal consistency does not yet guarantee the model to give correct prices, but it merely tells that no mistakes have been made in the implementation. The internal consistency is rarely an issue in simple models, the implementation of which requires no compromises. In more complex models instead, the internal consistency can become a problem due to various numerical problems, such as complex number logarithms, complex number exponentials, numerical integration, and the sampling from unknown distributions, to mention a few.

The simplest way to test the internal consistency is to compare the model output to a known external benchmark. If no external benchmark is available, another alternative is to compare the model against itself, and to search for any inconsistencies. As the model of this thesis has both semi-closed form and Monte Carlo solutions for a European call option, a natural test for the internal consistency is to test the convergence of these two. That is indeed a highly efficient test for the internal consistency of both, as on one hand, both solutions should theoretically give the same result, while on the other, the solutions are implemented independently on each others.

The comparison between the semi-closed form and the Monte Carlo solutions was conducted with a model parameter set calibrated against the implied market data on 16<sup>th</sup> August 2007. Table 3 presents the option prices given by both the semi-closed form and the Monte Carlo solutions, obtained by setting the number of simulation replications to

1,000,000 and the simulation time step length to  $T/500$ , where (T) denotes the time to option expiry. As seen from the table, the option prices converge well, disregarding a small simulation noise that could not be eliminated at any reasonable number of simulation replications. As a consequence, the model seems internally consistent.

**Table 3: Comparison of semi-closed form and Monte Carlo solution option prices.**

| Semi-closed form solution option prices |       |       |       |        |        | Monte Carlo solution option prices |       |       |       |        |        |
|---|-------|-------|-------|--------|--------|------------------------------------|-------|-------|-------|--------|--------|
|   | 10D   | 25D   | 50D   | 75D    | 90D    |                                    | 10D   | 25D   | 50D   | 75D    | 90D    |
| 1M                                      | 0.12% | 0.39% | 1.02% | 2.20%  | 3.77%  | 1M                                 | 0.12% | 0.39% | 1.03% | 2.20%  | 3.77%  |
| 3M                                      | 0.21% | 0.67% | 1.78% | 3.85%  | 6.67%  | 3M                                 | 0.21% | 0.68% | 1.79% | 3.85%  | 6.68%  |
| 6M                                      | 0.30% | 0.96% | 2.54% | 5.48%  | 9.67%  | 6M                                 | 0.30% | 0.97% | 2.55% | 5.49%  | 9.68%  |
| 1Y                                      | 0.44% | 1.37% | 3.64% | 7.89%  | 14.27% | 1Y                                 | 0.44% | 1.38% | 3.65% | 7.89%  | 14.29% |
| 2Y                                      | 0.63% | 1.92% | 5.15% | 11.46% | 24.23% | 2Y                                 | 0.63% | 1.94% | 5.18% | 11.50% | 24.24% |
| 3Y                                      | 0.76% | 2.31% | 6.26% | 14.50% | 26.99% | 3Y                                 | 0.77% | 2.32% | 6.31% | 14.52% | 27.01% |
| 5Y                                      | 0.97% | 3.01% | 8.39% | 22.13% | 28.72% | 5Y                                 | 0.98% | 3.03% | 8.44% | 22.17% | 28.77% |

| Absolute difference |       |       |       |        |       | Relative difference |       |       |       |        |        |
|---------------------|-------|-------|-------|--------|-------|---------------------|-------|-------|-------|--------|--------|
|                     | 10D   | 25D   | 50D   | 75D    | 90D   |                     | 10D   | 25D   | 50D   | 75D    | 90D    |
| 1M                  | 0.00% | 0.00% | 0.00% | 0.00%  | 0.00% | 1M                  | 1.35% | 0.84% | 0.20% | -0.01% | -0.08% |
| 3M                  | 0.00% | 0.00% | 0.00% | -0.01% | 0.01% | 3M                  | 0.67% | 0.68% | 0.16% | -0.15% | 0.09%  |
| 6M                  | 0.00% | 0.01% | 0.01% | 0.01%  | 0.01% | 6M                  | 0.97% | 0.71% | 0.43% | 0.24%  | 0.14%  |
| 1Y                  | 0.00% | 0.01% | 0.01% | 0.00%  | 0.02% | 1Y                  | 0.09% | 0.39% | 0.27% | 0.05%  | 0.13%  |
| 2Y                  | 0.00% | 0.02% | 0.03% | 0.04%  | 0.00% | 2Y                  | 0.40% | 1.14% | 0.56% | 0.32%  | 0.01%  |
| 3Y                  | 0.01% | 0.01% | 0.04% | 0.02%  | 0.02% | 3Y                  | 0.76% | 0.36% | 0.69% | 0.13%  | 0.08%  |
| 5Y                  | 0.01% | 0.02% | 0.05% | 0.04%  | 0.05% | 5Y                  | 1.46% | 0.62% | 0.60% | 0.18%  | 0.16%  |

## 6.2 Market Consistency

An option pricing model is market consistent, if the model output prices are within the market bid-offer spread (Galluccio & Le Cam 2005, pp. 1-40). As it was not possible to test the model of this thesis with exotic options due to lacking price records, the market consistency was tested with vanilla options. More precisely, the market consistency was tested by comparing the market and the model implied volatilities, not option prices as such. The first reason for this is that the implied volatilities are easier to compare across the different expiry tenors and strike levels. The second reason is that the implied volatility is used in the calibration cost function, which makes it a natural measure for the goodness-of-fit as well. The results are in any case equal, as the BS option price is explicitly determined by the implied volatility, and vice versa.

The market consistency was tested on a 45-business-day period from the beginning of July to the end of August 2007. On each business day, the implied volatility was recorded across seven different expiry tenors and five different strike levels, forming an implied volatility surface of 35 points, so that the total number of studied implied volatility points was 1,575. The expiry tenors used in the test surface were one month (1m), three months (3m), six months (6m), one year (1y), two years (2y), three years (3y), and five years (5y), and the strike levels the ones corresponding EUR<sub>call</sub>USD<sub>put</sub> option deltas of 0.10, 0.25, 0.50, 0.75, and 0.90.

The first test was to compare the mean absolute volatility difference between the market and the model mid volatilities to the mean market spread. The absolute volatility difference is defined to be the absolute value of difference between the market and model mid volatilities at a given surface point, and the spread the distance from the market mid to the bid/offer volatility at a given surface point. The mean absolute volatility difference and the mean spread, in turn, are defined as the arithmetic averages of the absolute volatility difference and the spread across all the 35 volatility surface points at a given observation date. Figure 1 plots the mean absolute volatility difference and the mean spread over the whole test period. As seen from the figure, the mean absolute volatility difference stays well below the mean spread over the whole observation period, indicating that the market consistency of the model is good.

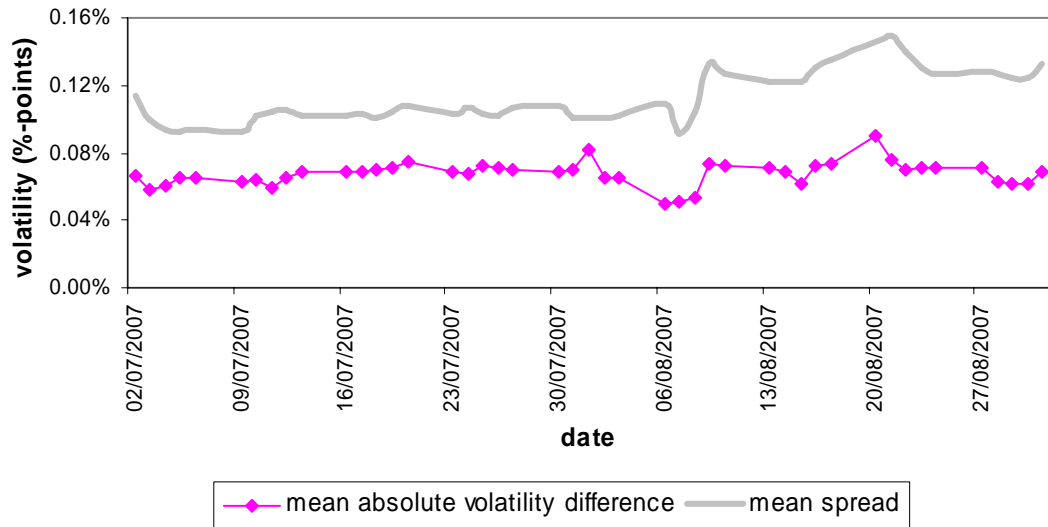


**Figure 1: Mean absolute volatility difference and mean spread.**

The second test was to compare the maximum absolute volatility difference between the market and the model mid volatilities to the mean and maximum market spreads. The absolute volatility difference, spread, and mean spread are defined similarly as above. The maximum absolute volatility difference and the maximum spread in turn, are defined as the maximum values of the absolute volatility difference and the spread across all the 35 volatility surface points at a given observation date. Figure 2 plots the maximum absolute volatility difference, the mean spread, and the maximum spread over the whole observation period. As seen from the figure, the maximum absolute volatility difference is always above the mean spread, but on the other hand, on the vast majority of the observation points, still below the maximum spread, which indicates the model to be adequately in line with the market.

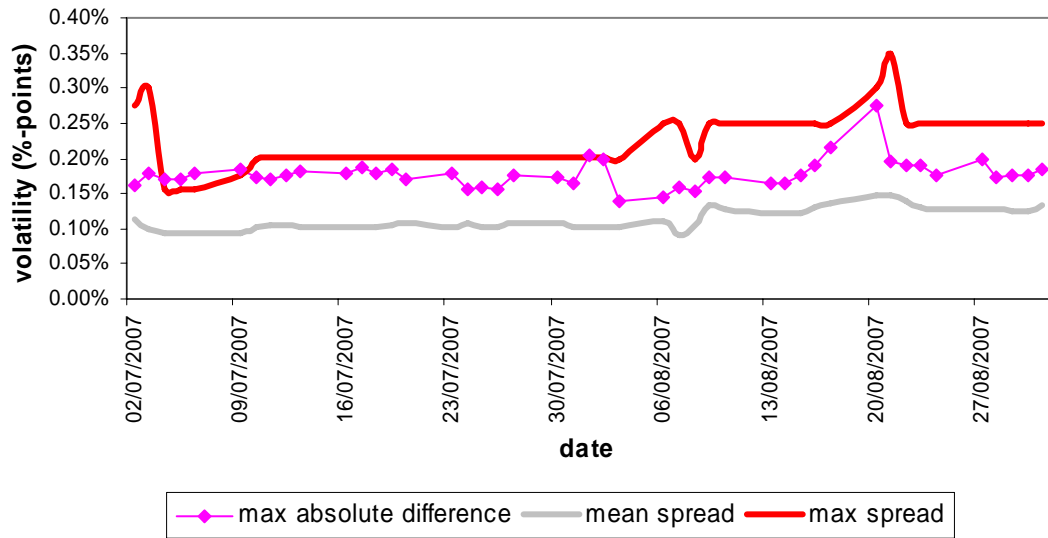


**Figure 2: Maximum absolute volatility difference and mean and maximum spreads.**

The third test was to analyze the term structure of the model fit over the whole observation period. All the model volatility surface points followed the corresponding market volatility points well, and no systematic error patterns or any other symptoms of the model misspecification were detected. As an example, Figure 3 plots the market mid, market bid, market offer, and model mid volatilities for one month at-the-money tenor over the whole observation period. As can be seen, the model mid volatility stays very close to the market mid volatility, also during the volatility peak of “subprime” crisis, which indicates the model to be market consistent. Similar behavior was detected with the other volatility tenors as well.

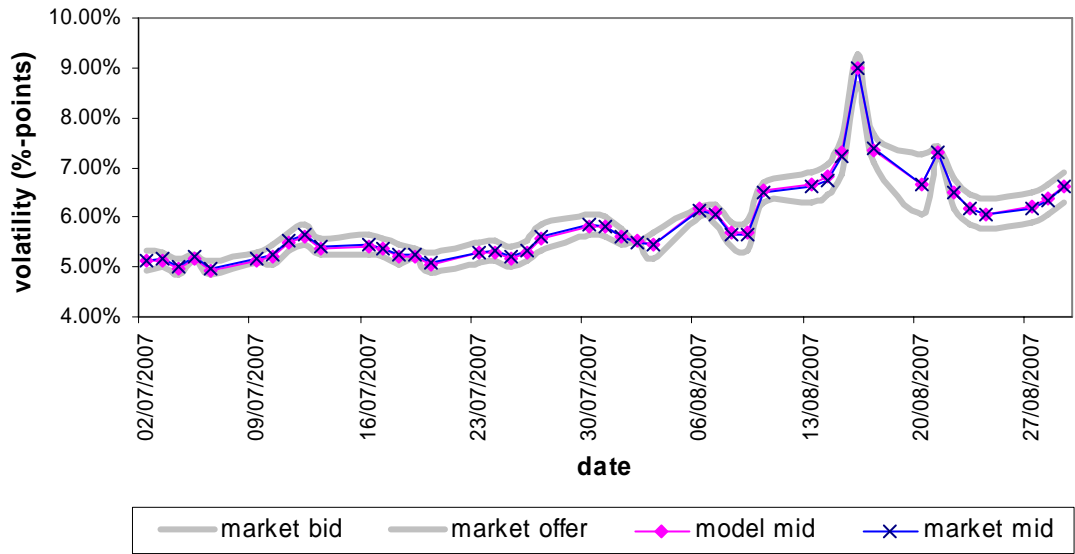


Figure 3: Market and model implied volatilities for one month at-the-money tenor.

The fourth test was a qualitative comparison of the market and model implied volatility surfaces under different kind of market conditions. Figure 4 illustrates the market and model implied mid volatilities on 11<sup>th</sup> July 2007, which was an ordinary day in a stable market period before the market stress. As seen from the figure, the market and model implied volatility surfaces look very similar, both being characterized by an increasing volatility term structure and a symmetric smile around the at-the-money level.

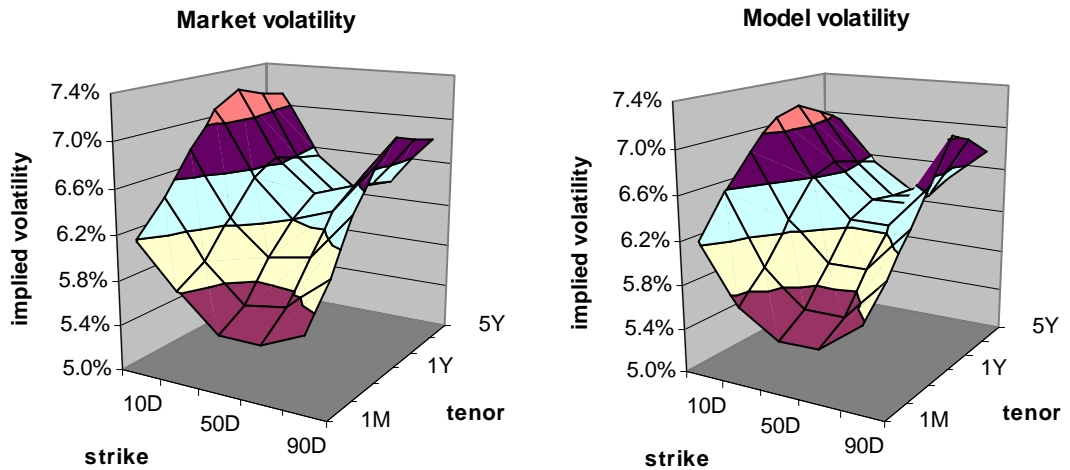


Figure 4: Market and model implied volatility surfaces on 11<sup>th</sup> July 2007.

Figure 5 illustrates the market and model implied mid volatilities on 16<sup>th</sup> August 2007, which was the most turbulent day of the “subprime” crisis in the FX market. As seen from the figure, the market and model implied volatility surfaces look somewhat similar, both being characterized by a highly irregular surface shape across both the expiry tenors and the strikes.

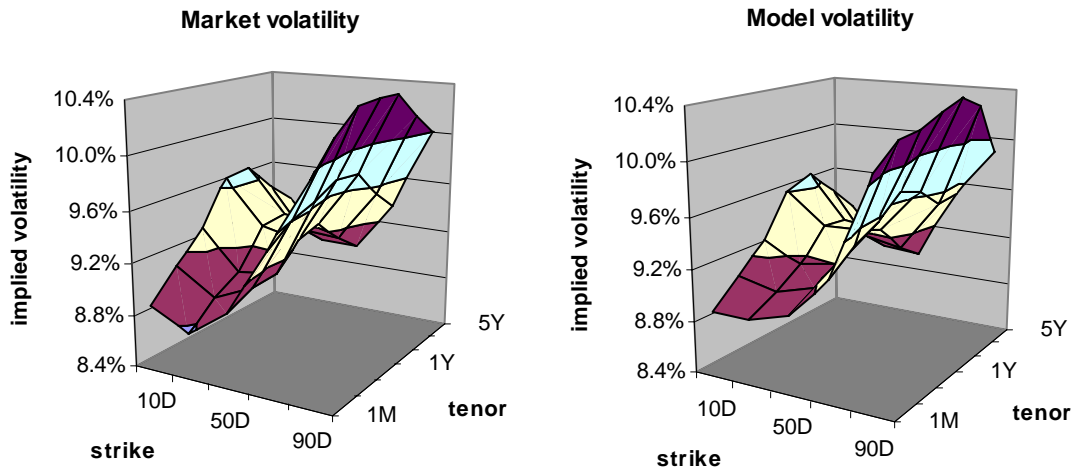


Figure 5: Market and model implied volatility surfaces on 16<sup>th</sup> July 2007.

Figure 6 illustrates the market and model implied mid volatilities on 28<sup>th</sup> August 2007, which was an ordinary day in a stabilizing market period after the market stress. As seen from the figure, the market and model implied volatility surfaces look rather similar, both being characterized by a hump-shaped at-the-money volatility term structure and a skewed smile around the at-the-money level.

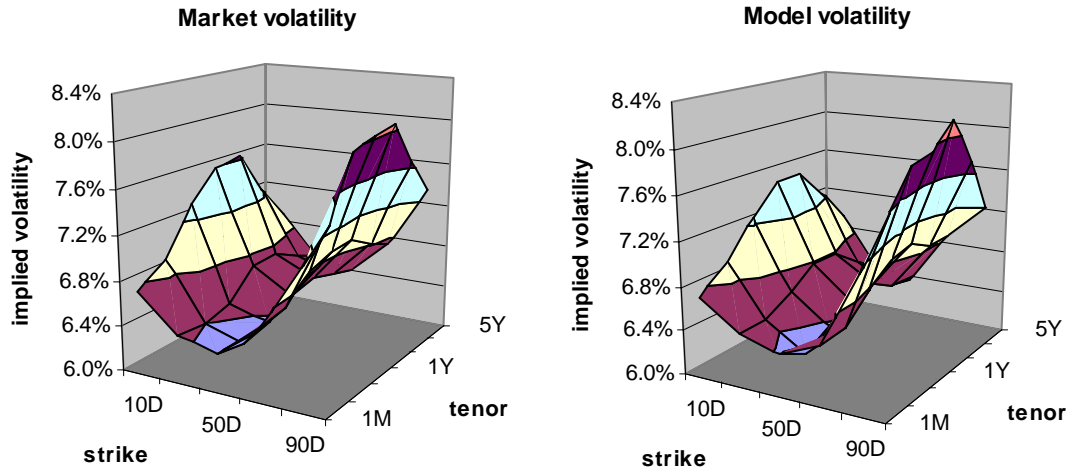


Figure 6: Market and model implied volatility surfaces on 28<sup>th</sup> August 2007.

All in all, the model mid volatility stayed within the market bid-offer spread in 1,187 out of 1,575 studied points, whereas the model mid volatility was outside the market bid-offer spread in 388 points. However, when the model mid volatility was outside the market bid-offer spread, it was on average only 0.038 %, and at maximum only 0.225 % outside the spread. Based on the test results above, the option pricing model of this thesis appears market consistent with the vanilla option prices. The key statistics of the market consistency tests are presented in Table 4.

Table 4: Key statistics of the market consistency tests.

|   |       |
|---|-------|
| Number of volatility observation points                           | 1,575 |
| Number of model volatility points inside market bid-offer spread  | 1,187 |
| Number of model volatility points outside market bid-offer spread | 388   |

|   | Minimum | Mean   | Maximum |
|---|---------|--------|---------|
| Market mid volatility   | 4.979%  | 6.697% | 10.425% |
| Model mid volatility  | 4.940%  | 6.696% | 10.587% |
| Absolute difference between model and market mid volatilities | 0.000%  | 0.068% | 0.275%  |
| Market bid-offer spread                                       | 0.025%  | 0.226% | 0.700%  |
| Spread violation  | 0.000%  | 0.038% | 0.225%  |

### 6.3 Robustness

In this thesis, an option pricing model is defined robust, if the fluctuation of the model parameters can be explained by the changing market conditions, instead of the fluctuation being generated by the structure of the model itself. Different researchers refer to the feature with different terms, for example Bates (Bates 1996, pp. 69-107) using “stability” and Eraker (2003, pp. 1269-1300) “parameter uncertainty”. Despite the different terms, the main reason to test it is to ensure that the model fits the market due to mathematically meaningful underlying dynamics and a successful model calibration, instead of over-fitting the market by incorporating too many free parameters.

The parameters of a robust model evolve smoothly over time, provided that no particular market stress exists. The parameters of a non-robust model instead, may fluctuate heavily from one point of time to another, either due to defective model dynamics, an incorrect calibration, or both. As a result, heavily fluctuating model parameters in a steady market environment are a clear indication of robustness problems, whereas smoothly evolving model parameters indicate a model to be robust.

Figure 7 illustrates the behavior of the jump frequency ( $\lambda$ ) over the whole observation period. As seen from the figure, the jump frequency stays between 0.15 and 0.40, which indicates the market to expect the EUR/USD foreign exchange rate to jump, on average, once in every 2.5 – 6.5 years. The jump frequency stays nicely within the optimization boundaries 0.01 and 5.00. As a result, the behavior of ( $\lambda$ ) does not suggest that the model would not be robust.

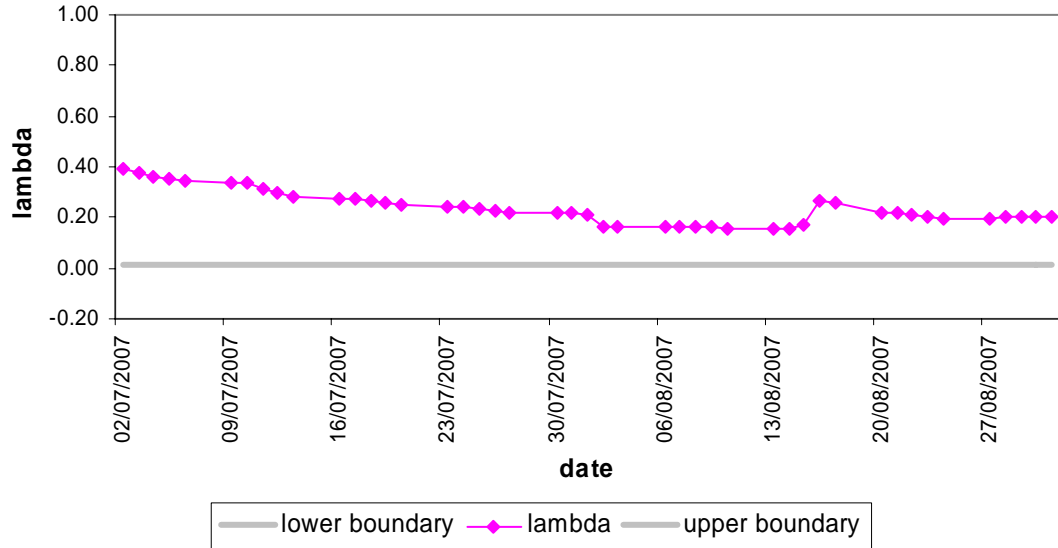


Figure 7: Time series of jump frequency ( $\lambda$ ).

Figure 8 illustrates the behavior of the average jump size ( $\epsilon$ ) over the whole observation period. The behavior of ( $\epsilon$ ) suggests no robustness problems either, as the average jump size stays between -0.07 and 0.02, which indicates the Euro to suddenly drop from 7% against the Dollar to the Dollar to suddenly drop 2% against the Euro, which is well between the optimization boundaries -0.10 and 0.10. Furthermore, the largest fluctuation takes place between 14<sup>th</sup> and 20<sup>th</sup> August, which is the time of the “subprime” crisis.

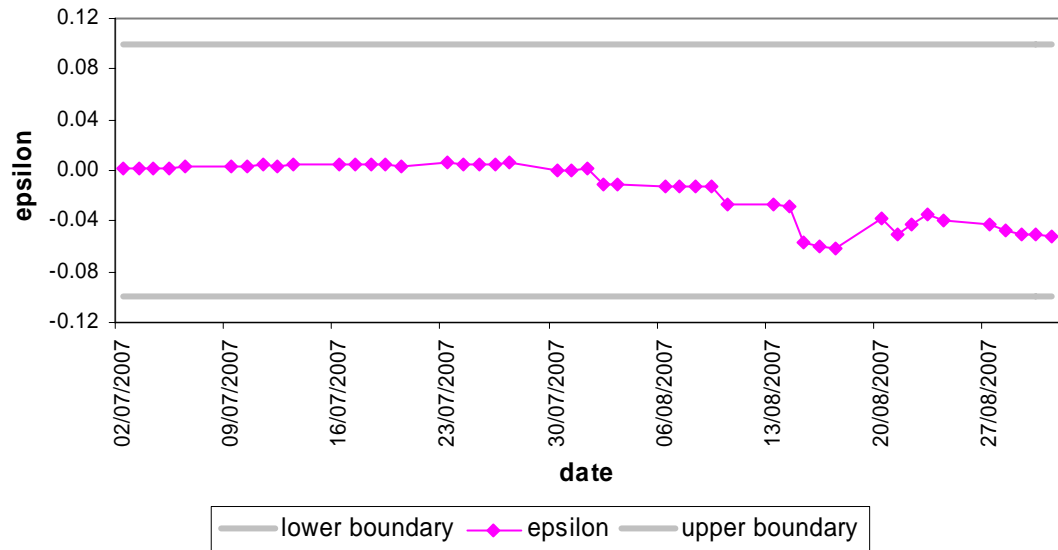
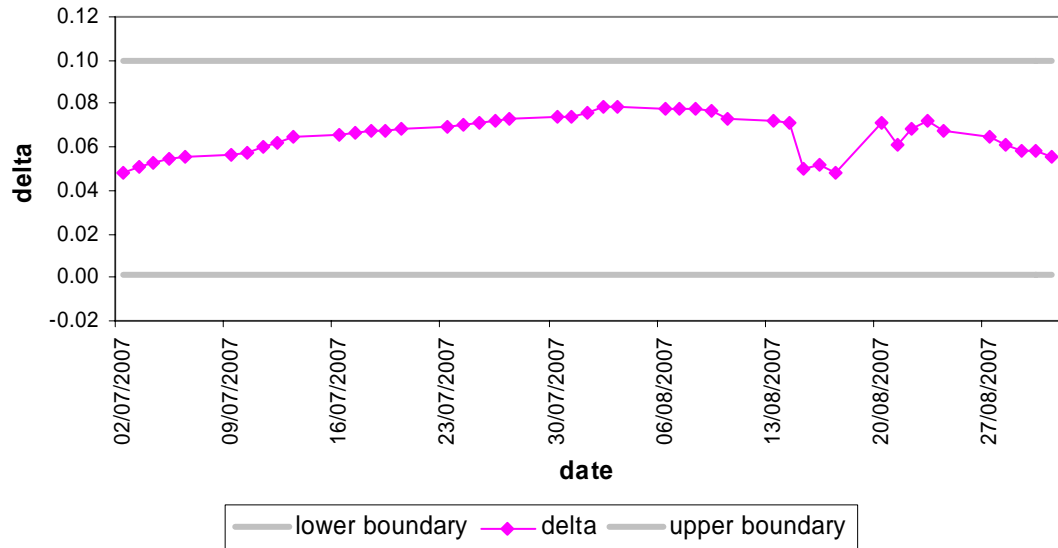


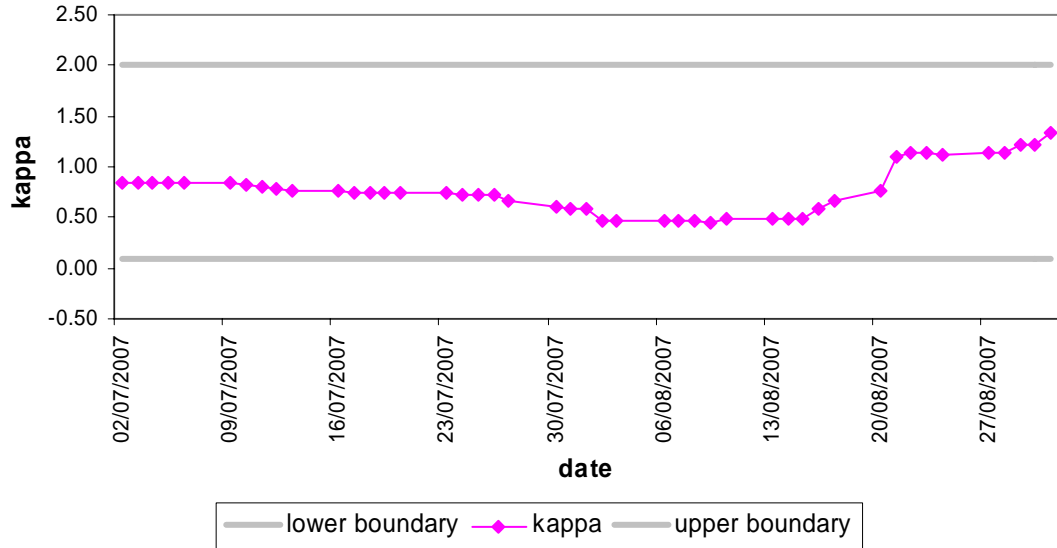
Figure 8: Time series of average jump size ( $\epsilon$ ).

Figure 9 illustrates the behavior of the jump size standard deviation ( $\delta$ ) over the whole observation period. Similarly to the other jump parameters, the behavior of ( $\delta$ ) does not suggest any robustness problems, but the parameter value stays between 0.04 and 0.08, which is well within the optimization boundaries 0.001 and 0.10. Similarly to ( $\epsilon$ ), the largest fluctuation takes place at the time of the “subprime” crisis.



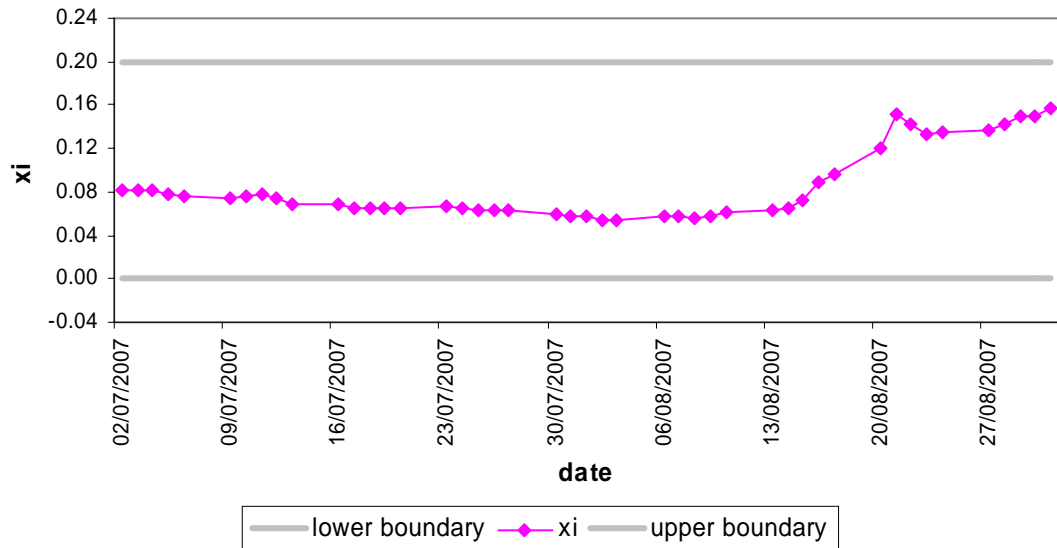
**Figure 9: Time series of jump size standard deviation ( $\delta$ ).**

Figure 10 illustrates the behavior of the volatility mean reversion rate ( $\kappa$ ) over the whole observation period. Similarly to the earlier parameters, it indicates no robustness problems, as the volatility mean reversion rate stays between 0.45 and 1.35. That is well between the optimization boundaries 0.10 and 2.00, and the largest fluctuation takes place between 14<sup>th</sup> and 20<sup>th</sup> August, which is the time of the “subprime” crisis.



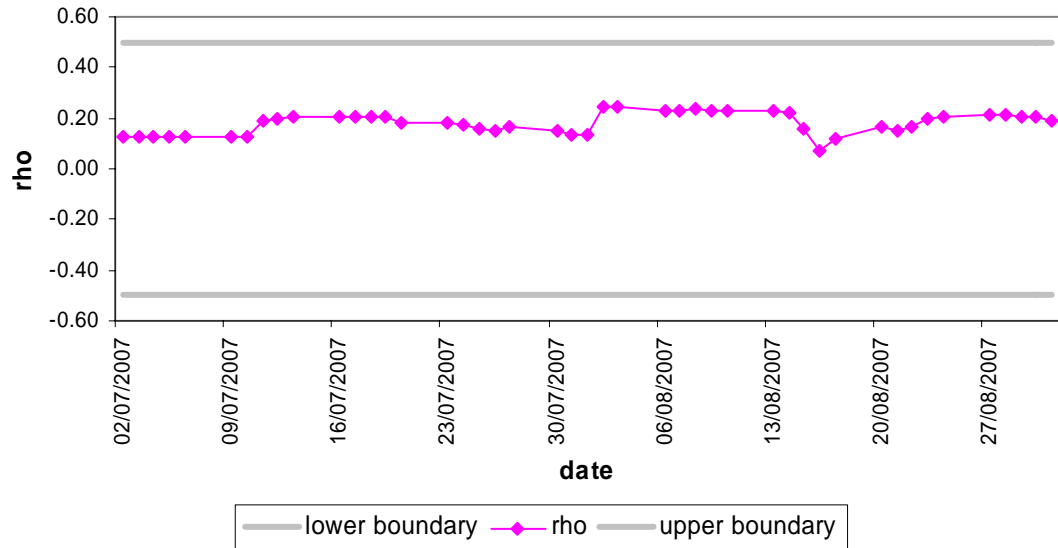
**Figure 10: Time series of volatility mean reversion rate ( $\kappa$ ).**

Figure 11 illustrates the behavior of the volatility of volatility ( $\xi$ ) over the whole observation period. The behavior of ( $\xi$ ) gives no reason to suspect the model not to be robust, as the parameter stays between 0.04 and 0.16, which indicates the market to expect the volatility of the EUR/USD FX rate to be between 4% and 16%. That is both within the optimization boundaries 0.001 and 0.20, and intuitively reasonable.



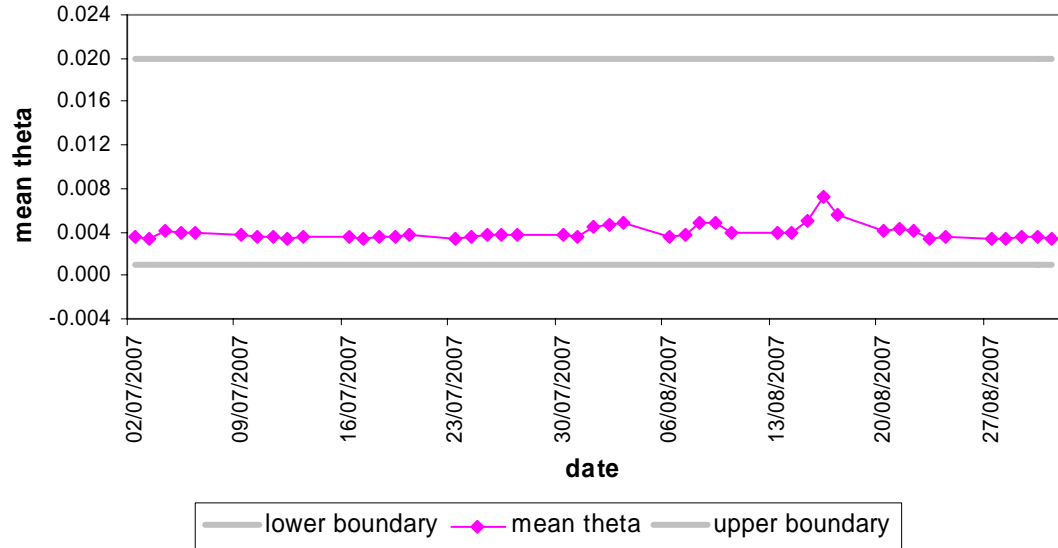
**Figure 11: Time series of volatility of volatility ( $\xi$ ).**

Figure 12 illustrates the behavior of the correlation between the spot and volatility processes ( $\rho$ ) over the whole observation period. As can be seen, the correlation stays between 0.11 and 0.25, without even getting close to the optimization boundaries -0.50 and 0.50. The behavior of ( $\rho$ ) therefore gives no reason to suspect the model not to be robust.



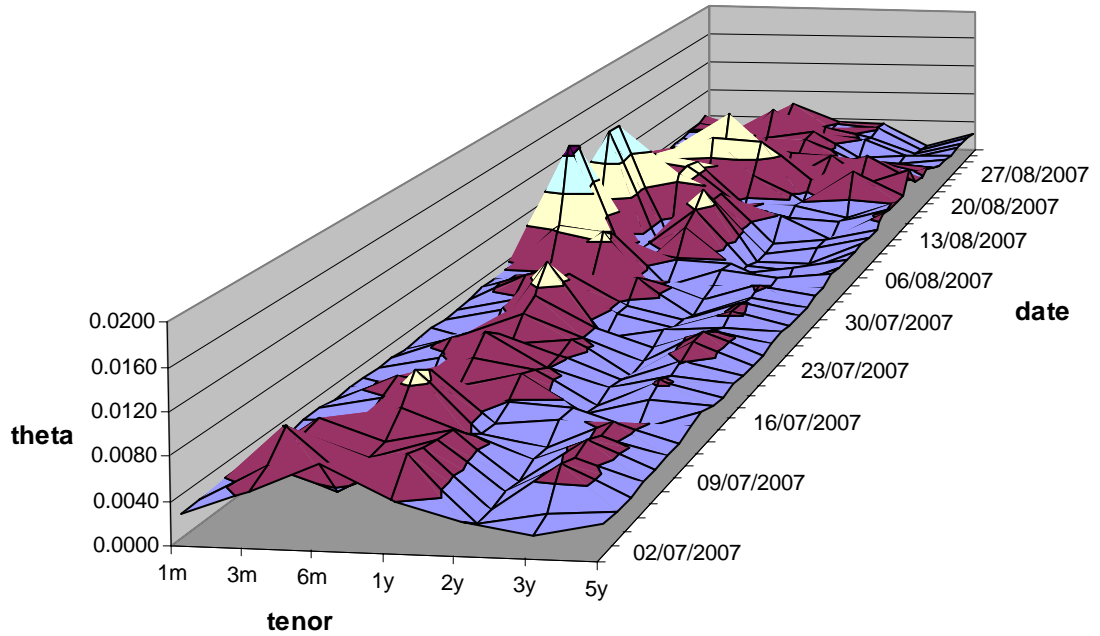
**Figure 12: Time series of spot-volatility correlation coefficient ( $\rho$ ).**

Figure 13 illustrates the behavior of the average value of the volatility mean reversion level ( $\theta$ ) over the different expiry tenors as a time series over the whole observation period. As seen from the figure, the average value of the volatility mean reversion level stays between 0.0034 and 0.0072, which indicates the market to expect the volatility mean reversion level of the EUR/USD FX rate, calculated as the square root of ( $\theta$ ), to be between 5.80% and 8.50%. That is both intuitively reasonable and within the optimization boundaries, so it gives no reason to suspect the model not to be robust.



**Figure 13: Time series of the average value of volatility mean reversion level ( $\theta$ ).**

In order to analyze the expiry tenor term structure of the volatility mean reversion level, caused by the piecewise constant ( $\theta_t$ ), Figure 14 illustrates the behavior of ( $\theta_t$ ) as a function of both time and expiry tenor. As seen from the figure, ( $\theta_t$ ) behaves smoothly over time, the largest fluctuation taking place on the short tenors during August. Surprisingly though, the largest fluctuation takes place on 8<sup>th</sup> and 9<sup>th</sup> August, which is before the “subprime” crisis. However, if analyzing the market volatility on those days in a more in-detailed manner, one can see that there is a steep increase in the market volatility from the one month tenor to the six month tenor, which enforces the model to have a high ( $\theta_{3m}$ ) value in order to hit the market. Otherwise, the behavior of ( $\theta_t$ ) is smooth over both the time and the expiries, which gives no reason to suspect the model to be non-robust.



**Figure 14: Time series of piecewise constant volatility mean reversion level ( $\theta$ )**

As none of the model parameters reached the optimization boundaries, fluctuated heavily over time, or had intuitively unreasonable values, the option pricing model of this thesis appears robust.

## 7 Discussion and Conclusions

The research problem of this thesis was to build a pricing model for exotic foreign exchange rate options. More precisely, the objective was to develop and implement a model that is theoretically sound and consistent with the market implied option prices. The thesis was divided into theoretical and empirical parts, where the theoretical part discussed the modeling of FX rates, option pricing, and model calibration. The empirical part built an option pricing model for exotic FX options, and tested the model performance with real market data. This Chapter first summarizes the key results of both the theoretical and empirical parts; and then analyses the strengths and weaknesses of the thesis, and presents suggestions for the future research.

### 7.1 Summary

The modeling of the foreign exchange rates has drawn plenty of attention, and numerous authors have proposed different stochastic models for the FX rates. Most popular ones are typically extensions of the geometric Brownian motion, and use stochastic volatility, add discrete jumps into the spot and volatility processes, and allow rich correlation structures between the model parameters. Even though they do not fully capture the behavior of the FX rates, they explain the historical returns and the implied option prices far better than their simpler counterparts.

Despite that it has been known for decades that the FX rates do not follow the geometric Brownian motion, the traditional option pricing models have assumed so and still remained popular among the industry practitioners. One likely reason for this is the local volatility concept, which allows vanilla options to be priced market consistently by using different volatilities for different expiry and moneyness tenors. However, the exotic options are often sensitive to the higher moments of the FX returns, which mean that

they cannot be priced correctly using the local volatility concept, but one has to use a more realistic underlying data generating process.

However, the more complex data generating process is challenging from the viewpoint of model implementation. First, the more complex data generating process makes the analytical pricing of options far more difficult. In practice, the current standard is to use the characteristic functions technique by Heston (1993, pp. 327-343), which can be correctly implemented only with elaborate numerical techniques. Second, the more complex data generating process also complicates model calibration, especially if the model is calibrated against the implied option prices. Third, the more complex data generating process often requires a non-trivial approximated sampling scheme, which is needed for pricing exotic options with Monte Carlo.

Given the above conclusions from the theoretical part, the empirical part of this thesis modeled the behavior of the FX rates as a nested stochastic volatility – jump process with piecewise constant model parameters. In order to price exotic options, the model was implemented in both continuous and discrete times. The continuous time model was used for the efficient model calibration against the implied option prices, whereas the discrete time model was used for the actual pricing of exotic options. The empirical part also created a model calibration method specifically for the purposes of this thesis, because no methods with an acceptable calibration quality were found in the literature.

The model performance was analyzed by testing the model with real market data during a two-month period from the beginning of July to the end of August 2007. For each business day, the model was calibrated against the implied option prices using the latest market data. The market consistency of the model was good, as 75.4% of the model output option prices stayed within the market bid-offer spread, and the ones outside the spread, were on average only 0.038% outside it. The model was also robust, as all the model parameters behaved steadily over time, and the parameter values stayed at plausible levels. Furthermore, the output option prices of the analytical and Monte Carlo solutions converged well, which indicates that the model is internally consistent.

## 7.2 Concluding Remarks

The main contribution of the thesis is the development of a comprehensive and market consistent framework for the pricing of exotic FX options in the SVJ model. Galluccio and Le Cam (2005, pp. 1-40) provide a similar framework for equities, but corresponding models for FX have apparently not been developed. In the thesis, the full model implementation process from the definition of the data generating process to the market consistency tests is covered. In contrast to most earlier studies, the model is also tested with real market data. As a result, the model is simultaneously up-to-date with recent theoretical findings while it also meets the practical business needs of an industry practitioner.

The weakness of the thesis is that it does not test the model with exotic options, due to the lacking price records. Even though the sound theoretical background and the successful numerical tests with vanilla options indicate the model and the calibration method to be mathematically meaningful and correctly implemented, one still cannot be sure about the capability of the model to price exotic options without explicit tests.

As a result, an obvious objective for the future study is test the market consistency of the model with exotic options in the OTC market. Furthermore, the used numerical methods for numerical integration, calibration, and random number generation were proven adequate, but they are still by no mean optimized in terms of numerical performance or accuracy. As a result, it is likely that both the computational performance and the accuracy of the model can be enhanced by fine tuning the numerical implementation.

Furthermore, the thesis also restricted the research scope to non-quanto and non-exercisable options on one underlying currency pair. However, many exotic FX options do include quanto and basket elements, making the extension of model to the quanto and basket options another interesting direction for the future research. The same naturally applies for the exercisable options as well, even though the early exercise feature is not too common in the foreign exchange rate options.

## References

Acklam, P. J. 2004. *An algorithm for computing the inverse normal cumulative distribution function* [online]. [2007-06-24]. Available in www-format at:  
<URL:<http://home.online.no/~pjacklam/notes/invnorm/index.html>>

Aït-Sahalia, Y. 2004. *Disentangling jumps from volatility*. Journal of Financial Econometrics, Vol. 74, No.3. (Dec., 2004), pp. 487-528.

Aït-Sahalia, Y., Kimmel, R. 2007. *Maximum likelihood estimation of stochastic volatility models*. Journal of Financial Economics, Vol. 83, No. 2. (Feb., 2007), pp. 413-452.

Akgiray, V., Booth, G. G. 1988. *Mixed diffusion-jump process modelling of exchange rate movements*. The Review of Economics and Statistics, Vol. 70, No. 4. (Nov., 1988), pp.631-637.

Albrecher, H., Mayer, P., Schoutens, W., Tistaert, J. 2007. *The little Heston trap*. Wilmott Magazine, (Jan., 2007), pp. 83-92.

Alizadeh, S., Brandt, M. W., Diebold, F. X. 2002. *Range-based estimation of stochastic volatility models*. The Journal of Finance, Vol. 57, No. 3. (Jun., 2002), pp. 1047-1091.

Andersen, L. 2007. *Efficient simulation of the Heston stochastic volatility model*. [online]. [2007-07-25]. Available in www-format at:  
<URL:<http://ssrn.com/abstract=946405>>.

## References

---

Andersen, T. G., Bollerslev, T. 1998. *Answering the sceptics: yes, standard volatility models do provide accurate forecasts*. International Economic Review, Vol. 39, No. 4. (Nov., 1998), pp. 885-905.

Andersen, T. G., Bollerslev, T., Diebold, F. X., Labys, P. 2001. *The distribution of realized exchange rate volatility*. Journal of American Statistical Association, Vol. 96, No. 453. (Mar., 2001), pp. 42-55.

Bachelier, M. L. 1900. *Théorie de la spéculation*. Annales scientifiques de l'É.N.S. 3e série, tome 17 (1900), pp. 21-86.

Bakshi, G., Cao, C., Chen, Z. 1997. *Empirical performance of alternative option pricing models*. The Journal of Finance, Vol. 52, No.5. (Dec., 1997), pp. 2003-2049.

Bali, T. G. 2000. *Testing the empirical performance of stochastic volatility models of the short-term interest rate*. The Journal of Financial and Quantitative Analysis, Vol. 35, No.2. (Jun., 2000), pp. 191-215.

Ball, C. A., Torous, W. N. 1983. *A simplified jump process for common stock returns*. The Journal of Financial and Quantitative Analysis, Vol. 18, No.1. (Mar., 1983), pp. 53-65.

Bank for International Settlements. 2007. *Triennial and semiannual surveys on positions in global over-the-counter (OTC) derivatives markets at end-June 2007* [online]. [2007-11-28]. Available in www-format at:  
<URL:[http://www.bis.org/publ/otc\\_hy0711.pdf](http://www.bis.org/publ/otc_hy0711.pdf)>

Bates, D. S. 1996. *Jumps and stochastic volatility: exchange rate processes implicit in Deutsche mark options*. The Review of Financial Studies, Vol. 9, No. 1. (Spring, 1996), pp. 69-107.

Bates, D. S. 2000. *Post-'87 crash fears in S&P 500 futures option market*. Journal of Econometrics, Vol. 94, No. 1-2. (Jan. - Feb., 2000), pp. 181-238.

Berkaoui, A., Bossy, M., Diop, A. 2006. *Euler scheme for SDEs with non-Lipschitz diffusion coefficient: strong convergence*. INRIA working paper no. 5637, pp. 1-18.

Biger, N., Hull, J. 1983. *The valuation of currency options*. Financial Management, Vol. 12, No. 1. (Spring 1983), pp. 24-28.

Black, F., Scholes, M. 1973. *The pricing of options and corporate liabilities*. The Journal of Political Economy, Vol. 81, No. 3. (May – Jun., 1973), pp. 637-654.

Bollen, N. P. B., Rasiel, E. 2003. *The performance of alternative valuation models in the OTC currency options market*. The Journal of International Money and Finance, Vol. 22, No. 1. (Feb., 2003), pp. 33-64.

Bollerslev, T. 1986. *Generalized autoregressive conditional heteroskedasticity*. Journal of Econometrics, Vol. 31, No. 3. (Apr., 1986), pp. 307-327.

Box, G. E. P., Muller, M. E. 1958. *A note on the generation of random normal deviates*. The Annals of Mathematical Statistics, Vol. 29, No. 2. (Jun., 1958), pp. 610-611.

Boyle, P. P. 1977. *Options: a Monte Carlo approach*. The Journal of Financial Economics, Vol. 4, No. 3. (May, 1977), pp. 323-338.

Boyle, P., Broadie, M., Glasserman, P. 1997. *Monte Carlo methods for security pricing*. Journal of Economic Dynamics and Control, Vol. 21. (1997), pp. 1267-1321.

Broadie, M., Kaya, Ö. 2006. *Exact simulation of stochastic volatility and other affine jump diffusion processes*. Operations Research, Vol. 54, No. 2. (Mar., 2006), pp. 217-231.

Calderon-Rossell, J. R., Ben-Horim, M. 1982. *The behavior of foreign exchange rates*. The Journal of International Business Studies, Vol. 13, No. 2. (Autumn, 1982), pp. 99-111.

Canina, L., Figlewski, S. 1993. *The informational content of implied volatility*. The Review of Financial Studies, Vol. 6, No. 3. (1993), pp. 659-681.

Chen, A. H. Y. 1970. *A model of warrant pricing in a dynamic market*. The Journal of Finance, Vol. 25, No. 5. (Dec., 1970), pp. 1041-1059.

Chinn, M. 2007. *Interest rate parity* [online] (entry written for the Princeton Encyclopedia of the World Economy). [2007-01-19]. Available in www-format at: <URL:<http://www.ssc.wisc.edu/~mchinn/IRP.pdf>>.

Churchill, R. V. 1963. *Fourier series and boundary value problems*. 2nd edition. McGraw-Hill. New York (NY), the United States of America.

Cont, R., Tankov, P. 2004. *Non-parametric calibration of jump-diffusion option pricing models*. Journal of Computational Finance, Vol. 7, No. 2. (Spring, 2004), pp. 1-43.

Courtault, J. M., Kabanov, Y., Bru, B., Crépel, P., Lebon, I., Le Marchand, A. 2000. *On the centenary of théorie de la spéculation*. Mathematical Finance, Vol. 10, No. 3. (Jul., 2000), pp. 341-353.

Cox, J. C., Rubinstein, M. 1985. *Options markets*. Prentice-Hall. Englewood Cliffs (NJ), the United States of America.

Das, S. R., Sundaram, R. K. 1999. *Of smiles and smirks: a term structure perspective*. The Journal of Financial and Quantitative Analysis, Vol. 34, No. 2. (Jun., 1999), pp. 211-239.

Deelstra, G., Delbaen, F. 1998. *Convergence of discretized stochastic (interest rate) processes with stochastic drift term*. Applied Stochastic Models and Data Analysis, Vol. 14, No. 1. (Mar., 1998), pp. 77-84.

Derman, E., Kani, I. 1994. *The volatility smile and its implied tree*. Goldman Sachs, Quantitative Strategies Research Notes (Jan., 1994), pp. 1-20.

Duffie, D., Pan, J., Singleton, K. 2000. *Transform analysis and asset pricing for affine jump-diffusions*. Econometrica, Vol. 68, No. 6. (Nov., 2000), pp. 1343-1376.

Durham, G. B. 2006. *Monte Carlo methods for estimating, smoothing, and filtering one- and two-factor stochastic volatility models*. Journal of Econometrics, Vol. 113, No. 1. (Jul., 2006), pp. 273-305.

Engle, R. F. 1982. *Autoregressive conditional heteroscedasticity with estimates of the variance of United Kingdom inflation*. Econometrica, Vol. 50, No. 4. (Jul., 1982), pp. 987-1008.

Engle, R. F. 2001. *GARCH 101: The use of ARCH/GARCH models in applied econometrics*. The Journal of Economic Perspectives, Vol. 15, No. 4. (Autumn, 2001), pp. 157-168.

Eraker, B. 2001. *MCMC analysis of diffusion models with application to finance*. Journal of Business & Economic Statistics, Vol. 19, No. 2. (Apr., 2001), pp. 177-191.

Eraker, B., Johannes, M., Polson, N. 2003. *The impact of jumps in volatility and returns*. The Journal of Finance, Vol. 58, No. 3. (Jun., 2003), pp. 1269-1300.

Eraker, B. 2004. *Do stock prices and volatility jump? Reconciling evidence from spot and option prices*. The Journal of Finance, Vol. 59, No. 3. (Jun., 2004), pp. 1367-1404.

Fridman, M., Harris, L. 1998. *A maximum likelihood approach for non Gaussian stochastic volatility models*. Journal of Business and Economic Statistics, Vol. 16, No. 3. (Jul., 1998), pp. 284-291.

Froot, K. A., Thaler, R. H. 1990. *Anomalies: foreign exchange*. The Journal of Economic Perspectives, Vol. 4, No. 3. (Summer, 1990), pp. 179-192.

Galluccio, S., Le Cam, Y. 2005. *Implied calibration of stochastic volatility jump diffusion models* [online]. [2007-04-06]. Available in www-format at:  
<<http://129.3.20.41/eps/fin/papers/0510/0510028.pdf>>

Garber, P. M. 1989. *Tulipmania*. The Journal of Political Economy, Vol. 97, No. 3. (Jun., 1989), pp. 535-560.

Garman, M. B., Kohlhagen, S. W. 1983. *Foreign currency option values*. Journal of International Money and Finance, Vol. 2, No. 3. (Dec., 1983), pp. 231-237.

Glasserman, P. 2003. *Monte Carlo methods in financial engineering*. Springer-Verlag. New York (NY), the United States of America.

Grabbe, J. O. 1983. *The pricing of call and put options on foreign exchange*. Journal of International Money and Finance, Vol. 2, No. 3. (Dec., 1983), pp. 239-254.

Hansen, L. P. 1982. *Large sample properties of generalized method of moments estimators*. Econometrica, Vol. 50, No. 4. (Jul., 1982), pp. 1029-1054.

Harrison, P. 1998. *Similarities in the distribution of stock market price changes between the eighteenth and twentieth centuries*. The Journal of Business, Vol. 71, No. 1. (Jan., 1998), pp. 55-79.

- Harvey, A., Ruiz, E., Shephard, N. 1994. *Multivariate stochastic variance models*. The Review of Economic Studies, Vol. 61, No. 2. (Apr., 1994), pp. 247-264.
- Haug, E. G. 1998. *The complete guide to option pricing formulas*. McGraw-Hill. New York (NY), the United States of America.
- Heston, S. L. 1993. *A closed-form solution for options with stochastic volatility with applications to bond and currency options*. The Review of Financial Studies, Vol. 6, No. 2. (1993), pp. 327-343.
- Heston, S. L., Nandi, S. 2000. *A closed-form GARCH option valuation model*. The Review of Financial Studies, Vol. 13, No. 3, (Autumn, 2000), pp. 585-625.
- Heynen, R. C., Kat, H. M. 1994. *Volatility prediction: a comparison of stochastic volatility, GARCH(1,1) and EGARCH(1,1) models*. Journal of Derivatives, Vol. 2, No. 2. (Winter, 1994), pp. 50-65.
- Higham, D., Mao, X. 2005. *Convergence of Monte Carlo simulations involving the mean-reverting square root process*. Journal of Computational Finance, Vol. 8, No. 3. (Spring, 2005), pp. 35-62.
- Hol, E., Koopman, S. J. 2000. *Forecasting the variability of stock index returns with stochastic volatility models and implied volatility*. Tinbergen Institute Discussion Paper, TI 2000-104/4, pp. 1-27.
- Honoré, P. 1998. *Pitfalls in estimating jump-diffusion models*. University of Aarhus Working Paper Series, No. 18. (Nov., 1998), pp. 1-36.
- Hull, J., White, A. 1987. *The pricing of options on assets with stochastic volatilities*. The Journal of Finance, Vol. 42, No. 2. (Jun., 1987), pp. 281-300.

Hull, J. C. 2005. *Options, futures, and other derivatives*. 6th edition. Pearson Prentice Hall. Upper Saddle River (NJ), the United States of America.

Jacquier, E., Polson, N., Rossi, P. 1994. *Bayesian analysis of stochastic volatility models*. Journal of Business and Economic Statistics, Vol. 12, No. 4. (Oct., 1994), pp. 371-389.

Johannes, M., Polson, N. 2006. *MCMC methods for continuous-time financial econometrics* [online]. [2007-02-08]. Available in www-format at:  
<URL:[http://www0.gsb.columbia.edu/faculty/mjohannes/PDFpapers/JP\\_2006.pdf](http://www0.gsb.columbia.edu/faculty/mjohannes/PDFpapers/JP_2006.pdf)>.

Johannes, M., Polson, N., Stroud, J. 2006. *Optimal filtering of jump-diffusions: extracting latent states from asset prices* [online]. [2007-02-08]. Available in www-format at:  
<URL:<http://www-stat.wharton.upenn.edu/~stroud/papers/sdejump.pdf>>.

Jorion, P. 1988. *On jump processes in the foreign exchange and stock markets*. The Review of Financial Studies, Vol.1, No. 4. (Winter, 1988), pp. 427-445.

Jorion, P. 1995. *Predicting volatility in the foreign exchange market*. The Journal of Finance, Vol. 50, No. 2. (Jun., 1995), pp. 507-528.

Kahl, C., Jäckel, P. 2005. *Not-so-complex logarithms in the Heston model*. Wilmott Magazine, (Sep., 2005), pp. 94-103.

Kahl, C., Jäckel, P. 2006. *Fast strong approximation Monte-Carlo schemes for stochastic volatility models*. Journal of Quantitative Finance, Vol. 6, No. 6. (Dec., 2006), pp. 513-536.

Kalvelagen, E. 2005. *Some notes on random number generation with gams* [online]. [2007-02-11]. Available in www-format at:  
<URL:<http://www.gams.com/~erwin/random.pdf>>.

Knuth, D. E. 1997. *The art of computer programming, volume 2: seminumerical algorithms*. 3rd edition. Addison Wesley. Reading (MA), the United States of America.

Kythe, P. K., Schaferkotter, M. R. 2005. *Handbook of Computational Methods for Integration*. Chapman & Hall/CRC Press. Boca Raton (FL), the United States of America.

Lipton, A. 2002. *The vol smile problem*. RISK Magazine, Vol. 15, No. 2. (Feb., 2002), pp. 61-65.

Lord, R., Kahl, C. 2006. *Why the rotation count algorithm works*. Tinbergen Institute Discussion Paper, TI 2006-065/2, pp. 1-31.

Lord, R., Koekkoek, R., van Dijk, D. 2006. *A comparison of biased simulation schemes for stochastic volatility models*. Tinbergen Institute Discussion Paper, TI 2006-046/4, pp. 1-32.

Malkiel, B. G., Quandt, R. E. 1969. *Strategies and rational decisions in the securities options market*. MIT Press. Cambridge (MA), the United States of America.

McFarland, J. W., Richardson Pettit, R., Sung, S. K. 1982. *The distribution of foreign exchange price changes: trading day effects and risk measurement*. The Journal of Finance, Vol. 37, No. 3. (Jun., 1982), pp. 693-715.

Melino, A., Turnbull, S. 1990. *The pricing of foreign currency options with stochastic volatility*. Journal of Econometrics, Vol. 24, No. 1-2. (Jul.-Aug., 1990), pp. 239-265.

## References

---

Merton, R. C. 1973. *Theory of rational option pricing*. Bell Journal of Economics and Management Science, Vol. 4, No. 1. (Spring, 1973), pp. 141-183.

Merton, R. C. 1976. *Option pricing when underlying stock returns are discontinuous*. Journal of Financial Economics, Vol. 3, No. 1-2. (Jan.-Mar., 1976), pp. 125-144.

Metropolis, N., Ulam, S. 1949. *The Monte Carlo method*. Journal of the American Statistical Association, Vol. 44, No. 247. (Sep., 1949). pp. 335-341.

Mikhailov, S., Nögel, U. 2003. *Heston's stochastic volatility model implementation, calibration and some extensions*. Wilmott Magazine (Jul., 2003), pp. 74-79.

Nelson, D. B. 1992. *Filtering and forecasting with misspecified ARCH models I: Getting the right variance with the wrong model*. Journal of Econometrics, Vol. 52, No. 1-2. (Apr., 1992), pp. 61-90.

Nelson, E. 1967. *Dynamical theories of Brownian motion*. 2nd edition. Princeton University Press. Princeton (NJ), the United States of America.

Oldfield, G. S., Messina, R. J. 1977. *Forward exchange price determination in continuous time*. The Journal of Financial and Quantitative Analysis, Vol. 12, No. 3. (Sep., 1977), pp. 473-479.

Pan, J. 2002. *The jump-risk premia implicit in options: evidence from an integrated time-series study*. Journal of Financial Economics, Vol. 63, No. 1. (Jan., 2002), pp. 3-50.

Philadelphia Stock Exchange. 2004. *A user's guide to currency options* [online]. [2006-10-14]. Available in www-format at:

<URL:<http://www.phlx.com/products/currency/cug.pdf>>

Poon, S.-H., Granger, C. W. J. 2003. *Forecasting volatility in financial markets: a review*. The Journal of Economic Literature, Vol. 41, No. 2. (Jun., 2003), pp. 478-539.

Roweis, S. 2007. *Levenberg-Marquardt optimization* [online]. [2007-09-10]. Available in www-format at:

<URL:<http://www.cs.toronto.edu/~roweis/notes/lm.pdf>>

Samuelson, P. A. 1965. *Rational theory of warrant pricing*. Industrial Management Review, Vol. 6, No. 2. (Spring, 1965), pp. 13-31.

Samuelson, P. A., Merton, R. C. 1969. *A complete model of warrant pricing that maximizes utility*. Industrial Management Review, Vol. 10, No. 2. (Winter, 1969), pp. 17-46.

Schlögl, E., Schlögl, L. 2000. *A square-root interest rate model fitting discrete initial term structure data*. Applied Mathematical Finance, Vol. 7, No. 3. (Sep., 2000), pp. 183-209.

Scholes, M. S. 1998. *Derivatives in a dynamic environment*. The American Economic Review, Vol. 88, No. 3. (Jun., 1998), pp. 350-370.

Sepp, A. 2007. *Affine models in mathematical finance: an analytical approach*. Doctoral Dissertation, University of Tartu. Tartu, Estonia.

Shephard, N., Pitt, M. K. 1997. *Likelihood analysis of non-Gaussian measurement time series*. Biometrika, Vol. 84, No. 3. (Sep., 1997), pp. 653-667.

Stein, E. M., Stein, J. C. 1991. *Stock price distributions with stochastic volatility: an analytic approach*. The Review of Financial Studies, Vol. 4, No. 4. (1991), pp. 727-752.

Structured Products Association. 2007. Article library [online]. [2007-08-15]. Available in www-format at:

<URL:<http://www.structuredproducts.org/library>>

Student. 1908a. *The probable error of a mean*. Biometrika, Vol. 6, No. 1. (Mar., 1908), pp. 1-25.

Student. 1908b. *Probable error of a correlation coefficient*. Biometrika, Vol. 6, No. 2/3. (Sep., 1908), pp. 302-310.

Sønderby, N. E. 2003. *Simulationsbaseret prisfastsættelse af amerikanske optioner i en model med stokastisk volatilitet og spring*. Master's Thesis, Handelshøjskolen i København. Copenhagen, Denmark.

Taylor, M. P. 1995. *The economics of exchange rates*. Journal of Economic Literature, Vol. 33, No. 1. (Mar., 1995), pp. 13-47.

Tucker, A. L., Pond, L. 1988. *The probability distribution of foreign exchange price changes: tests of candidate processes*. The Review of Economics and Statistics, Vol. 70, No. 4. (Nov., 1988), pp. 638-647.

## Appendix A: Abbreviations

|        |   |
|--------|---|
| 2F     | = Two-factor  |
| AML    | = Approximated maximum likelihood                           |
| ARCH   | = Autoregressive conditional heteroscedasticity             |
| BS     | = Black-Scholes   |
| CET    | = Central European time                                     |
| CIP    | = Covered interest rate parity                              |
| DPS    | = Duffie-Pan-Singleton                                      |
| FX     | = Foreign exchange  |
| GARCH  | = Generalized autoregressive conditional heteroscedasticity |
| GMM    | = Generalized method of moments                             |
| i.i.d. | = Independent and identically distributed                   |
| IMM    | = Implicit Milstein method                                  |
| JD     | = Jump-diffusion  |
| MC     | = Monte Carlo   |
| MCMC   | = Markov-chain Monte Carlo                                  |
| MM     | = Method of moments   |
| OTC    | = Over-the-counter  |
| PDE    | = Partial differential equation                             |
| QE     | = Quadratic exponential                                     |
| QML    | = Quasi-maximum likelihood                                  |
| RNG    | = Random number generator                                   |
| SDE    | = Stochastic differential equation                          |
| SI     | = Stochastic interest rate                                  |
| SSE    | = Sum of squared errors                                     |
| SV     | = Stochastic volatility                                     |
| SVCDJ  | = Stochastic volatility – correlated double jump            |

## Appendix A: Abbreviations

---

|        |  |
|--------|--|
| SVDJ   | = Stochastic volatility – double jump                            |
| SVIDJ  | = Stochastic volatility – independent double jump                |
| SVJ    | = Stochastic volatility – jump                                   |
| SVSCDJ | = Stochastic volatility – state-dependent correlated double jump |
| UIP    | = Uncovered interest rate parity                                 |

## Appendix B: Symbols

|              |   |
|--------------|---|
| $C$          | = The price of a European call option                           |
| $E(\bullet)$ | = Expectation operator  |
| $F_t$        | = Forward foreign exchange rate                                 |
| $H$          | = Hessian matrix  |
| $J$          | = Jacobian matrix   |
| $J_t$        | = Random jump size  |
| $I$          | = Identity matrix   |
| $K$          | = Option exercise price   |
| $N$          | = The number of Monte Carlo simulation replications             |
| $N_e$        | = The number of expiry tenors in the implied volatility surface |
| $N_s$        | = The number of strike levels in the implied volatility surface |
| $N_t$        | = The number of random jump occurrences                         |
| $N(\bullet)$ | = Standard normal distribution                                  |
| $P_1$        | = Option delta  |
| $P_2$        | = The conditional probability of option expiring in-the-money   |
| $S_t$        | = Spot asset price  |
| $T$          | = Time to option expiry   |
| $U_V$        | = Uniform distributed random number                             |
| $V_t$        | = Stochastic volatility   |
| $W_t$        | = Standard Wiener process                                       |
| $X_t$        | = The logarithm of the spot asset price                         |
| $Z_S$        | = Standard normal distributed random number                     |
| $Z_t$        | = Two-dimensional jump process                                  |
| $Z_V$        | = Inverse-normal distributed random number                      |
| $a$          | = Lower truncation barrier in the Gaussian quadrature algorithm |
| $b$          | = Upper truncation barrier in the Gaussian quadrature algorithm |

## Appendix B: Symbols

---

|                 |  |
|-----------------|--|
| $b_t$           | = The interest rate difference between the foreign and domestic interest rates |
| $dt$            | = Time differential  |
| $i$             | = Imaginary unit   |
| $m$             | = First moment of the stochastic volatility process                            |
| $p$             | = The number of autoregressive lags in the ARCH and GARCH models               |
| $q$             | = The number of moving average lags in the GARCH model                         |
| $q_c$           | = Continuous dividend yield  |
| $r_t$           | = Domestic risk free interest rate   |
| $r_t^*$         | = Foreign risk free interest rate  |
| $s$             | = The second moment of the stochastic volatility process                       |
| $t$             | = Time   |
| $t_i$           | = Abscissa $i$ in the Gaussian quadrature algorithm                            |
| $w$             | = Dumping factor in the Levenberg-Marquardt algorithm                          |
| $w_i$           | = Weight $i$ in the Gaussian quadrature algorithm                              |
| $\Gamma_V$      | = The market price of volatility risk  |
| $\Delta$        | = Time discretization step length in the Monte Carlo simulation                |
| $\Theta$        | = Model parameter set  |
| $\Phi$          | = Integration variable   |
| $X$             | = State variable set   |
| $\Psi$          | = The characteristic function of the data generating process                   |
| $\alpha_p$      | = The weighting factor of autoregressive lag $p$ in the ARCH and GARCH models  |
| $\beta_q$       | = The weighting factor of moving average lag $q$ in the GARCH model            |
| $\gamma$        | = Time integral weighting factor in the Quadratic Exponential scheme           |
| $\delta_t$      | = The jump size standard deviation of the jump process                         |
| $\varepsilon_t$ | = The average jump size of the jump process                                    |
| $\varepsilon_p$ | = Random error term for autoregressive lag $p$ in the ARCH and GARCH models    |
| $\theta_t$      | = The mean reversion level of the stochastic volatility process                |
| $\kappa_t$      | = The mean reversion rate of the stochastic volatility process                 |
| $\lambda_t$     | = The jump intensity of the jump process                                       |
| $\mu_t$         | = The instantaneous drift of the spot asset price process                      |
| $\xi_t$         | = The volatility of the stochastic volatility process                          |

## Appendix B: Symbols

---

|           |   |
|-----------|---|
| $\rho_t$  | = The correlation between the spot asset price and volatility processes           |
| $\sigma$  | = The constant volatility of the spot asset price process                         |
| $\tau$    | = Time from the option expiry   |
| $\varphi$ | = The drift of the stochastic volatility process                                  |
| $\psi$    | = The ratio of the first two squared moments of the stochastic volatility process |
| $\omega$  | = New volatility information in the ARCH and GARCH models                         |